SLIP CASTING OF SILICON NITRIDE

by
Pawan Saxena

Department of Mining and Metallurgical Engineering
McGill University, Montreal
November, 1992

A Thesis submitted to the Faculty of Graduate Studies and Research
in partial fulfilment of the requirements for the degree of
Masters of Engineering

ABSTRACT

Slip casting is a well established technique for the manufacture of traditional ceramic bodies, such as clays and whitewares. It combines complex shaping with high green densities, resulting in low shrinkage and good densification behaviour.

This method, however, has received little attention in the field of engineering ceramics especially with regard to silicon nitride Commercial fabrication of silicon nitride, a major contender for high temperature applications due to its excellent thermomechanical properties, has been confined to hot pressing. This is an expensive process and has geometrical limitations

Slip casting, followed by sintering, has been identified as a potentially economical alternative fabrication method, however a number of parameters have to be optimized before a good slip cast silicon nitride body can be made. The aim of the present work is to control parameters such as pH, viscosity and deflocculation in order to form dense, homogeneous, slip cast silicon nitride bodies.

A detailed investigation of the rheological properties of Si_3N_4 and careful control of processing parameters, made it possible to produce slip cast Si_3N_4 bodies having upto 97% TD on sintering. Mechanical strength values obtained by slip casting were compared with those obtained by die-pressing. Strength values of the slip cast material was limited by iron inclusions entrained in processing.

RÉSUMÉ

La coulée en barbotine est une technique très utilisée dans la fabrication de produits domestiques en céramique, comme de la poterie et des bibleleaux Elle permet l'élaboration d'objets aux formes complexes tout en obtenant une haute densite des pièces avant cuisson Cette dernière propriété reduit considerablement les risques de défaults associés à la contraction de la pièce durant la cuisson et le refroidissement

Cependent, cette méthode de fabrication a reçu peu d'attention de la part le l'industrie en céramique, spécialement concernant le nitrure de silicium Les produits commerciaux en nitrure de silicium, réputés pour leur très bonne tenue thermo-méchanique à haute température, sont surtout obtenus à partir du pressage isostatique à chaud. Cette technique est coûteuse et est limitée quant à la complexité des formes réalisables.

Par contre, la coulée en barbotine représente une alternative économiquement avantageuse, même si elle exige l'optimisation d'un certain nombre de parametres avant de réussir des pièces de nitrure de silicium acceptables. Le but de cette etude consiste à déterminer les paramètres de la barbotine comme le pH, la viscosité, la concentration en défloculant qui donnerant des pièces en nitrure de silicium de haute densité et de grande homogénéité.

Une étude minutieuse des propriétés rhéologiques du Si_3N_4, ainsi qu'un contrôle serré des parametres de coulée ont permis de produire des pieces dont la densité après frittage pouvait atteindre 97% de la densité théorique. La résistance mécanique des pièces ainsi obtenues a été comparée avec celle de pieces produites par pressage à matrices La résistance mécanique des pièces issues de la coulée en

barbotine est présentement limitée par l'introduction d'inclusions ioniques dans le matériau lors du procédé

ACKNOWLEDGEMENTS

I wish to express my sincere thanks to my research supervisor Professor R A.L.Drew for his continuous advice, encouragement and guidance throughout the course of study

I also wish to express my thanks to Professor Martin D.Pugh and Dr Kartik Shanker for their suggestions and criticism through several discussions during the course of this research.

It has been a pleasure knowing and working with my colleagues at the ceramics lab: Holly Hampton, Joe McDermid, Cheryl Brayman, Daniel Muscat, Ali Hadian, Serge Grenier, Youngmin Baik and Kevin Jaansalu

Finally, I would like to thank my wife Dr. April L.Wootten, for sharing the housework.

to

my parents

CONTENTS

LIST OF FIGURES

LIST OF TABLES

CHAPTER I INTRODUCTION

A ceramic can be defined as an inorganic compound formed by the chemical combination of a metal and a non-metal. Traditional ceramic products derived from clay minerals, as well as structural and electronic ceramics (which are often manufactured by chemical synthesis) are all made up of elements which are found abundantly in the earth's crust

There presently exists, a great deal of interest in the development of structural ceramics throughout the industrialized world. The increasing importance of fuel conservation[1], and interest in increasing the operating efficiency have stimulated renewed interest in the use of ceramic components in heat engines. The advantages of ceramics for such applications as compared to the metals, currently used, are their capability for operating at higher temperatures and low densities, the greater abundance of raw materials, their availability, and their potential low cost.

The most important materials[2] for potential high temperature applications in the energy conversion systems and heat engines are silicon nitride (Si_3N_4), silicon carbide (SiC) and zirconia (ZrO_2) Silicon Nitride, which is a leading candidate, has gained increasing importance as a structural material This is due to a favourable combination of properties[3] of dense Si_3N_4 such as high strength at high temperatures, good thermal shock behaviour, high wear and good chemical resistance. However, one major disadvantage of this material, is the difficulty of producing dense Si_3N_4 parts from starting powders by a solid state sintering process. To achieve sufficient densification, the use of additives which react to form a liquid phase at high temperature and thus promote densification by liquid phase sintering, is necessary.

For higher densities, the simultaneous application of a high pressure, can be utilised This process, known as hot pressing, though renders good properties, allows only the fabrication of simply shaped parts and therefore the mass production of complex silicon nitride components is limited. Thus, to obtain dense silicon nitride bodies with the flexibility of complex shaping it is essential to divide the manufacturing process into two steps, namely, green forming and sintering

In green forming (the word "green" implying unfired or unsintered product) the Si_3N_4 powder along with the sintering additives is consolidated to the desired shape by a purely physical process This process may involve suspending the multicomponent powder mix in a liquid, usually water and drying the suspension whilst creating the desired shape of the component as in slip casting, or compacting the semi-dry suspension, as in extrusion and injection moulding The suspension may also be fully dried and compacted under high pressure as in dry pressing

The powder compact, or the "green body" can contain anywhere from 25% to 60% porosity, which must be removed by sintering, in order to achieve properties close to that of a theoretically dense material Sintering ensures further densification by removal of the porosity, leading to shrinkage, combined with growth together and strong bonding between adjacent particles

Slip casting is a well established technique for the manufacture of clays and whitewares. In the past decade, it has been identified as being a potentially appropriate fabrication method for making silicon nitride components. It combines complex shaping with high green densities resulting in low shrinkage and good densification behaviour.

The present thesis deals with the study of slip casting of silicon nitride, in an

attempt to optimise the processing parameters for this particular technique. The slip casting process requires a slip which, in this case is a multicomponent powder, suspended in a liquid vehicle. This suspension exhibits colloidal properties and must therefore be characterised with respect to pH, stability with time and effects of flocculation and deflocculation. This thesis deals with a systematic study of these parameters with the aim of forming dense homogeneous slipcast Si_3N_4 bodies.

Outline of thesis

Chapter II of the thesis deals with the literature review of silicon nitride, the sialon system, and sintering of sialons. It will describe the processing of silicon nitride including green forming processes (such as die pressing, extrusion and slip casting) and sintering. Applications and powder requirements of colloidal processing in ceramic systems will also be discussed.

Chapter III will describe the slip casting process in detail. It will highlight various properties such as slip stability with time, the casting procedure and drying. The sub-sections will detail the properties, rheology of colloids and slip casting behaviour of non-clay ceramics.

Chapter IV describes the experimental work that was carried out. It begins by describing the slip preparation. The next section describes the viscosity experiments performed in order to control the rheology. The last two sections describe the slip casting, sintering and sample preparation for strength testing. Sample preparation for microstructure analyses is also given.

Chapter V is devoted to the results and discussion of the experiments performed and Chapter VI outlines the conclusions.

CHAPTER II LITERATURE REVIEW

2.1 Introduction

The bulk of the literature on silicon nitride has appeared during the last two decades, however, the earliest published literature dates as far back as the last century. A German patent of 1895 by Mehner[4] refers to the synthesis of silicon nitride in an electric arc furnace. Weiss and Engelhardt[5] later summarized certain properties of silicon nitride and recognized its composition to be Si_3N_4. A renewal of interest in silicon nitride appears to have been stimulated by a paper of Collins and Gerby[6] who reported some more physical and chemical properties, particularly its low coefficient of thermal expansion, a major reason for the current interest

The potential usefulness of silicon nitride in demanding engineering applications had been recognized by Collins and Gerby[6]; and Turkdogan's[7] publications Parr and his co-workers at Admiralty Materials Lab in the U K had generated interest in the applications and use of silicon nitride, as evident by their papers[8,9] Despite this interest, a large market for silicon nitride has failed to grow rapidly, the circumstances accounting for the failure arising largely from the demanding applications for which the material is being considered, e g poor mechanical design to cope with the high stress and high temperature environments found in heat engines, particularly for a relatively brittle material

Improved ceramic materials like silicon nitride, silicon carbide and zirconia renewed interest in research especially for energy conservation Mechanical properties of silicon nitride and silicon carbide are quite similar, however silicon nitride is preferred since it requires lower sintering temperatures and has higher toughness and

strength

Collins and Gerby have described in their paper about formation of free standing shapes from silicon powder by various means including dry pressing, slip casting and extrusion, and heating of those shapes at 1300°C in nitrogen to convert them to Si_3N_4. This process is known as reaction bonding. On the other hand, hot pressing of silicon nitride powder is expensive and is confined to shapes of simple geometry only. Reaction bonding, although can provide complex shapes, has limited application since the strength is low and it exhibits poor oxidation resistance due to residual porosity.

Addition of sintering additives to silicon nitride powder in a balanced ratio creates silicon nitride components by low pressure or pressureless sintering, and leads to a fully dense material These ratios can easily be determined by the Si-Al-O-N[10,11] system (an acronym for compositions containing Si, Al, O and N). This system is used currently in the fabrication of silicon nitride components, since it involves the use of processes such as slip and pressure casting, injection moulding and extrusion. A process for the large scale manufacture of silicon nitride components for reliable properties, however is yet to be developed.

Slip casting, one of the green forming processes defined earlier, is a traditional ceramic forming process with emerging applications in advanced materials processing. Most of the work in this field of processing for non-clay ceramics especially silicon nitride, has only been performed in the past decade Since the establishment of slip casting as an inexpensive process for mass production of alumina based ceramics, this process has gained key importance for both researchers worldwide and the industry, for its possible viability for the manufacture of silicon nitride components. Unfortunately very little literature has been published since this process for shaping

silicon nitride is novel and most of the work is being done currently at many research institutes.

Persson, Hermansson and Carlsson[12] in 1983 developed slip cast Si_3N_4. They investigated the electric mobility of the slip, in order to estimate the particle surface charge for slip stability. Later, in 1986 Whitman and Feke[13] carried out a study to see the effect of powder treatment strategies on the colloid chemistry of aqueous dispersions of silicon nitride by surface titration methods. Bellosi and Galassi[14] in 1986, and Siskens[15] also investigated property reactions of silicon nitride aqueous slips relating to rheology, zeta-potential and pH. Siskens, however, used Vanisperse CB as a dispersant to deliberately lower the zeta-potential.

Olagnon and Nagy[16], in 1989, further investigated slip casting of Si_3N_4 powders with respect to milling time and slip rheology. Their findings, and those of Nagel and Greil[17] both indicate that, though the green density of slip cast pieces may range between 45%-55% of theoretical density, the sintered density ranges between 95%-99% of theoretical density. They used ammonium based polymer dispersant and Dolapix PC 33, respectively, and have deduced that silicon nitride surface has physisorbed and chemisorbed ammonia. Surface chemistry and rheology are therefore, by far, the most important parameters for slip stability. These account for inter-particle forces in order to control dispersion in a suspension[18]. A detailed discussion of inter-particle potential theory is found in the work of Overbeek(1977) and Hunter(1981).

2.2 Silicon Nitride

The structure of silicon nitride was first evaluated by Turkdogan et al[7], who also established that silicon nitride could exist in two forms α and β. By alternative

interpretations of their powder x-ray diffraction data, Hardie and Jack[19] concluded that both forms are hexagonal with the c dimension of α-Si_3N_4 being approximately twice that of β-Si_3N_4 (Table II 1)

TABLE II 1: Unit cell data for silicon nitride (Å)

	α-Si_3N_4	β-Si_3N_4
a	7 749	7 609
c	5.617	2 911

Until recently, considerable disagreement has existed regarding the nature of the structure of α-Si_3N_4. Early structure determination by Hardie and Jack[19], Ruddlesden and Popper[20] seemed to be in agreement, but later Wild et al[21] proposed that α-Si_3N_4 was actually an oxynitride with O replacing N on some sites and with other N sites vacant. Kohatsu and McCauley[22] concluded that although oxygen might substitute for nitrogen in α-Si_3N_4, there is no structural requirement for its presence. The difference in structural dimension between the α and β phase is attributed to a change in the stacking sequence from ABCD. for α, to ABAB.. in β. These results were confirmed by Ruddlesden and Popper[20].

Both forms of silicon nitride are comprised of tetrahedra of four nitrogen atoms with a silicon atom located in the centre. A single layer of silicon nitride consists of six tetrahedra with each nitrogen shared between three adjacent tetrahedra (Figure 2.1) β-Si_3N_4 has a structure based on that of phenacite (Be_2SiO_4)[2].

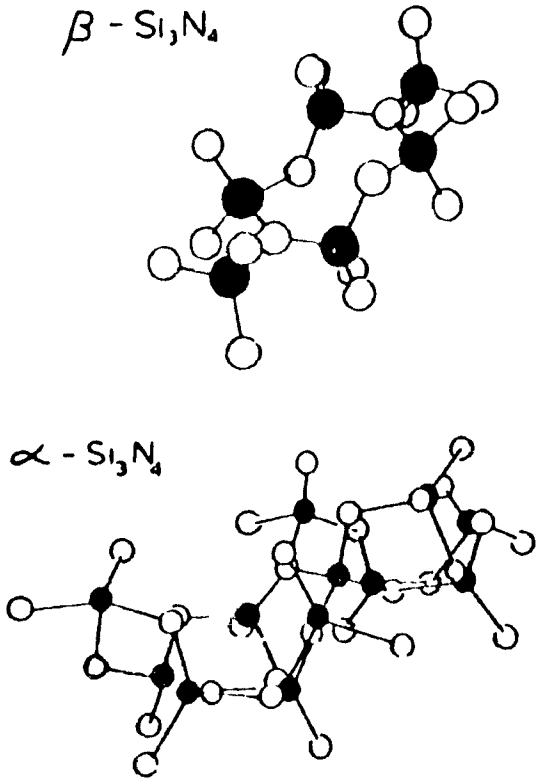

FIGURE 2.1: The two polymorphs of silicon nitride (solid spheres are Si)

The experimental evidence is that both the structures co-exist over a broad range of temperatures but that the β phase is more prevalent at higher temperatures (>1500°C). Madelung energy calculations indicate that β-Si_3N_4 should be more stable at room temperatures; the magnitude of this difference is however small, i.e. only 1.3% of the absolute value, so that the co-existence of the two phases is possible. Gruen[23] suggests that this energy difference is the explanation for the fact that the transformation of α to β is possible, whereas the reverse has not been observed. A

review[24] of the reaction mechanisms between silicon and nitrogen postulates that the formation of α-Si_3N_4 involves reaction of molecular nitrogen, whereas β-Si_3N_4 is formed by reaction of atomic nitrogen. The transformation from α to β phase can only be accomplished by a 180° rotation of the basal plane. A lattice reconstruction is required, which must involve solution of the α phase and precipitation of β. Such transformations are observed in the presence of a liquid phase and Jennings[24] suggests that the dissolution of silicon nitride must result in the formation of atomic nitrogen in the liquid, which leads to the transformation of the β-Si_3N_4 upon precipitation from that liquid.

In the following sections we shall explore the different powder consolidation methods used in the ceramic industry; and the silicon nitride sintering mechanism, involving the formation of a liquid phase to promote precipitation of dense β-Si_3N_4.

2.3 Green Forming in ceramics

Different processes used in the formation of ceramics may combine consolidation and densification in one step. These processes are expensive and have geometrical limitations.

Increased automation and mechanization in the rapidly growing electronic, electrical, aeronautical and other industries has made it necessary to maintain an economic production of ceramic components. In addition to this, realization that statistical quality control can be applied to ceramic processes with substantial economic advantage has led to a desire for better control of the process. A number of

powder consolidation methods such as slip casting, die-pressing and plastic forming not only provide the flexibility of complex shaping, but also allows a better control of the process itself. These methods have been successful, especially for traditional ceramics and are gaining importance in the field of advanced ceramic components. The green forming processes used in the consolidation of silicon nitride and relevant to this thesis are described in general below.

1. Slip casting

This process has been applied for many years for clay articles of complicated shapes and geometry. A slip or slurry is a fluid suspension of ceramic powder in a liquid. The process refers to filling a plaster mould with such a slip. The capillary forces due to the pores in the mould withdraw the liquid from the slip. This results in the formation of a consolidated layer, at the slip-mould interface, which increases in thickness with time. This process can be divided in two classes:

(a) Drain casting, in which slip is poured into the mould, left for a short time, and then drained out, leaving a thin shell against the inside of the mould; and *(b) Solid casting*, in which the mould is filled with a slip and left until it casts into a solid piece.

This method is used in large scale production of ceramic wares, as it is possible to reproduce very complicated shapes in plaster moulds. Schematics of drain casting and solid casting are shown in figures 2.2 and 2.3 respectively.

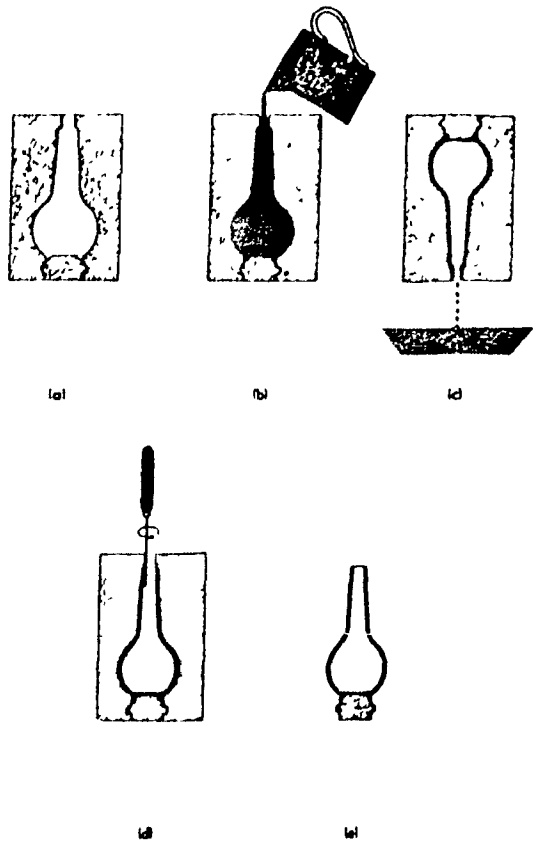

FIGURE 2.2: Drain casting

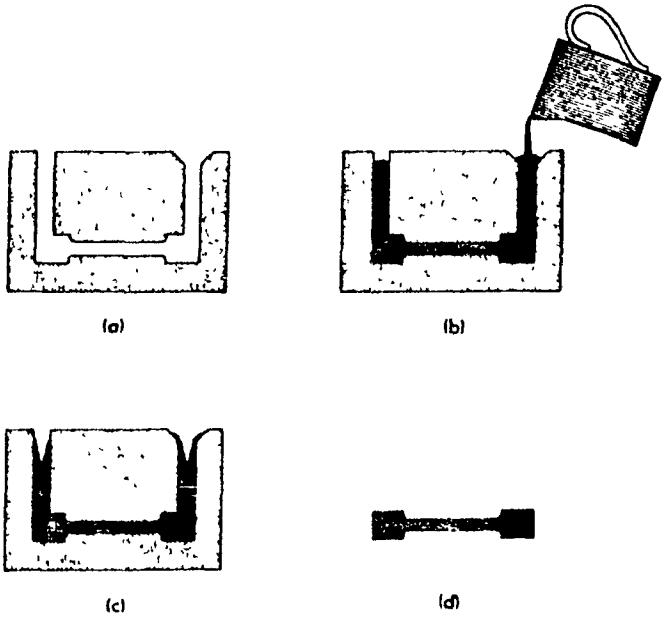

FIGURE 2.3: Solid casting

The slip consisting colloidal size particles, and suspended in a vehicle, usually water, contains certain species known as deflocculants These species may be ionic or polymers, and markedly affect viscosity and flow properties of the slip by controlling the "ion exchange" Ion exchange in slip casting is related to the charge sharing or transfer between suspended particles; suspending medium and the deflocculants This interaction leads to electrostatic forces and polymer adsorption (depending on the choice of deflocculant) and controls the settling of the particles and thus affecting the rheology of the slip This has been discussed extensively in books by Kelle[25], Overbeek[26] and Kruyt[27] Different properties are required for slips to be used for drain casting and solid casting Table II 2 lists desirable properties of casting slips

Slip casting process is used extensively in the ceramic industry, since the slip cast pieces have a higher and more uniform density than pressed ones The firing temperatures required to produce zero apparent porosity for slip cast ceramics is lower than for pressed ones[28].

A detailed discussion of properties of slips will be given in the next chapter

TABLE II.2: Properties of casting slips

Property	Drain casting	Solid casting
Low viscosity to drain	+	
Good stability on storing	+	+
Ability to drain cleanly	+	
Low rate of settling on standing	+	+
Quick mould release	+	+
Fast casting rate	+	
Low shrinkage in cast	+	+
High green strength	+	
Low degree of thixotropy	+	
High degree of thixotropy		+

2. Dry pressing

Dry pressing as applied to the production of technical ceramics, comprises the compacting of dry, granulated ceramic powder in a die under high pressure. The moisture content of the dry granulated powder can range between 0-4%, and the granules are free flowing and non-plastic The powder is pre-mixed with binders and lubricants to ease compaction and quick mould release. This method has the advantage that the process can be fully automated, however only simple die constructions can be used. Figure 2.4 shows schematic of a simple dry press.

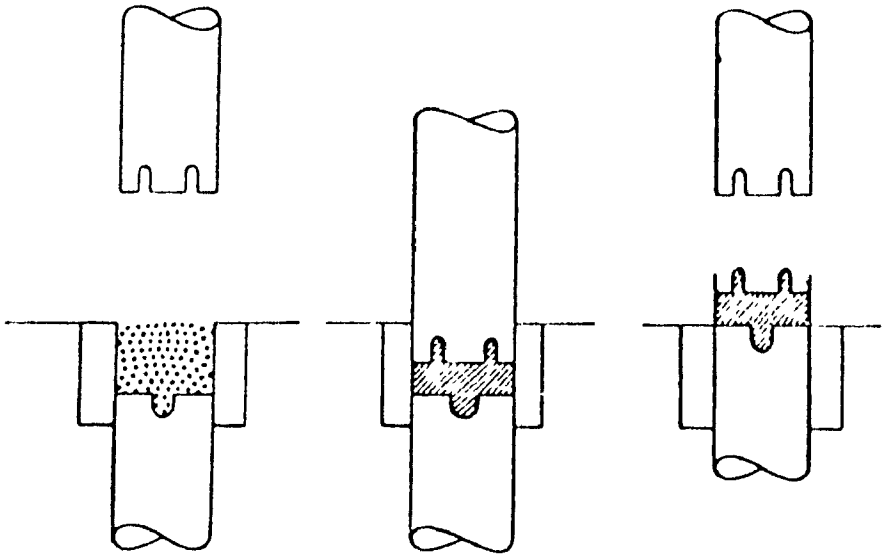

FIGURE 2.4: Dry Press

Pressing is used for large scale production of refractories and tiles. The linear shrinkage of dry pressed articles upon sintering is between 12-15% with dimensional tolerances upto 2%. This process, however, has a disadvantage of differential shrinkage, due to improper mould filling, and leads to non-uniformity in density, warpage and cracking. Pressure differential due to wall friction leads to uneven green density and therefore shrinkage, and is especially pronounced in long shapes with a small area of cross-section Length to diameter ratios greater than unity can cause problems and selection of binders and lubricants, becomes more critical This problem is overcome by pressing the powder equally from all sides using isostatic pressing.

3. Isostatic pressing

In this process the dry powder is filled in a rubber mould and inserted in a liquid medium, and subjected to high pressure of upto 50,000 psi Compression takes place from all directions and wall friction is eliminated. A schematic in figure 2.5 shows a typical isostatic pressing apparatus. Glycerine, hydraulic oil, water or other non-compressible fluids are used to maintain high pressures. The disadvantages of isostatic pressing are limited production rates and difficulties in achieving close tolerances and good surface finish. A typical application of this process is in the manufacture of alumina spark plugs.

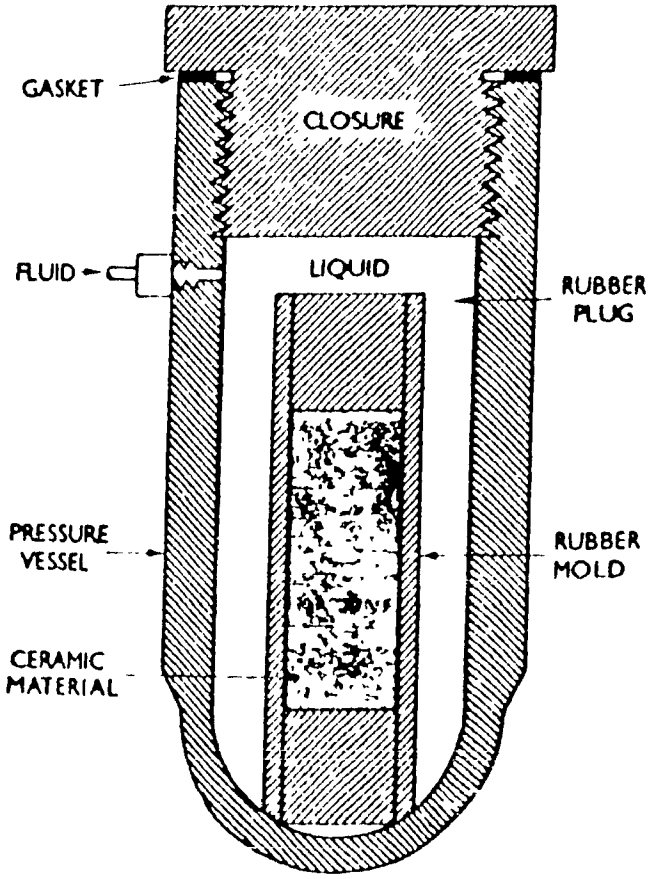

FIGURE 2.5: Schematic of an isostatic press

Few other processes like extrusion, injection moulding and tape casting are used for consolidating ceramic powders. The consolidated powders contain moisture (depending on the processing route), which must be removed before they are subjected to high temperature for sintering. Usually a burn out step is introduced to remove the moisture and other organic impurities entrained during the processing Subsequently, the green ceramics are sintered to form dense components as described below

2.4 Sintering Mechanisms

1. Solid state sintering

The green compacted powder as described above contain 35-60% porosity; whether they are obtained from slip casting or pressing. This porosity must be removed in order to obtain physical properties close to that of a theoretically dense material The changes that occur during sintering are mainly concerned with the reduction in porosity which also leads to alterations in the microstructure. This change is initiated by two fundamental criteria which should be met, i e

i. material transport mechanism; and

ii. source of energy to activate this mechanism.

Various routes are possible by which material transport can be achieved Material transport may take place by surface or lattice diffusion, by vapour transport or by boundary diffusion in ways which always increase the bonding between particles leading to shrinkage i e a decrease in the particle-particle separation distance x (Figure 2 6), and elimination of porosity For all, or any of these changes the capillary driving force depends on the radius of curvature of the neck which forms between particles Various material transport routes have been identified by Ashby[29] and are

shown in figure 2.6.

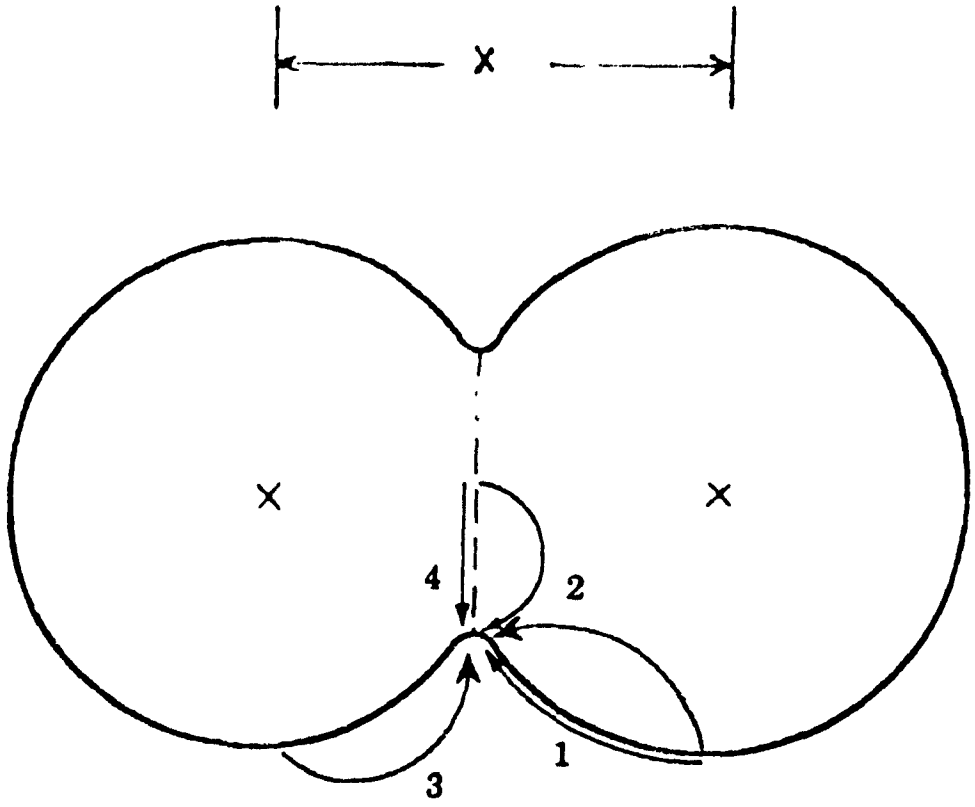

FIGURE 2.6 Paths for material transport during sintering

1. Surface diffusion, 2. Bulk diffusion,
3. Vapour diffusion & 4. Grain boundary diffusion.

Each path involves the transport of material from a source at the grain boundary to a sink which is the neck region. The smaller the particles, the greater is the difference in the curvatures between the particle and the neck, and the greater is the driving force for sintering. Material transport paths 2 and 4 lead to elimination of porosity and shrinkage; and routes 1 and 3 result in pore closure.

2. Liquid phase sintering

Silicon nitride ceramics are highly covalent and therefore, exhibit a very low diffusion coefficient, even at high temperatures of 1400°C. Self diffusion is limited since the interatomic bonds are short, strong and highly directional. Greskovich and Rosolowski[30] have shown that it is practically impossible to achieve densification of pure silicon nitride without the addition of sintering aids. Some self diffusion coefficients of various species[31] are given in Table II.

TABLE II.3: Self diffusion coefficients for Al_2O_3 and Si_3N_4

Material	Diffusion Species	Temperature (°C)	Diffusion Coefficient (cm^2/sec)
Al_2O_3	Al	1500	$2\ 10^{-12}$
	O	1400	$5\ 10^{-13}$
α-Si_3N_4	Si	1400	$8\ 10^{-12}$
	N	1400	$1\ 10^{-19}$

The commercially viable process for forming high purity, high density sintered silicon nitride components is by the use of additives which form a viscous grain boundary, or liquid phase, at sintering temperatures. Thus complete densification to β-Si_3N_4 is possible by using ultrafine starting powders, consolidation, increasing sintering temperature (preferably with a slight N_2 overpressure), and addition of sintering aids to form a liquid phase.

Liquid phase sintering, as the name implies, requires the presence of liquid phase during sintering. In this the liquid acts as a means of material transport. The

wetting of the particles by the viscous phase, leads to substantial capillary pressure. The capillary pressure aids densification by particle re-arrangement (through a creep process) and increased particle-particle contact pressure. This further increases the rate of material dissolution and transport and also leads to reprecipitation[32] of the dissolved material This is mainly due to differences in chemical potential between the neck regions and the remainder of the compact as shown in figure 2.7.

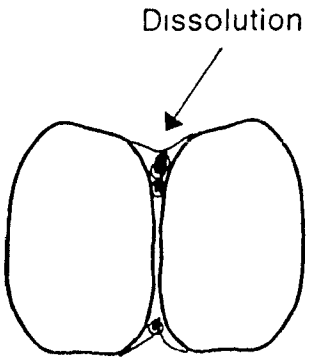

FIGURE 2.7: Dissolution of particles leading to shrinkage

In the case of α-silicon nitride, the sintering additives (e.g, Y_2O_3 and Al_2O_3) react with oxygen containing phases like SiO_2, or the oxynitride , which are present on the surface of silicon nitride powders to form a liquid phase. The amount of this oxynitride liquid phase and its viscosity, initiate rearrangement , induced by capillary forces This is followed by the solubility of silicon nitride particles at contact points

with the liquid phase.

Figure 2.8 shows the different steps typical of liquid phase sintering leading to the formation of dense β-Si_3N_4.

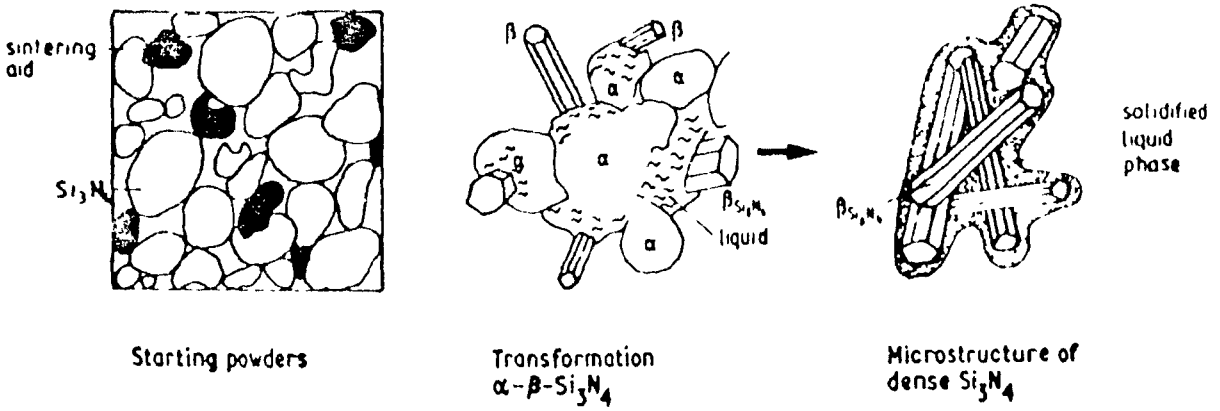

FIGURE 2.8: α to β transformation

The Si-Al-O-N system

Jack et al[10] and Oyama et al[11] in separate investigations in the UK and Japan, respectively, discovered the Si-Al-O-N system (Figure 2.9) In this system, combinations of additives of Al_2O_3, SiO_2, and AlN to silicon nitride can lead to complete densification. This is a four component system and can be represented by regular tetrahedra, each verticies representing one atom of the respective element The composition of any mixture within the tetrahedra can be expressed as a reciprocal

salt pair

$$\frac{3\,[Al]}{4\,[Si] + 3\,[Al]}$$

and

$$\frac{2\,[O]}{3\,[N] + 2\,[O]}$$

When these ratios (M/X) are plotted against each other a square (Figure 2.9) is formed. Each corner representing the molar equivalent, with respect to 1 mol of Si_3N_4. All possible phases that are formed, will lie within the square, with normal valencies. The phase diagram in Figure 2.9 is stable at 1700°C. O', β', X are various phases with different composition and unit cell dimensions.

O' sialon phase, is a combination of silicon oxynitride and alumina, extending along the 2M/3X line. This gives Si_2N_2O type structure.

β' *sialon* is generally along the 3M/4X line and has a hexagonal type structure. This sialon has lower thermal expansion coefficient, and higher oxidation resistance than β-Si_3N_4. This is the most important phase due to its excellent high temperature properties.

The *X sialon* has a typical composition of $3Al_2O_3.2Si_3N_4$. This phase has not been characterized in detail, and occurs in the production of β'.

Other phases closer to the bottom right corner are different polytypes of AlN. These are 15R, 8H, 12H, 21R, 27R and 2H. Their nomenclature, defined by Ramsdell notation, is primarily based on their varying unit cell dimensions, and specific M/X ratio.

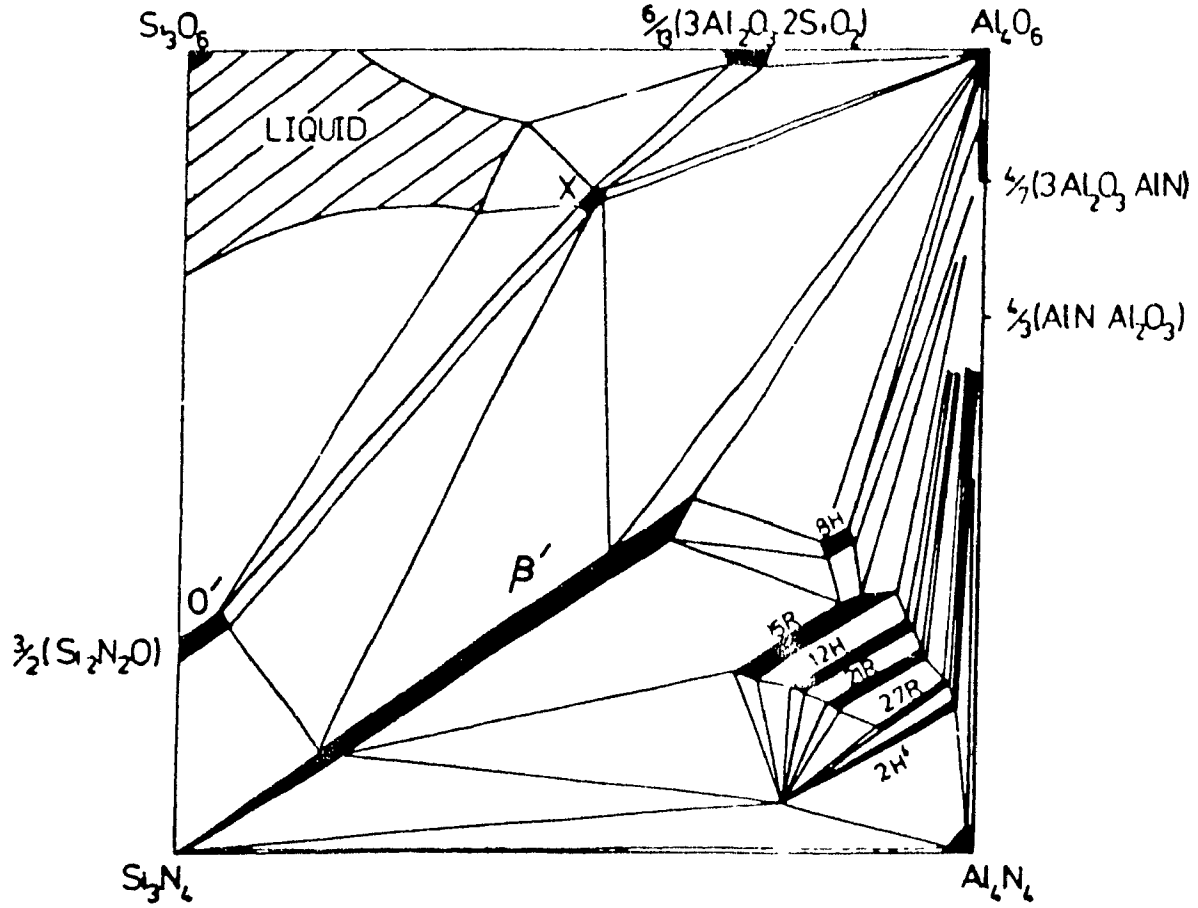

FIGURE 2.9· The Si-Al-O-N system (1700°C)

The sialon system discussed so far is a result of hot-pressing experiments performed at Newcastle The limitations of hot-pressing have already been described earlier For making sialons through pressureless sintering it is necessary to introduce metal oxides and nitrides Many additives have been tried in an atempt to achieve complete densification at lower temperatures. Jack et al[10] have described additives like MgO, Y_2O_3, HfO_2, BeO_2 etc. for enhancing liquid formation and material transport during the densification of silicon nitride Deeley[33] found that complete densification of silicon nitride can can be achieved by the addition of small amounts of MgO.

These additives react to form a liquid phase during sintering. One disadvantage in using the liquid phase, is the limitation to the high temperature properties of these materials This is due to the formation of low melting glassy phase (see Figure 2.7) Addition of 1-3 wt% of Y_2O_3 for the formation of β' phase results in 2-6 vol% of glass in the microstructure[33] This glassy phase has an approximate element proportion in the ratio of Si:Al:Y = 2·2·1 The amount of yttrium addition is limited since the oxidation resistance of β' sialon decreases with increasing yttria content This is due to the fact that the excess yttria remains as oxide at the intergranular phase boundary. The Oxygen diffusion is more rapid through the yttria-aluminium amorphous phase than the amorphous SiO_2 phase, which surrounds the β' Si_3N_4 The addition of yttria is therefore limited to about 4-5 wt% The total additive content is therefore very critical, since glassy phase is detremental to high temperature properties of β' Si_3N_4.

As in the case of present work, wet processing always introduces SiO_2 due to the hydrolysis of silicon nitride This requires minimum contact time of water with

silicon nitride and the additives This has been realized by the use of a high speed attrition mill, as shown in Chapter IV

CHAPTER III SLIP CASTING

Slip casting in ceramic systems takes two general forms; drain casting and solid casting. A good casting operation requires the following[34]:

1. Firmness of the cast under moderate stresses.
2. Sufficient plasticity to permit easy release of the cast from the mould.

A satisfactory slip which meets the above criteria should have[35]:

(i) Low enough viscosity to flow into the mould easily.

(ii) No settling of the solids

(iii) Fairly, but not too, rapid casting rate.

(iv) Low drying shrinkage.

(v) High green strength after casting.

(vi) Ability to drain cleanly.

The basic factors which control casting slip performances are ion exchange capacity and the presence of colloids[36]. These parameters will be discussed further in the following sections.

In order to understand the usefulness of slip casting it is customary to know its rate limiting step for kinetics[37] of material transport while casting. As the cast thickness increases the overall rate of material transport decreases due to increased permeation distance (Figure 3.1).

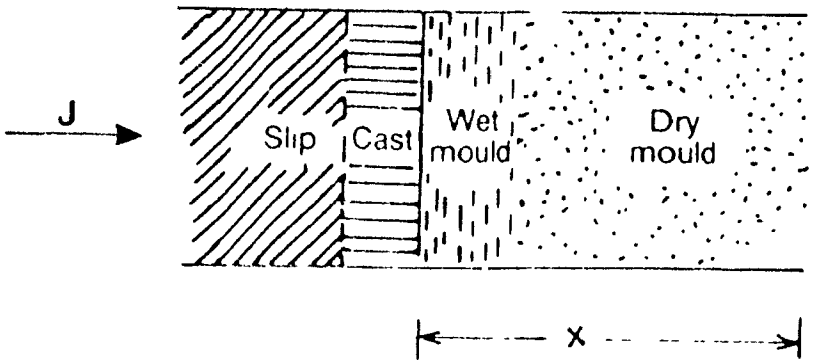

FIGURE 3.1: Water extraction by capillary action of plaster

Assuming planar (unidirectional) deposition, the flux equation for water can be written as

$$J = -K\frac{(dP)}{(dx)}$$

(III-1)

Where J is the flux, K is a material constant, dP is the differential capillary pressure across the plaster mould and x is the thickness of plaster

This equation takes the general parabolic form:

$$x = (K't)^{1/2} \qquad \text{(III-2)}$$

(In equation III-2, K' is a new constant which which takes into account cake build up at the slurry/plaster interface) This equation states that the volume of water removed from the slip is a linear function of the square root of time The casting rate is therefore time dependent, and depends on complicated interaction between the mould, cast and slip This interaction is also dependent on the nature and amount of deflocculants which control the slip stability, and assumes an incompressible cast layer An incompressible cake is one with constant porosity throughout. Tiller and Tsai[38] have extended this model for compressible layers.

The role of deflocculants in a slip system is of extreme importance, since it affects the particle interaction in suspension This interaction, typical of colloidal suspensions is a function of electrostatic forces and/or steric hinderance.

3.1 Colloidal suspensions

Particles having linear dimensions between 10nm and 1000nm are considered to be colloids The particle size distribution of a ceramic mix can be expressed graphically in terms of weight or volume percentages of particles finer or coarser than the particle size[39] As the particle size becomes smaller, certain size related physical properties change These are increase in specific surface area, increase in diffusion rate, reduction in sedimentation velocities and increase in coagulation rates. At a linear dimension region of 0.2 to 0 5 μm, rate of change of the above properties is drastic[39]

Small particles, well within the colloidal range exhibit good densification behaviour[4,40] In case of α-Si_3N_4 as a starting material the finer the particles, for a

given oxygen content, the higher the resulting sintered densities[10] Thus in order to make dense β-Si_3N_4 the starting α powders must be very small The oxygen content, however, increases with the specific surface area Due to small size of the particles they exhibit characterstic colloidal properties

(a) Brownian Motion.

Colloidal suspensions when subjected to dark field illumination of a ultramicroscope exhibit random movement of the particles. This random kinetic motion causes change in particle velocity and direction. The transitional diffusion can be measured by treating this brownian motion as a three dimensional random walk

(b) van der waals forces·

These are short range, weak attractive forces between individual atoms or molecules. In ceramic slips containing polyelectrolytes as deflocculating agents, presence of van der waals forces can result in both constructive or destructive attractive forces[41] At approximately 1μm, van der waals adhesion forces acting on particles are about six orders of msgnitude greater than the gravitational forces[12]

(c) Charge effects

Charge effects are almost always present in a colloidal suspension α-Si_3N_4 powder when left in water for an extended period of time renders a basic pH, indicating slight negative charge on the surface The addition of electrolytes or surface active polmer ions in the form of deflocculants, can greatly reduce coagulationn and settling rates These aditives, give an apparent charge to the slip by attaching themselves to the particles, or by inducing a charge by surrounding the particle in close vicinity A thin electrostatic layer coats each particle depending on the nature of the charge of the parent particle, that of the medium and the affinity of the particle

towards ionic groups This thin film then interacts with other particles and controls agglomeration and settling kinetics

3.2 Ineraction of colloid particles

Fine ceramic powders have a high surface area and a low solubility, and surface chemistry controls their charging behaviour. Surface of a particle may become charged by (1) the desorption of ions at the surface of the particles,
(2) chemical reaction between the surface and the liquid medium changing the composition of the surface, and (3) preferrential adsorption of specific additive groups from the liquid medium

For oxides with a hydrated surface, the surface chemistry in water is dominated by the following reactions.

$$MOH_2^{+}{}_{(surface)} = MOH_{(surface)} + H^{+}{}_{(solution)} \qquad \text{(III-3)}$$

and

$$MOH_{(surface)} = MO^{-}{}_{(surface)} + H^{+}{}_{(solution)} \qquad \text{(III-4)}$$

Here M, represents a metal ion such as Ba^{+2}, Al^{+3}, Si^{+4}, Ti^{+4} etc. The point of zero charge (PZC) of the surface may be defined as ·

$$PZC = \frac{pK_1 + pK_2}{2} \qquad \text{(III-5)}$$

PZC indicates the average acid-base character of the surface.

pK_1 and pK_2 are rate constants for equations III-3 and III-4 respectively

Ions and polar molecules in the solution surrounding a particle will respond to the charge surface Coulombic forces will repel like charged ions and attract polar

molecules, thus attraction may be ionic or may be initiated by polymer bridging, depending on the nature of the liquid medium If a repulsive force of sufficient magnitude exists between particles, the suspension is stable; however if the repulsive forces are absent or revert to attractive forces the stability is lost and the system coagulates.

The electrical double layer

Colloidal particles in aqueous medium possess an electrical charge The suspension, however, must be electrically neutral and a difference in electrical potential between the surface and bulk solution is affected as shown in figure 3 2 The potential gradient is not sharp, because the thermal vibration of the molecules of the liquid medium causes the diffusion of the counterions Counterions are ions of the opposite charge with respect to the species at the surface of the particle However most of the counterions will be centred around the charged particle, forming a so called diffuse double layer or the electrical double layer around it[13].

When two such particles approach each other, their double layers start to overlap and, if the charges are of different species, interaction leads to repulsion (figure 3.3), and the suspension is stable This electrostatically stable suspension will form a good slip for casting The magnitude of repulsion depends on the zeta potential, ξ(figure 3.4). The ξ potential is the potential difference developed between the tightly adhered layer due to adsorbed ions, and the dispersion medium The ξ potential is related to the surface charge of the particle, Q; and the diffuse double layer thickness, for spherical particles, by the following relation

$$\xi = \frac{Q}{\epsilon_r(\frac{1}{r} - \frac{1}{R})}$$

(III-6)

where ϵ_r = dielectric constant

r = radius of the particle

R = radius of the particle plus the diffuse double layer.

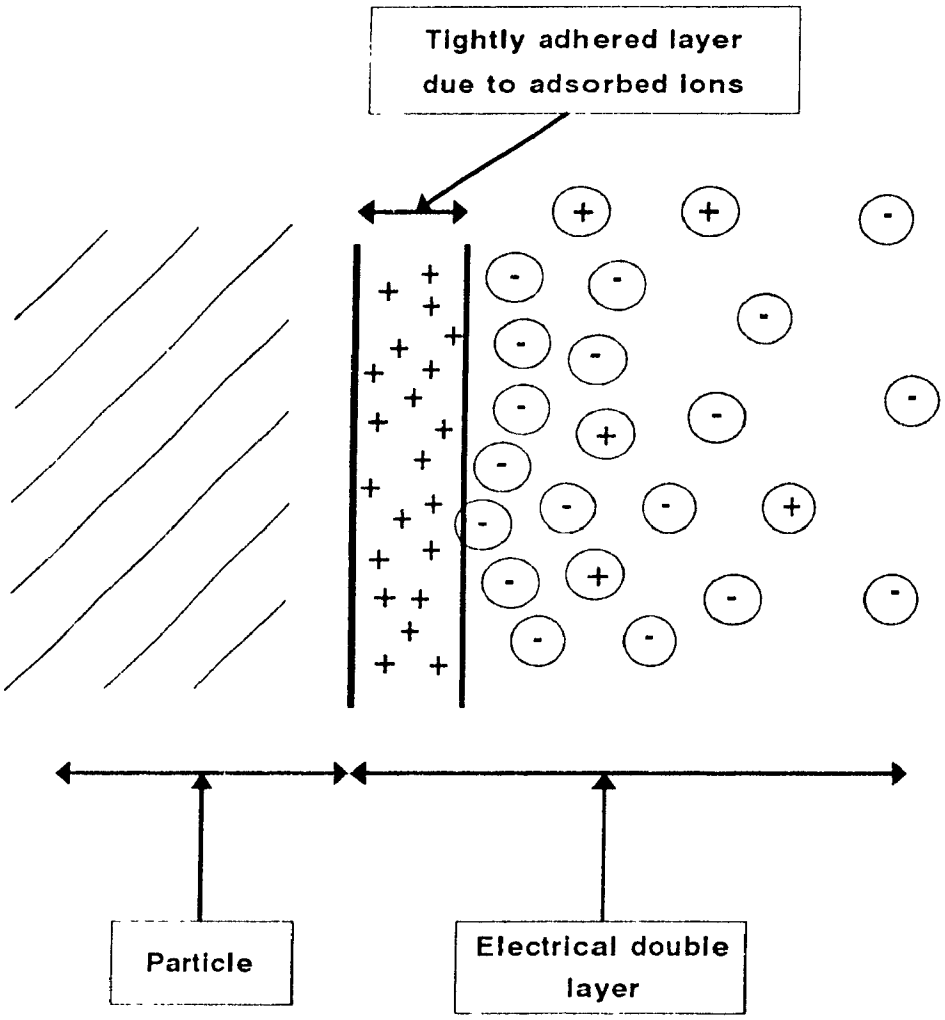

FIGURE 3.2: The electrical double layer model

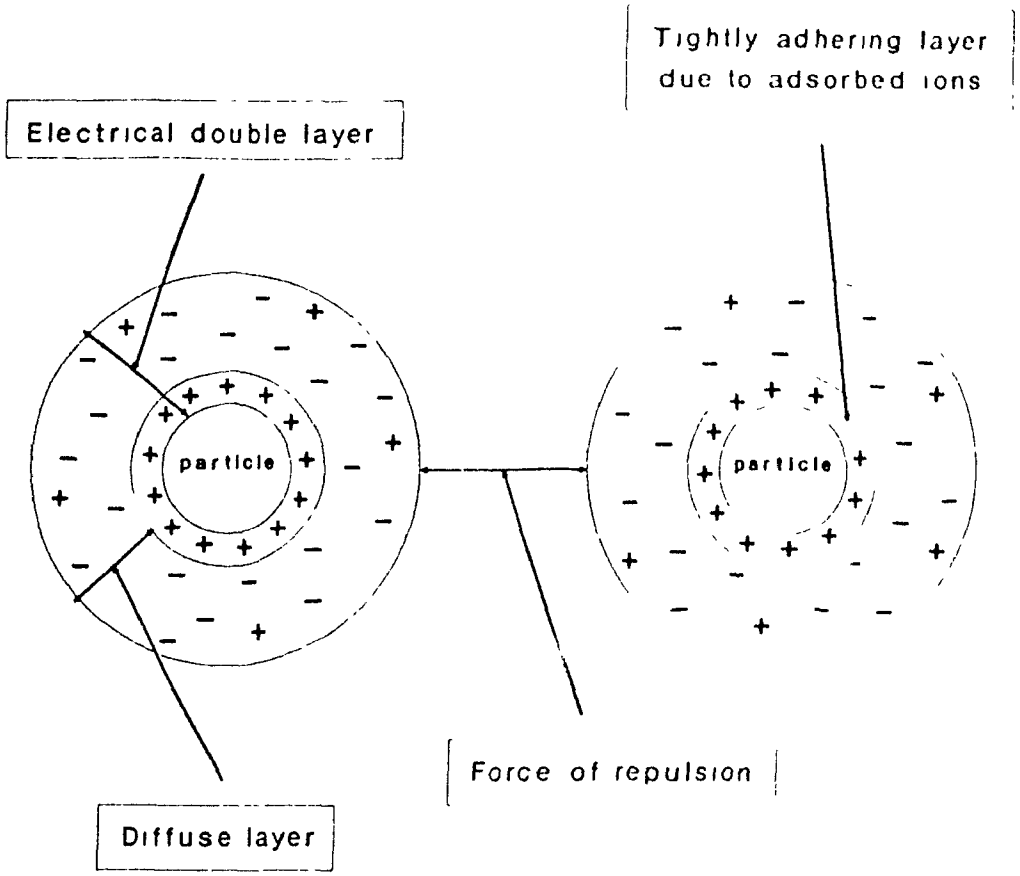

FIGURE 3.3: Electrostatic repulsion due to diffuse double layer

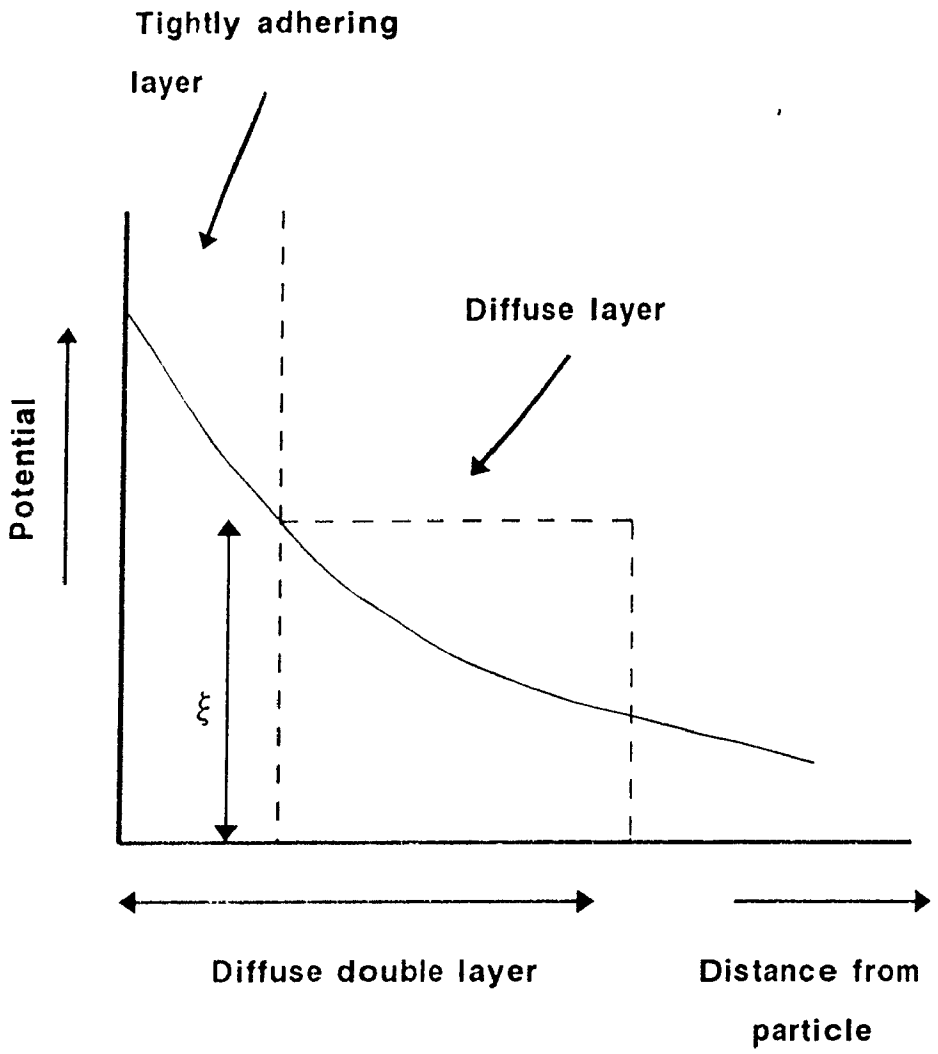

FIGURE 3.4: The zeta potential, ξ

By measurements of electrophoretic mobility, the zeta potential of charged particles can be estimated. The zeta potential is related to the electrophoretic mobility by the following relation[50].

$$u = \frac{2\epsilon\xi}{(3\eta)f_1(\kappa r)} \qquad \text{(III-7)}$$

where u = electrophoretic mobility

ϵ = permittivity

ξ = zeta potential

η = viscosity of the fluid

$f_1(\kappa r)$ = constant for spherical particles, and is expressed by the equation

$$f_1(\kappa r) = \frac{3}{2} - \frac{9}{2\kappa r} + \frac{75}{2\kappa^2 r^2} - \frac{330}{\kappa^3 r^3} \qquad \text{(for } \kappa r > 1\text{)} \qquad \text{(III-7)}$$

Equation III-6 is valid for zeta potentials less than 25mV At higher zeta potentials and mixed electrolytes the equation is not valid and it is more accurate to report the electrophoretic mobilities

Polymer-colloid interaction

The electrostatic double layer is characteristic of ionic interactions initiated by the addition of electrolytes. Addition of polymers, for stability, to colloids also leads to a similar interaction Polymers may adsorb onto colloid particles, or may break up into smaller free moving chains in the medium (figure 3.5)

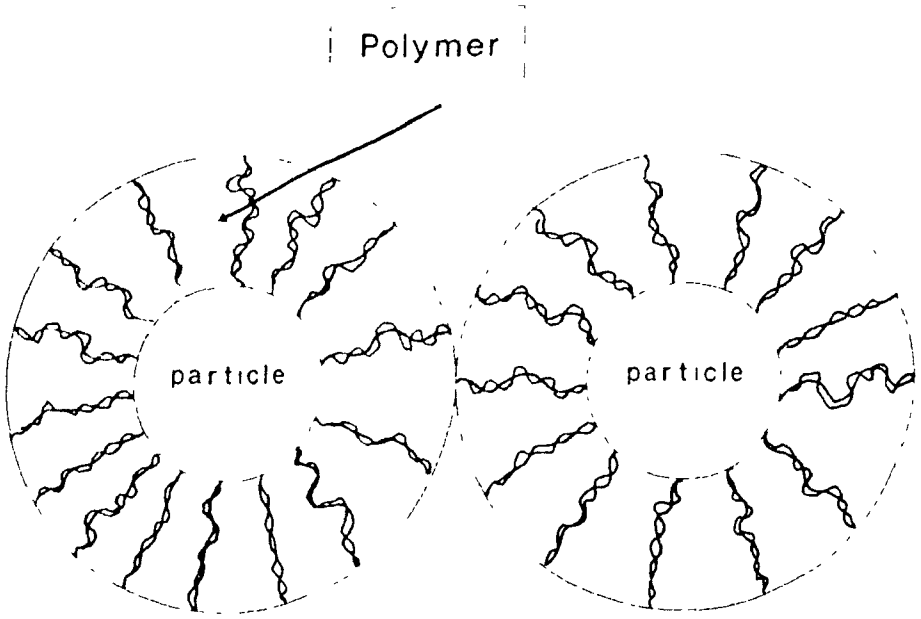

FIGURE 3.5: Polymer adsorbed on the particle

Polymer based electrolytes used for colloidal processing can be anionic or cationic. When a polymer is added to the system, the free moving and charged chains get adsorbed onto the particles. This can lead to repulsion when two polymer adsorbed particles approach one another (steric repulsion, adsorption stabilization). When an excess of polymer is added to the system, it can lead to attractive forces by polymer bridging (steric attraction, adsorption flocculation).

In some cases polymers may have no affinity to the surface of the particle and remain free in the solution. Thus when two polymer coated particles approach each other, there is repulsion at large distances, due to the fact that free polymers are squeezed out of the gap There is however attraction at smaller distances due to osmotic pressure differences between the gap and the solution[11](figure 3 6) The choice and amount of commercially available polyionic dispersants for slip casting Si_3N_4 is one of the main objects of this thesis

When two polymer coated surfaces approach each other, the density and configuration of the polymer segments changes This leads to a change in the enthalpy and increases the entropy of the system resulting in attractive or repulsive forces

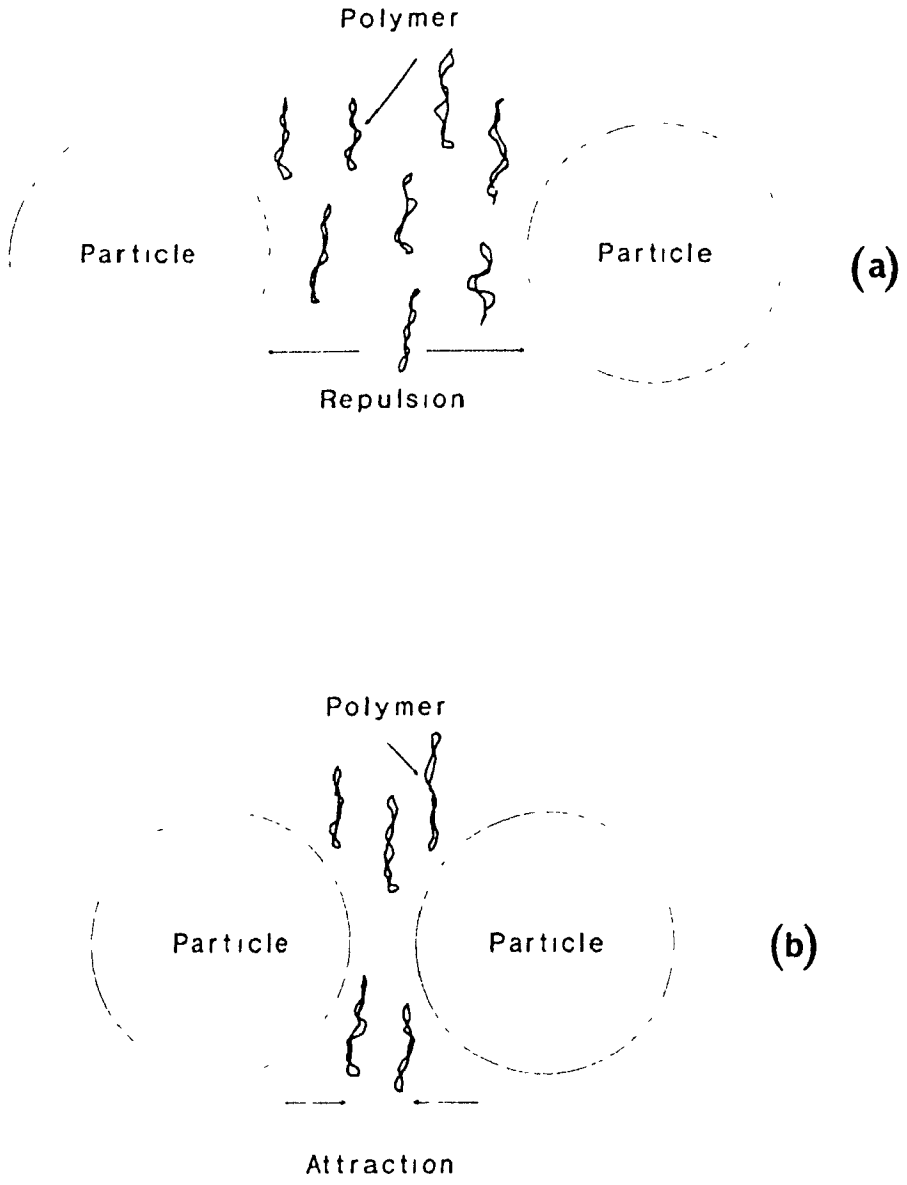

FIGURE 3.6: Polymer having no affinity to the surface of the particle (a) repulsion at large distances, (b) Attraction at smaller distances

3.3 Rheology

Rheology in ceramic systems is concerned mainly with the deformation of the cohesive bodies such as slips and plastic masses. Slip casting involves flow in the mixing, pumping, pouring and draining of the slip. Some slips are known to thicken somewhat upon standing. Therefore the draining of the excess slip from the mould must be preceded by deformation of the gelled structure. This is particularly important in drain casting.

The deformation of substances can be divided in two groups:

(a) Spontaneously reversible deformation, or elasticity and (b) an irreversible deformation, called flow. The deformation, in general, can change considerably with different solid loadings, particle sizes and size distributions. Viscosity measurements are important for quality control and is an important aspect in process engineering, especially in industries involved in large scale production of slip cast ceramic articles. Viscosity, η, is defined as the ratio of the applied shear stress τ, to the shear rate D. Fluids can be classified into four categories:

1. Newtonian (A)
2. Pseudoplastic (B)
3. Dilatant (C), and
4. Plastic

The flow behaviour is shown in figure 3.7. For Newtonian fluids the viscosity is a material constant and

$$\tau = \eta_l D \qquad \text{(III-7)}$$

where: η_l is the coefficient of viscosity

D is the shear rate

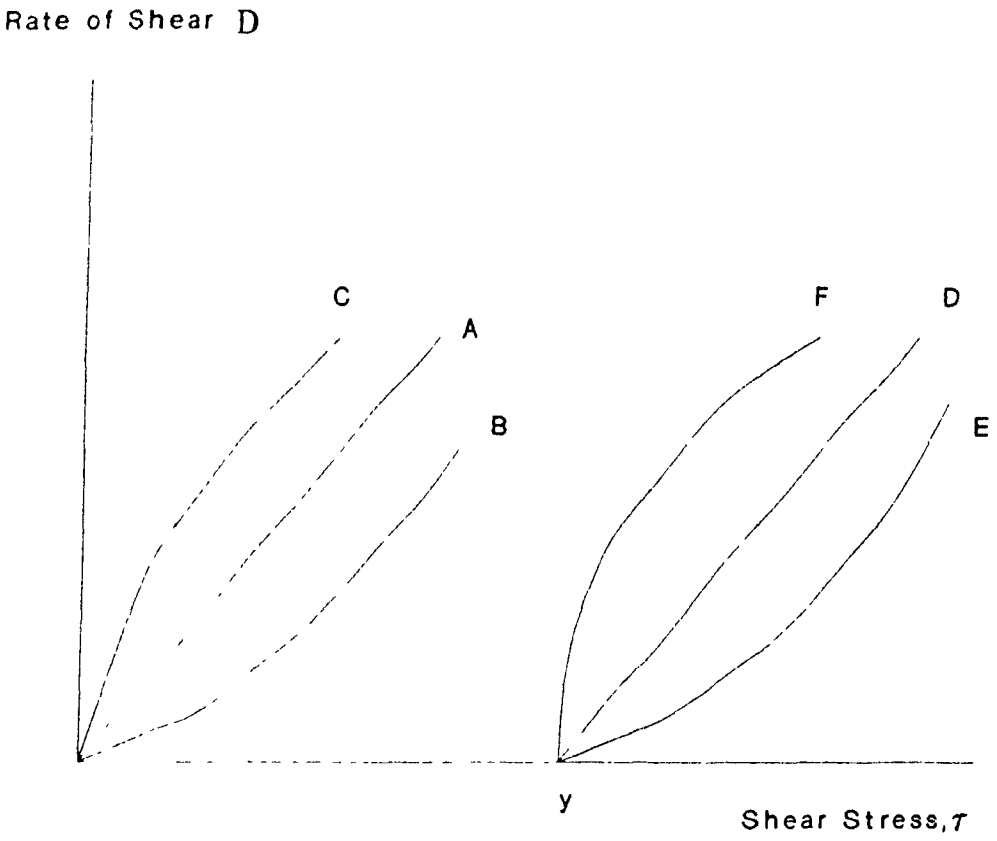

FIGURE 3 7: Flow curves for different rheological suspensions. y=yield value A:Newtonian Fluid, B: Pseudoplastic, C: Dilatant, D: Newtonian with yield value E: Pseudoplastic with yield value, F: Dilatant with yield value.

When a suspension contains large molecules and anisometric particles, laminar flow partially orients the particles. This orientation reduces resistance to shear and the viscosity decreases with increasing shear rate This behaviour is called pseudoplastic or shear thinning. In cases of concentrated deflocculated slurries, particle displacement may reduce interference at low flow rates However at high shear rates the particle interference increases thus raising the viscosity This behaviour is known as dilatant or shear thickening Suspensions showing yield values are classified as plastic Curves D, E and F in figure 3 7 represent plastic flow.
In these cases when the shear stress greater than the yield value is applied, the suspension will start to flow and will show characteristics of A, B or C

3.4 Colloidal processing in ceramic systems

For the reliability of ceramics, methodologies must be developed to ensure, with a high probability, that heterogenities are eliminated from starting powders, and these should not be reintroduced in subsequent processing steps

The two major aspects of colloidal processing require repulsive and attractive interparticle forces Repulsive forces, required to break weak agglomerates, can be generated with the addition of electrolytes

A major issue for exploiting colloidal processing in ceramic systems is to directly form powder compacts from the slurry state. Slip casting and tape casting are two major fabrication processes which can be directly used with colloidally prepared powders The concept of colloidal methodology has been developed partly due to cost economics, and partly due to the need to eliminate hetrogenities that produce flaws in structural ceramics[45].

Colloidal methodology has been successfully adapted for alumina based ceramics. Polyacrylic acid has been used to disperse alumina. In addition, surface modification of other oxide and non-oxide ceramics with Al-alkoxide to create alumina-like surface has been suggested by Cesarano et al[45] In case of silicon nitride, a thorough and detailed study of the colloidal and rheological properties is required before any surface modifications can be proposed This work is primarily an attempt to investigate such properties for viable use of slip casting for large scale production of silicon nitride components

CHAPTER IV EXPERIMENTAL PROCEDURE

4.1 Raw Materials

The silicon nitride powder used for slip casting was obtained from UBE Industries Ltd. The powder, grade SN E-10, had manufacturers specifications as shown in Table IV.I. It is a fine grained, high purity powder previously been shown to have good densification characteristics.

Table IV.I : Manufacturers specifications of UBE silicon nitride powder used.

Grade	**SN-E10**
N (wt%)	>38 0
O (wt%)	1 45
Cl (ppm)	<100
Fe (ppm)	<100
Ca (ppm)	<50
Al (ppm)	<50
Crystallinity (wt%)	>99 5
$\beta/(\alpha+\beta)$	<5
SSA (m^2/g)	12.4

The sintering additives used for densification were Al_2O_3, AlN and Y_2O_3.

The gravimetric composition of the powder mixture prior to sintering is shown in Table IV II This had previously been determined as a suitable composition, giving good sintered density and strength values.

Table IV.II Gravimetric ratio of powder mix

Powder	Manufacturer	Weight %
Si_3N_4	SNE-10, UBE Industries	87.97
Al_2O_3	A 16SG Alcoa, USA	4.72
Y_2O_3	5603, Molycorp, USA	4.65
AlN	Grade C, H.C Starck, West Germany	2.66

The theoretical sintered density of the above composition was calculated to be 3.28g/cm^3.

Two commercial polymer dispersants were used to deflocculate the powders prior to slip casting, Darvan C and Darvan 821A. Darvan C® is an aqueous solution of ammonium salt of a polyelectrolyte; and Darvan 821A® is an aqueous solution of ammonium polyelectrolyte Room temperature properties of both the dispersants are given in Table IV III. Preliminary viscosity measurements with another

---

® R.T Vanderbilt Co, Norwalk, CT, USA

commercial dispersant ET-85 (Ester) showed similar behaviour, though Darvan C and Darvan 821A showed minimum viscosities.

Table IV.III Room temperature properties of Darvan C and Darvan 821A.*

Physical property	**Darvan C**	**Darvan 821 A**
Density at 25°C	1.11±0.02 Mg/m^3	1.25 Mg/m^3
Percent ash	0.04	0 01
Percent solids	25±1	40
pH	7 5-9.0	7 0
Viscosity at 25°C (undiluted)	75 cps	50 cps
Solubility charecteristics	Completely soluble in water systems	Completely soluble in water systems
Molecular weight	14,000-20,000	2,500-3,000

Solutions of both Darvan C and Darvan 821A were diluted in distilled water to reveal concentrations in the range of 0.2-2 volume %.

---

* Based on information given by the manufacturer

4.2 Processing

Two processing methods namely slip casting (wet processing) and die pressing (dry processing) were used to make samples for modulus of rupture measurements. Slip casting was investigated in detail with a view to optimizing slip conditions.

4.2.1 Slip Casting

A flow diagram for the process used to form slip cast samples is shown in Figure 4.1.

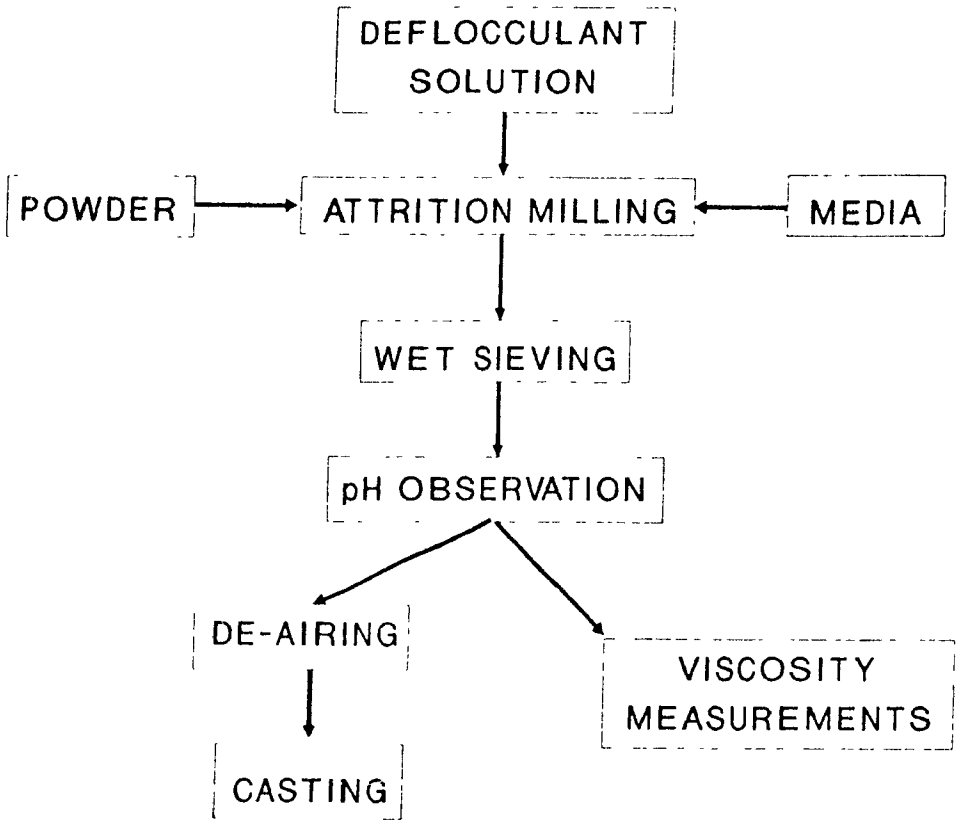

FIGURE 4.1: Flow diagram of Slip casting

(A) Slip preparation

The Si_3N_4 powder, and the additives were mixed in the wet state. Varying concentrations of the prepared dispersant solution were used as the suspending liquid This mixture was attrition milled for 30 minutes, at a speed of 200 rpm Hot pressed silicon nitride media, with a diameter of ~5mm, was used in equal weight proportion to that of the powder mix. The ratio of weight of powder mix, to the amount of dispersant solution used, i.e. the solids loading by weight, was varied from 1 1 to 2 5 1 in steps of 0.5. The slip obtained after attrition milling was poured through 212μm sieve into a beaker to separate the media After measuring the pH, a portion of the slip, (approximately 15ml) was used for viscosity experiments (Section 4 2 1 B), and the remainder was used for casting in plaster moulds (Section 4 2 1 D) The pH measurements were done using a hand held Cole Parmer pH meter using HI 1211S electrode.

(B) Viscosity Measurements

The viscosities of silicon nitride slurries with varying amounts of deflocculants and solids loading were measured using Contraves Rheomat 115 which employs the "cup and bob" technique.

The Rheomat 115 is a rotational viscometer, operating according to the Searle's principle.

Viscosities were calculated using the following equation

$$\eta = T/N \cdot T_{rep}/U_{rep} \qquad \text{(IV-1)}$$

η = viscosity in mPa.s; T = torque; N = rpm;

T_{rep} = 1 141, constant for DIN 125 system;

U_{rp} = 1 291, constant for DIN 125 system

The desired rpm was programmed and, using the SE 790 x-y plotter, torque was measured (on y-axis) as a function of rpm (on x-axis). Viscosities were measured at two different rotational speeds, 50rpm and 500rpm, to observe any shear thickening or shear thinning behaviour.

(C) Mould preparation

Commercial grade potters' plaster was used for making moulds. For every 100g of plaster, 80ml of distilled water were added, as moulds made with this plaster:water ratio have been shown to exhibit maximum water removal capacity[16]. The water was added to the plaster and allowed to stand for 1 minute. Using a small submerged propeller blade the mixture was rapidly stirred for 3 minutes and then quickly poured in cardboard boxes, previously greased with vaseline. Blocks of plaster were cast with approximate dimensions 15cm × 15cm × 3cm when dry. These were then machined to give final mould as shown in figure 4.2. Using this type of mould, samples in the shape of bars were cast having dimensions 9.4mm × 5.4mm × 63.6mm.

(D) Casting

The mould assembly shown in Figure 4 2 was clamped together and placed on a waxed surface. For each casting operation fresh slip was poured directly into the mould and the top of the mould assembly was then covered with a perspex sheet to avoid evaporation of water. Figure 4 3 shows the clamped assembly and the casts obtained In some experiments the whole assembly was enclosed in a perspex box to limit the rate of casting. This was possible since the humidity surrounding the mould,

and within the perspex box, reduced the net capillary pressure exerted by the plaster, thereby reducing the casting rate.

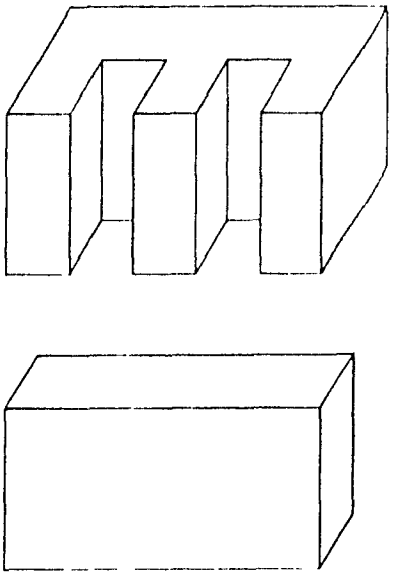

FIGURE 4.2 Mould for casting bars.

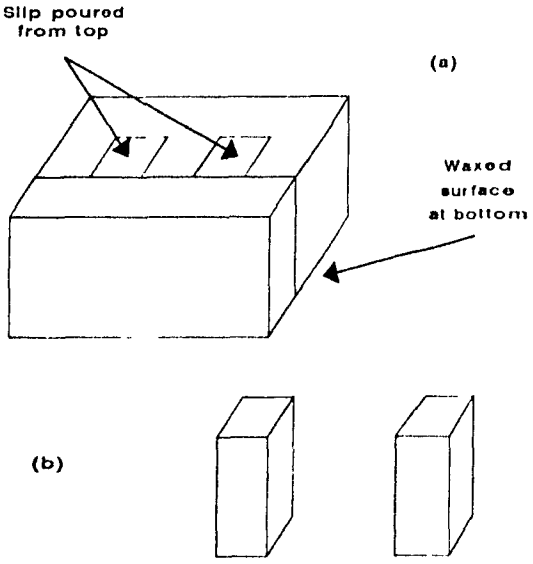

FIGURE 4.3 (a) Clamped mould assembly, (b) Casts obtained

4.2.2 Die pressing

Figure 4 4 shows a flow chart for making samples by this processing route. Silicon nitride slurries containing 0.5% deflocculant and sintering additives were attrition milled as described earlier. The slurries were poured through a 212μ and microwave dried The resulting soft agglomerates were granulated through the 212μ sieve so as to form a free flowing powder. For each sample approximately 5g of the dry granulated powder was uniaxially die-pressed at a pressure of 4.6MPa. The green bars obtained had dimensions of 8 9mm x 5mm x 60mm.

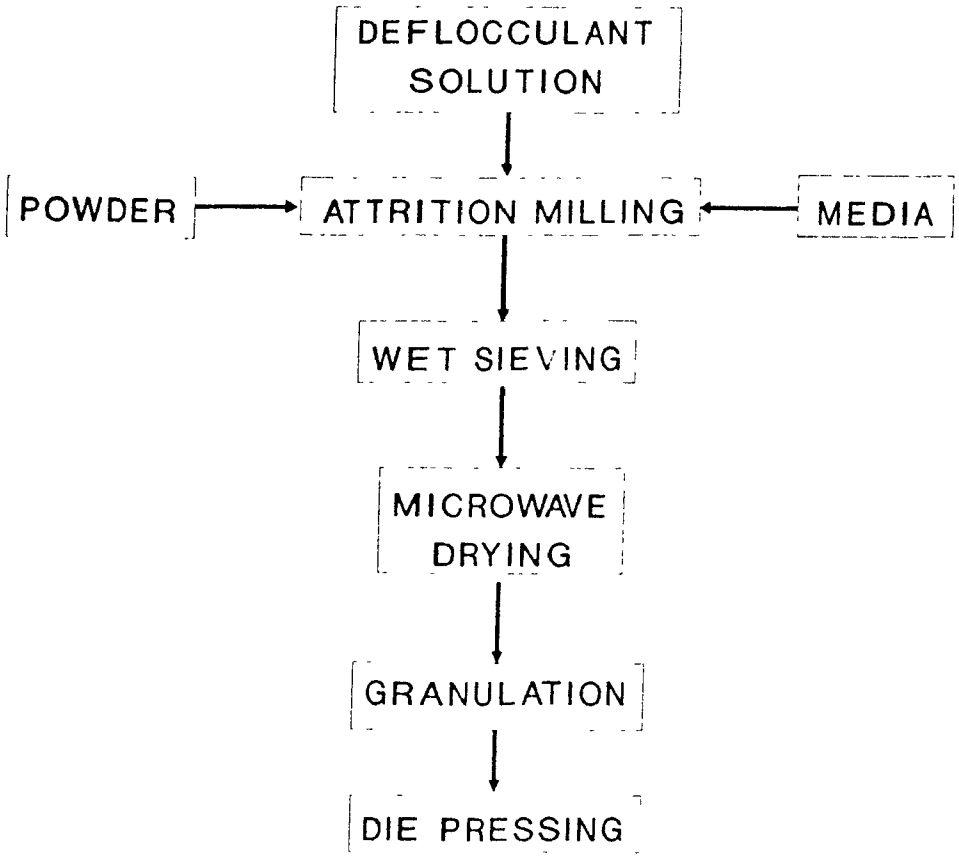

FIGURE 4.4 Flow chart for die pressing.

4.3 Drying and Iso-pressing

The slip cast samples cast, were air dried for 2 days after removal from the mould. These samples, together with those obtained by die-pressing, were placed in an air oven which was heated upto 500°C, from room temperature, in 3 hours Temperature was maintained at 500°C for an additional 3 hours, and then the samples were furnace cooled. This burn out treatment was performed to remove the polymer dispersant, and any entrained organic contaminants.

The uniaxially pressed samples, after burnout, were subsequently isostatically pressed at 340MPa, and air dried for 1 hour at 130°C

4.4 Sintering

Green densities for samples prepared by both the methods were measured, after drying, by calculations based on dry weights and dimensions

These samples were then embedded in a Si_3N_4/BN powder bed (within a graphite crucible) and tightly packed to avoid warpage Sintering was performed at 1800°C for 1 hour in a controlled atmosphere, graphite element furnace A high purity nitrogen atmosphere of ~125 kPa was maintained The sintering cycle is shown in figure 4.5. The furnace has graphite elements and double walled water cooled chamber A schematic of the furnace is shown in figure 4 6

Sintered densities were measured using Archimedes principle outlined in ASTM C373-72

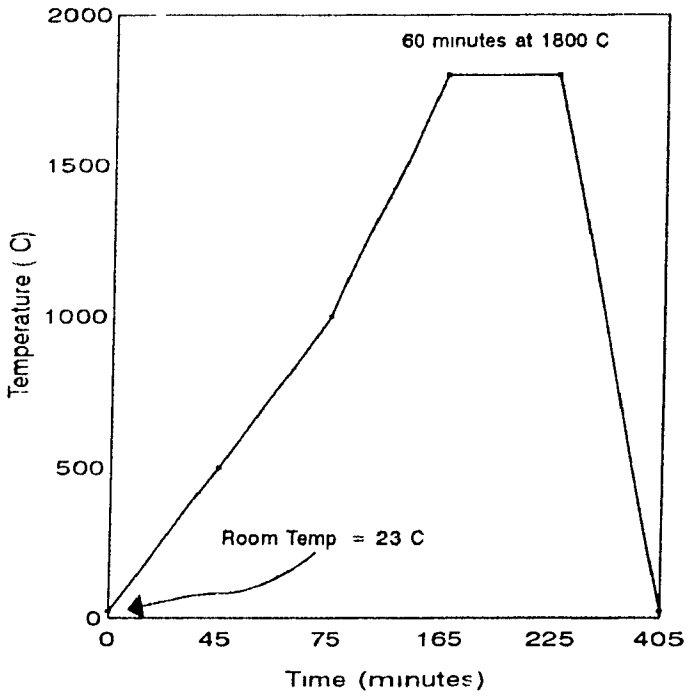

FIGURE 4.5: Sintering cycle used for densification.

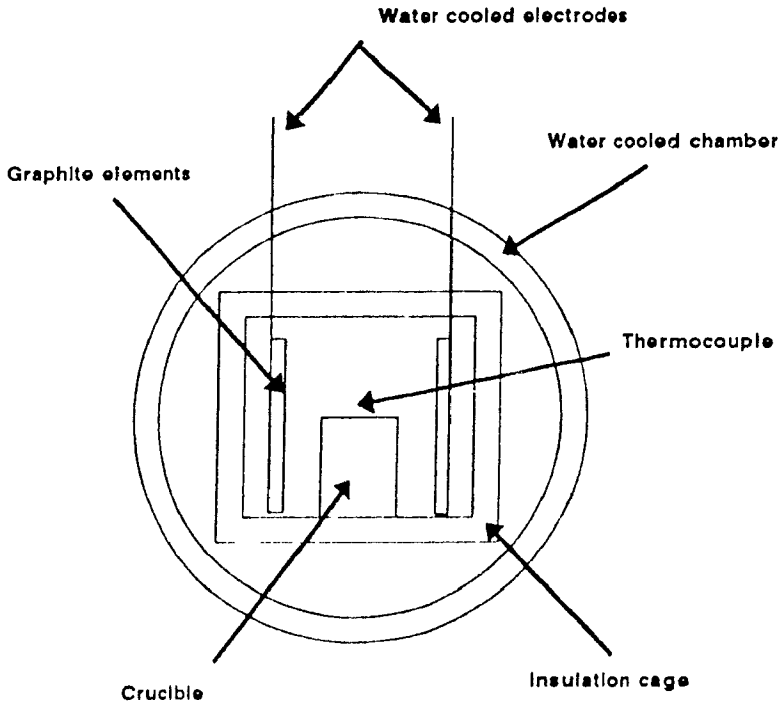

FIGURE 4.6: Schematic of the Sintering furnace

4.5 Sample preparation

(A) For Modulus of Rupture

A four point bending jig, shown in figure 4.7, was used to calculate the room temperature M.O R strength. Samples were longitudinally surface ground with a 240 grit diamond wheel to ensure parallel surfaces as per US Military Standards[47]. The edges of the tensile faces were bevelled using 240 and then 600 grit diamond wheels to remove stress concentrations.

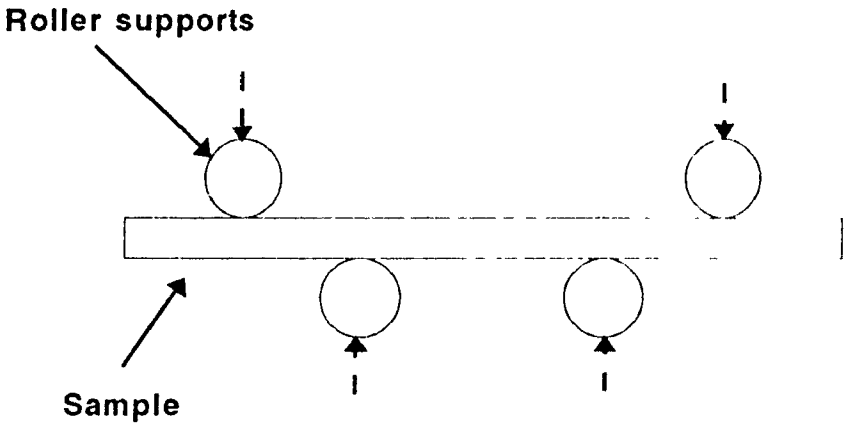

FIGURE 4.7 Four point bending test jig

M O R values were calculated using the following formula:

$$M.O.R. = 3Pa/(bd^2) \qquad \text{(IV-2)}$$

where

M.O.R = Modulus of Rupture (MPa)

P = load (Newtons)

a= the distance between adjacent upper and lower loading points (mm)

b,d are specimen width and thickness respectively (mm).

The relationship[51] proposed by Weibull for reliability of ceramics is given by:

$$f(\sigma) = \langle(\sigma-\sigma_\mu)/\sigma_0\rangle^m \qquad \text{(IV-3)}$$

where: σ is the applied stress

σ_μ is the threshold stress

σ_0 is a normalising parameter (at probability of failure = 0.632)

m is the Weibull modulus which describes the flaw size distribution.

Thus by plotting ln ln (1/(1-f)) against ln MOR, where

f= n(sample ranking)/(1+N(total number of samples)),

the Weibull modulus, m, is given by the slope of the line.

(B) For Microstructure analysis

Microstructural analysis was carried out using Scanning Electron Microscopy. Fractured surfaces of sintered, and green samples after burnout, were analysed. These were ultrasonically cleaned, mounted on SEM stubs, and subsequently gold coated. Fractography was carried out on broken M.O.R. bars to determine fracture initiation sites. These were more visible by tilting the specimens by ~20°. Energy dispersive X-

Ray analyses was used to determine the chemical composition of inclusions observed on the fractured surfaces.

CHAPTER V RESULTS AND DISCUSSION

The study analyses the rheological behaviour of silicon nitride slips using polymer dispersants By optimising slip properties, mechanical strength values of silicon nitride samples fabricated by slip casting, are compared with those obtained by die-pressing

5.1 Slip casting

5.1.1 Surface charge

Pure silicon nitride powder when mixed with deionized water at low concentrations of 10wt% and 15wt% solids, showed a pH of 8-9. A portion of the powder settled immediately, and the fines settled very slowly eventually forming a clear supernate. Presence of basic species in the supernate are clearly evident by its pH values A basic pH also indicates proton (H^+) adsorption by the silicon nitride surface leaving a defficiency in the solution If the pH of the supernate is adjusted to 7, it can be concluded that the silicon nitride surface is surrounded by a monomolecular layer of H^+ ions followed by a monomolecular layer of OH^- ions, in order to maintain electrical neutrality.

The hydrolysis of silicon nitride is thermodynamically plausible[13] according to the following equation.

$$Si_3N_4 + 12H_2O \rightarrow 3Si(OH)_4 + 4NH_3 \qquad \text{(V-1)}$$

The presence of ammonia is observed on sniffing freshly milled silicon nitride slip. AlN, also present in the slip, shows a stronger tendency to hydrolysis than silicon

nitride. AlN reacts with water, and becomes $Al(OH)_3$ and AlOOH as per the following equation; and changes the composition of the liquid phase

$$AlN + 3H_2O \rightarrow Al(OH)_3 + NH_3 \qquad (IV\text{-}2)$$

The ammonia released, therefore can be attributed to a result of hydrolysis of both Si_3N_4 and AlN. From this argument we can suspect that the silicon nitride surface is negatively charged and contains silanol (Si-OH) species, while the acidic species are adsorbed[12,16] Presence of NH_2 groups on the surface if silicon nitride have also been reported by Whitman and Feke[13]

Samples of UBE silicon nitride powder, as received, ball milled and attrition milled were analyzed for Oxygen content, by inert gas fusion method The results are given in Table V.1

TABLE V 1 Results of Oxygen analysis

Sample	Process	wt % Oxygen
A	Silicon Nitride powder as received	1 21
B	Powder attrition milled/ silicon nitride media/ methyl alcohol for 0 5h at 200 rpm/ microwave dried	1 24
C	Powder ball milled in distilled water for 2h and microwave dried	1 33
D	Powder attrition milled with silicon nitride media and distilled water for 0 5h at 200 rpm and microwave dried	2 5

A high Oxygen content is observed in sample D. Attrition milling decreases the particle size, thereby increasing the specific surface area of the powder. An increase in Oxygen content is related to the increase in the specific surface area The oxygen

rich surface layer is produced by the oxidation of the ultrafine powders, having been exposed to water containing atmosphere. Studies done at NASA, Lewis Research Centre[49] indicate an increase in specific surface area of almost four times when silicon nitride powder is attrition milled with silicon nitride media and ethanol at 100 rpm. Their studies indicate that the Oxygen pick-up was linear with time of milling, but eventually limited by subsequent breakdown of particles, indicating that hydrolysis, as well, is occuring after an increase in specific surface area.

Attrition milling in the present work was done for half hour. This is sufficient enough to breakdown agglomerates No experiments were done for longer periods of time, however, it can be safely assumed that breakdown of particles will reach a plateau with time This is because the tendency of the particles to re-agglomerate under grinding pressure and further fracture of the particles will decrease with time. Thus the increase in Oxygen content which is linear initially, would eventually reach a plateau with time

The Oxygen exists predominantly as Si-OH on the surface of the particle and gives a negative charge to the surface This again suggests the presence of negative species on the surface of the silicon nitride particles.

Figure 5 1 shows the electrophoretic mobility of silicon nitride powder using 0 001M KNO_3 as the background electrolyte.

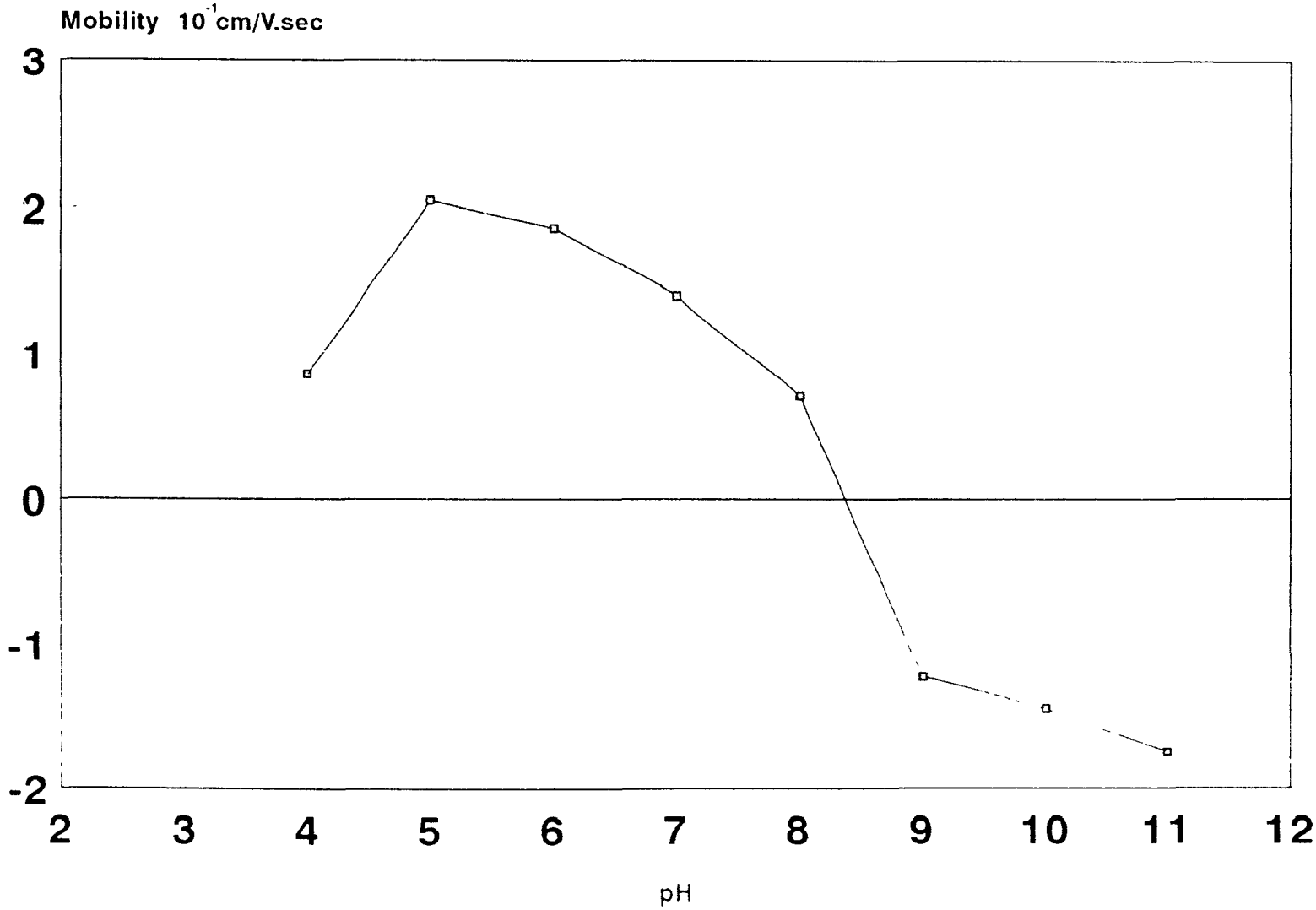

Figure 5.1: Electrophoretic Mobility of Silicon Nitride particles.
(Background Electrolyte: 0.001M KNO_3)

From the figure the Iso-electric point (IEP), which is proportional to the mobility, is between 8-9 This IEP is quite basic and does not strongly support that silanol species on the surface of silicon nitride are dominant This also indicates that even if silanol species do exist on the surface, the silanol layer is permeable to physisorbed and chemisorbed basic species. Presence of NH_2 groups have also been reported by others[13].

Figure 5 1 indicates that a slip containing silicon nitride particles will be most stable if the pH is less than 7 or greater than 9. At these pH ranges zeta potential would be high, resulting in a well dispersed system due to high electrostatic repulsion between particles Zeta potential of sintering additives Al_2O_3 and Y_2O_3 show higher stabilities in the ranges of pH<5 and pH>9 [15] Therefore for a slip containing silicon nitride and additives Al_2O_3 and Y_2O_3, pH>9 is preferable due to a relatively small difference in zeta potential between silicon nitride and the additives In addition, since acidic slips also affect the life of a plaster mould, they should be avoided

5.1.2 Slip Viscosity Behaviour

Figures 5 2-5 5 show the variation of viscosity with varying amounts of Darvan C, for solids loading 1 0 to 2.5. Viscosity was measured at two shear rates, 50 and 500rpm From these graphs it is apparent that for a given solids loading, viscosity decreases as the amount of Darvan C increases, until a minimum is obtained. On further increasing the Darvan C concentration, viscosity increases again.

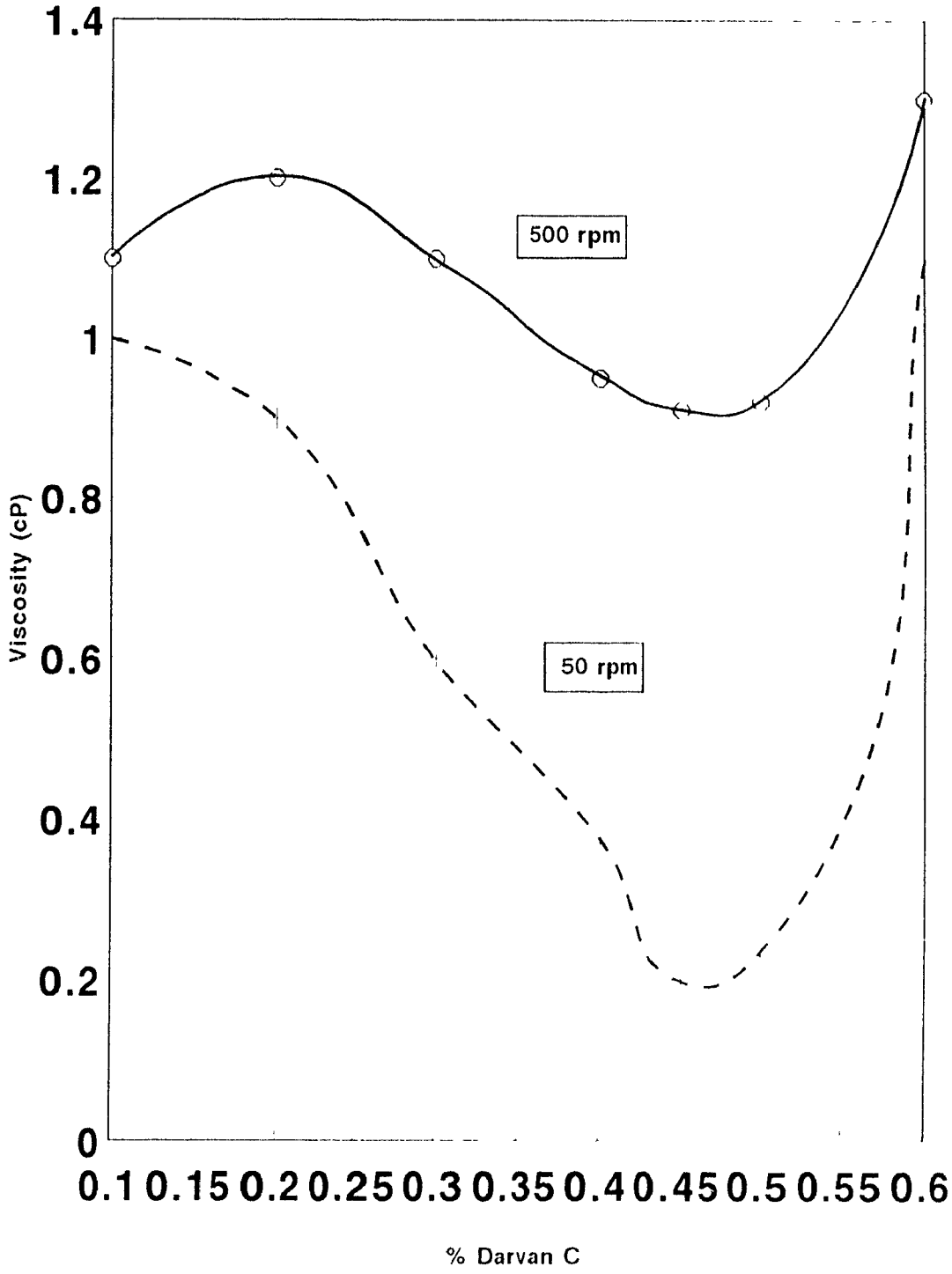

Figure 5.2: Viscosity vs % Darvan C
(Solids Loading: 1.0)

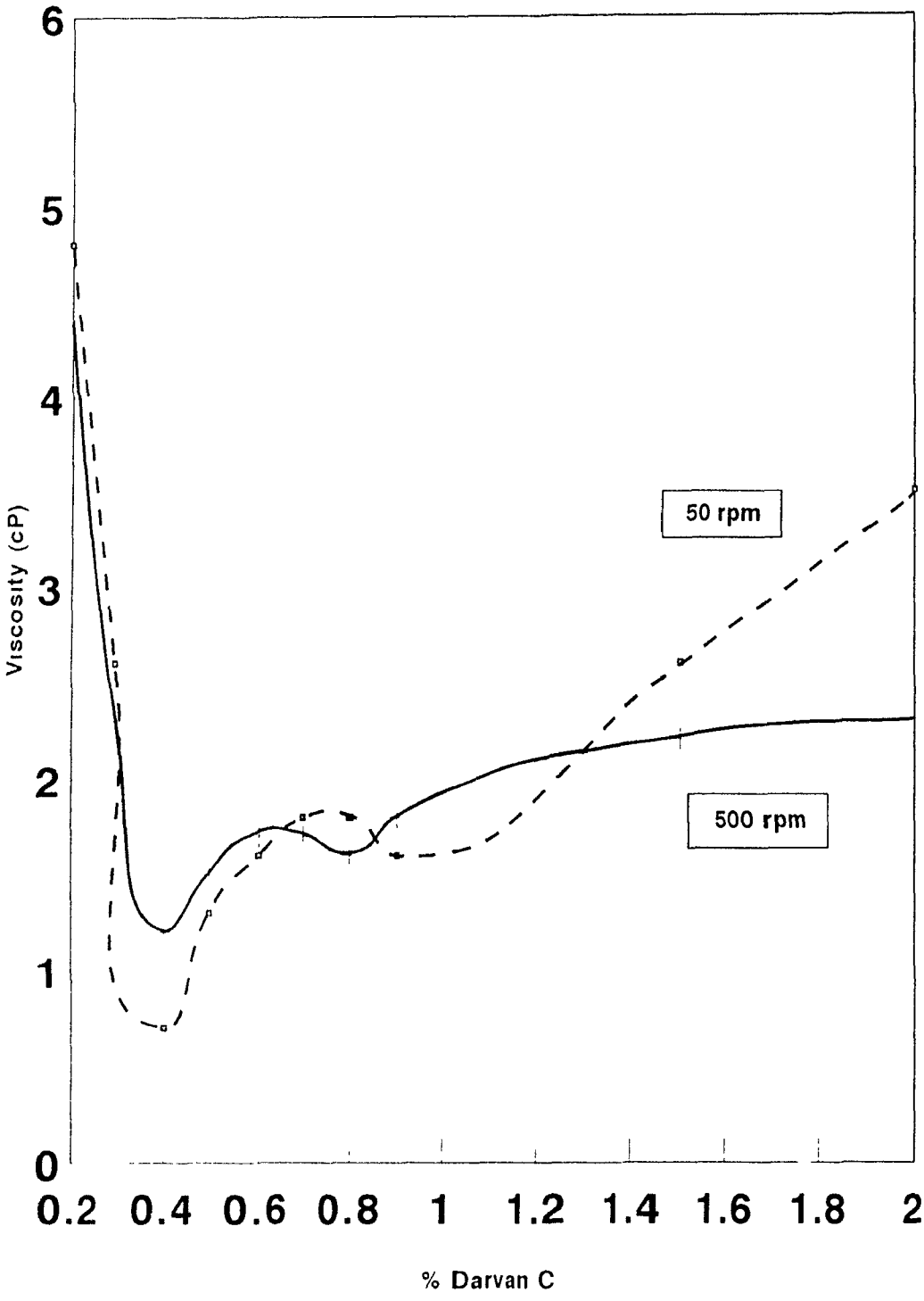

Figure 5.3: Viscosity vs % Darvan C (Solids Loading: 1.5)

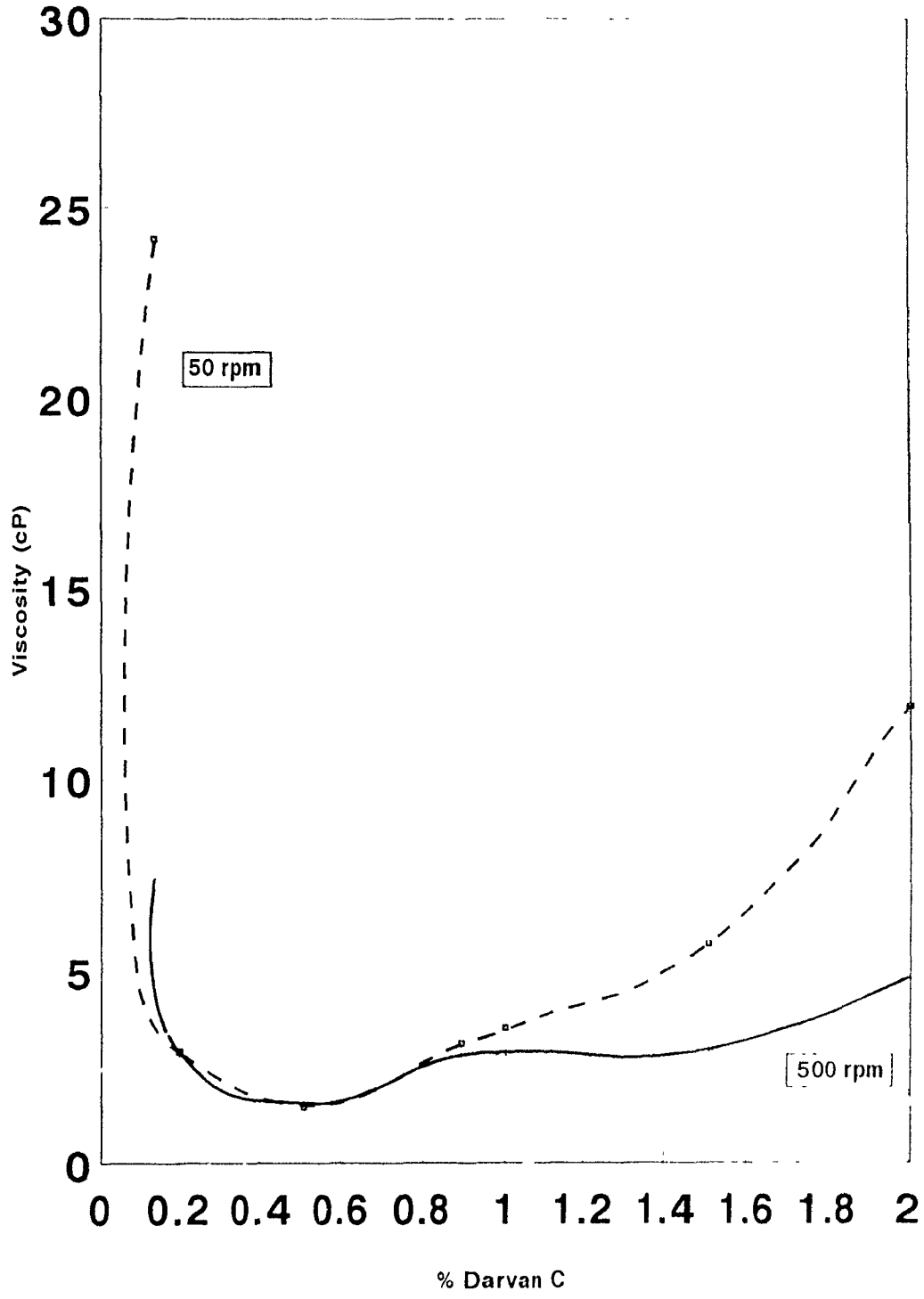

Figure 5.4: Viscosity vs % Darvan C (Solids Loading: 2.0)

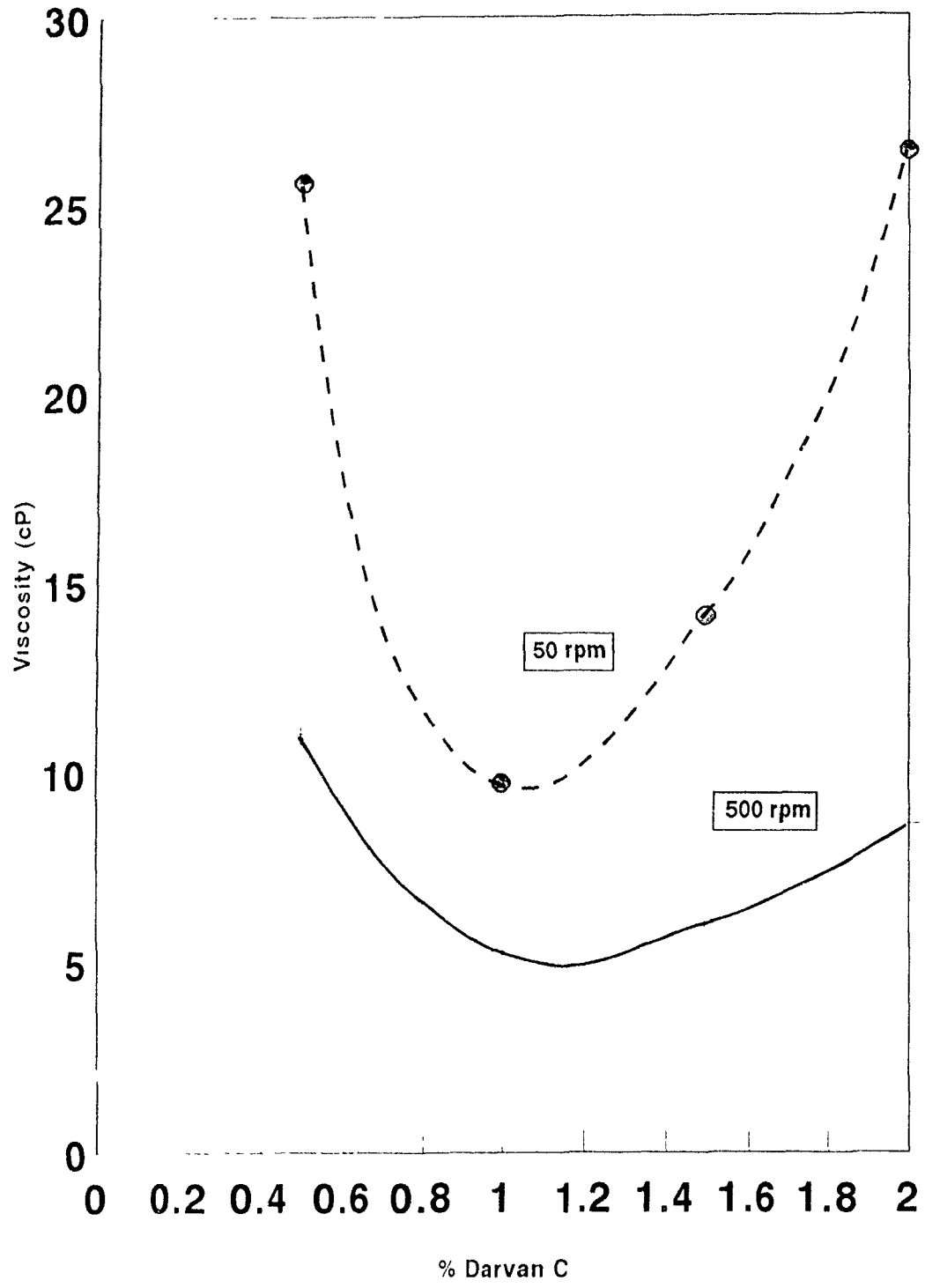

Figure 5.5: Viscosity vs % Darvan C (Solids Loading: 2.5)

Darvan C, a polyelectrolyte of Ammonium Methyl Methacrylate, is proprietary and the exact composition is not known This polyelectrolyte has been used earlier[18] and has been found to be an effective dispersant for ceramic slips. It is however, an ammonium salt of Methyl Methacrylate and dissociates in water to give NH_4^+ ions and methacrylate poly-ions Darvan C being ionic, the slurry is being stabilised by both electrostatic interactions and polymer adsorption

When Darvan C is added to a slip the methacrylate poly-ions tend to be adsorbed on the surface of particles. This diffuse layer gives the particles a negative charge. The excess of the positive ions(NH_2' and H^+) in the solution then surround the diffuse layer due to electrostatic attraction. The particles being negatively charged, repel each other and the system deflocculates It should be noted that repulsive forces can also arise due to non-ionic polymer adsorption on the particle surface Absorption of non-ionic polymers on the particle surface can result in both attractive and repulsive forces. Attractive forces can arise from polymer bridging when there is a direct link between two particles through a polymer bridge Repulsive forces arise in two ways when two polymer adsorbed particles approach each other (1) As the particles come close to each other, the polymer concentration increases more in the gap between the particles than in the general solution resulting in osmotic pressure difference between the gap and the solution This decreases the entropy of the system, and in turn increases the Gibbs free energy. This increase in energy causes repulsion between particles. (2) The polymer chains can also interpenetrate and compress each other which results in forcing the particles apart. This can be visualised by compressing a simple circular spring as shown in figure 5 6.

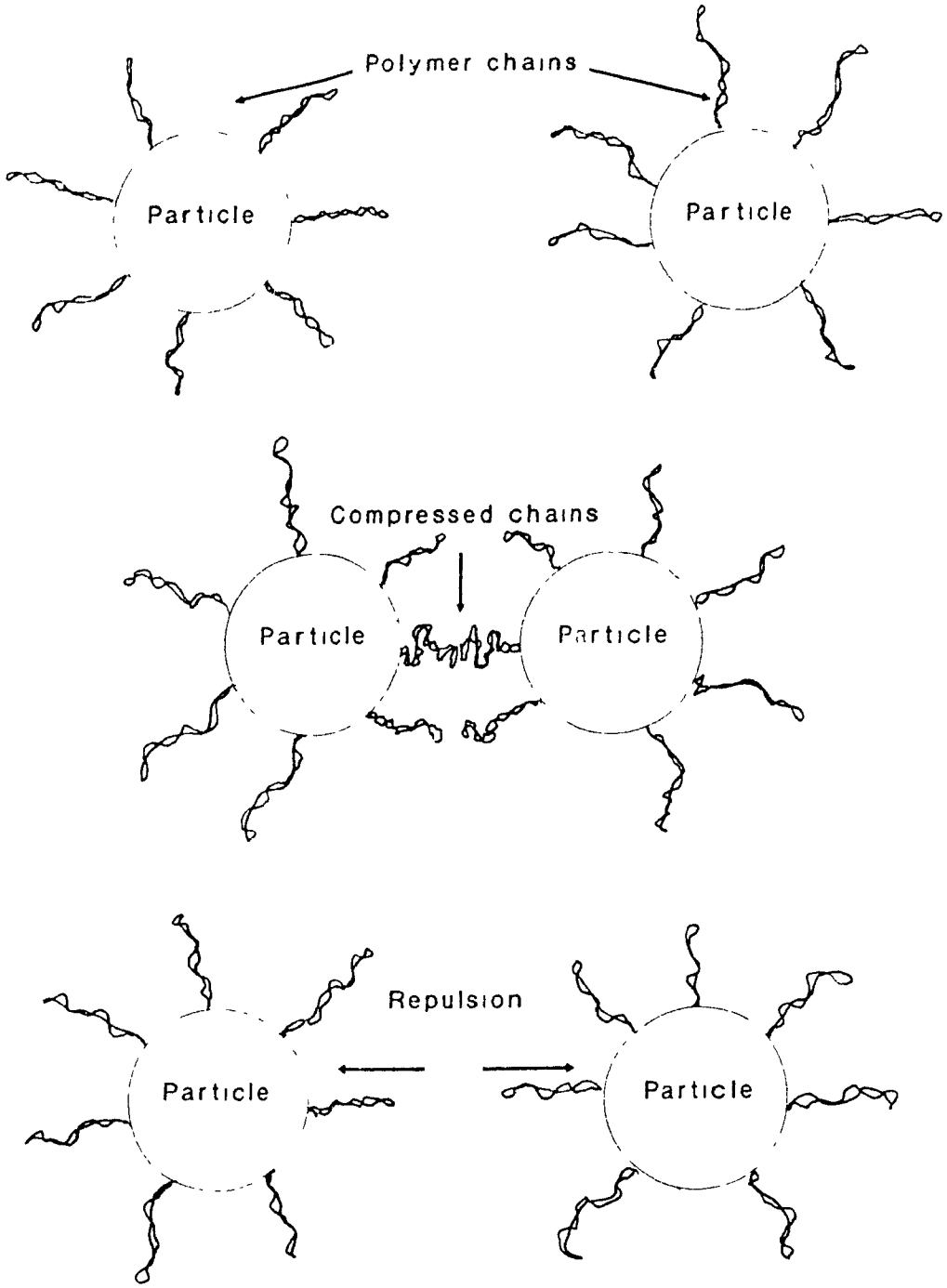

FIGURE 5.6· A. Two particles with polymer chains approaching one another, B. Compressed chains at closest approach; and C. Repulsion due to force exerted by the compressed chains.

Murray and Anderson[48] have shown that a low viscosity of a slip is associated with a high zeta potential and vice versa. Increasing the amount of Darvan C can have two opposing effects: (1) Increase in zeta potential (low viscosity) due to increased surface charge, and (2) decrease in zeta potential (high viscosity) due to a compressed diffuse layer. From the discussion so far an optimum amount of Darvan C must be added to the slurry to produce a fully deflocculated system From figures 5.2 to 5.5 minimum viscosities correspond to the optimum amount of Darvan C required for a given solids loading

Viscosities, for a given solids loading are also dependent on shear rates (see figure 5 7). These slips are non-Newtonian and exhibit thixotropy In thixotropy the agglomerates are broken by shear action and later recombine when the shear rate is reduced. Due to this, the viscosities at 500rpm are lower than the viscosities at 50rpm This, however is not true for low solids loading of 1 0(33 wt%) For this solids loading, the viscosities at 500rpm are higher than 50rpm indicating a shear thickening (dilatant) behaviour. The difference in viscosities at the two shear rates is, however small. Slurries with solids loading 2 5(71 wt%) are shear thinning(thixotropic) On increasing the solids loading, the shear thickening behaviour (observed clearly from figure 5 2), decreases and shear thinning behaviour increases (as shown in figure 5 5) The actual changeover from shear thickening to shear thinning takes place at a solids loading of slightly greater than 2 0(67 wt%) and 0 5% Darvan C (Figure 5 7)

The viscosity at this point is Newtonian. At high concentrations of Darvan C, in figures 5 3-5 5 a pronounced shear thinning behaviour is observed since the difference in viscosities at these points is high and increases with the solids loading. The rheological aspects will be discussed further in section 5 1 3

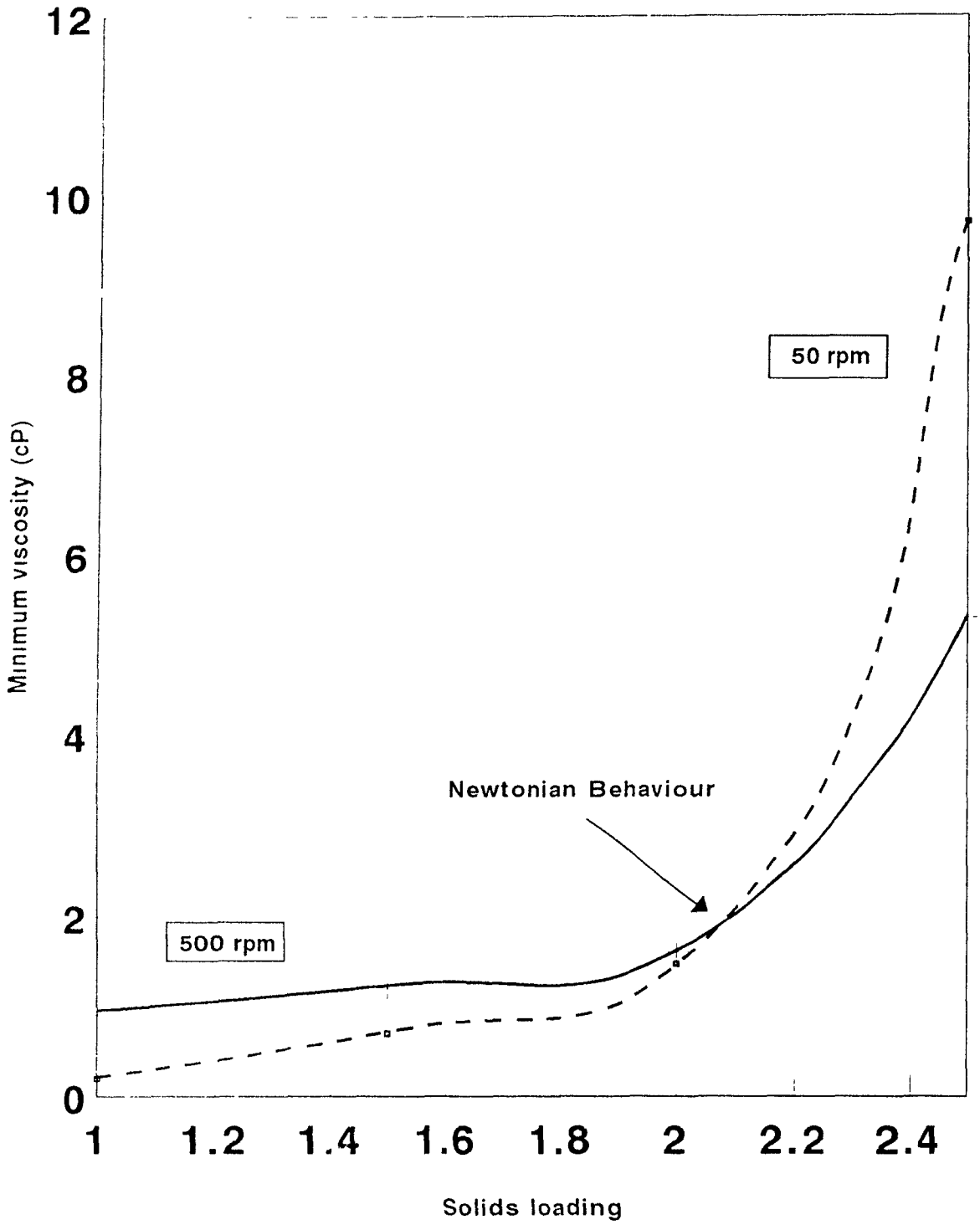

Figure 5.7: Minimum Viscosities at different Solids Loading

Figure 5 8 shows a plot of Darvan C content with different solids loadings at minimum viscosities. From the figure it can be observed that for solids loading upto 2.0(67 wt%), the amount of Darvan C required is about 0 5% However at a solids loading of 2 5(71 wt%) requires 0 9% of Darvan C This means that increasing the solids content by 6 wt% (from 2.0 to 2 5) requires a significant increase in the amount of Darvan C This can be explained as follows. as the solids loading increases beyond 2.0, a large percentage of water is used up to surround the particles This is due to the fact that the total particle surface area/volume of slurry increases Since the ratio of water.particle surface area at solids loading of 2 5(71 wt%) is much lower than the ratio of water particle surface area at solids loading of 2 0(67 wt%), a larger amount of Darvan C is required to surround the particles This indicates that a large number of particles are surrounded by Darvan C and very little water Such particles surrounded by high concentration of polymer tend to form polymer bridges, therefore adsorption at these concentrations leads to flocculation At higher solids loading, the average interparticle distance decreases Therefore the dispersant molecules suffer from stoic interference and are less effective

If we consider non-ionic polymer adsorption, because of overcrowding, the distance between two particles will be small This will lead to a reverse osmotic pressure between the gap and solution, and an attractive force, resulting in coagulation and flocculation Thus a compromise between the amount of dispersant and solids loading should be obtained to avoid overcrowding of particles and excess polymer.

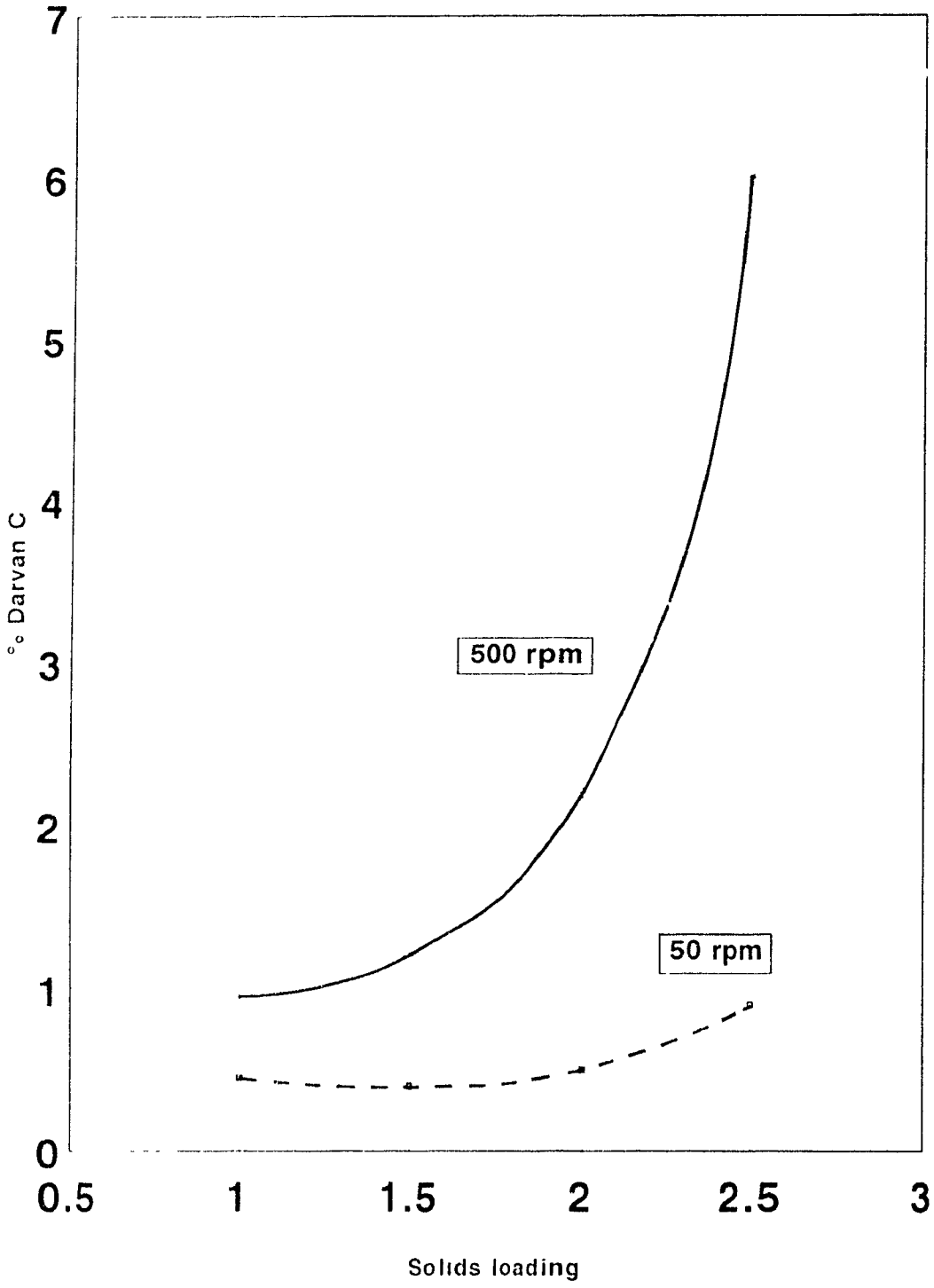

Figure 5.8: % Darvan C vs Solids Loading
(At Minimum Viscosities)

Figure 5.7 illustrates minimum viscosities at different solids loadings. A high viscosity can be observed at solids loading 2.5 As mentioned earlier, viscosities at both shear rates are the same at solids loading 2.0 (67wt%) Although no quantitative analysis was carried out on sedimentation, it was observed (while preparing the slurries) that sedimentation rate for solids loading 2.5 was the highest The more deflocculated a slurry, the lower are the sedimentation rates This is due to the fact that in a well deflocculated system the particles have high repulsive forces which keep them in motion If the repulsive forces are weak, and are overcome by attractive forces, the particles will tend to coalesce with each other and form "flocs" These flocs eventually coalesce with other particles and sediment Therefore in flocculated systems the gravitational forces overcome the electrostatic forces, leading to a high sedimentation rate.

Particle size also affects the sedimentation rates It was observed at solids loading 2.5, that for the first 10-15 minutes of attrition milling, the powder and the liquid in the mill rotated in one lump After that a few drops of liquid reappeared , and very slowly the formation of a liquid slurry took place Thirty minutes of attrition milling was carried out for all the samples, including the ones at lower solids loading Thus the effective milling time for a slurry for solids loading 2.5, was only 15-20 minutes This could have resulted in few larger sized particles which accelerated the sedimentation rates The slurry was extremely thick and very viscous in appearance It was also observed during casting that the slurry could not occupy the finer details of the plaster mould, due to a very high surface tension and viscosity

From the discussion so far, a solids loading of 2.0 (67 wt%) and 0.5% Darvan C appeared to be the best combination for making well dispersed slips The observed

pH values for the above were 8 5-10 0. Olagnon et al[16] have performed similar studies using Darvan C and Dispex 40 They optimised a solids content of 65 wt% which corresponds to a solids loading of 1.8. Their pH range for a well dispersed slip was in the range of 7 5 to 9 0 The results they obtained are quite consistent with the ones observed in the present work. An improvement in the present work has been the slightly higher solids content This increase in solids, alongwith the increase in the amount of dispersant (0 5%) is justified by the higher pH values obtained, which is primarily due to a higher oxygen content on the surface of the particles as a result of attrition milling

Two more polymer dispersants Darvan 821A (Ammonium Polyacrylate) and ET-85 were tested for their viability to aid slip formation Using the optimised solids loading of 2 0, and 0 5% dispersant concentration, viscosity was measured at different shear rates Table V 2 shows the viscosity behaviour of the two new dispersants in comparison to Darvan C, at 0 5% concentration. From the table, the viscosities for

Table V.2: Viscosity behaviour of various dispersants

Dispersant	Viscosity at 50 rpm (cP)	Viscosity at 500 rpm (cP)
Darvan C	2 6	2.6
Darvan 821A	2.0	2.7
ET-85	22.5	7.0

Darvan C and Darvan 821A are low with respect to ET-85 ET-85 also shows a high shear thinning behaviour due to a big difference in viscosities at different shear rates The choice of 0.5% dispersant and solids loading of 2 0 for the two new dispersants was used since this produced a good slip with Darvan C Also, based on the fact that both Darvan C and Darvan 821A are similar ammonium polyelectrolytes, it was assumed that the dispersion characterstics would be similar, which indeed they appear to be

Darvan 821A was further investigated since it appeared to be a good alternative dispersant For a solids loading of 2 1, viscosity was measured as a function of amount of Darvan 821A, as shown in figure 5 10 A very well defined minima is observed at 0 5% concentration This indicates a high zeta-potential of the particles and a well dispersed system This behaviour is very similar to the one shown in figure 5 4. Darvan 821A is an aqueous solution of Ammonium Polyacrylate The molecular weight of this polymer (2500-3000) is much lower than the molecular weight of Darvan C (14000-20000), indicating that 821A has shorter chains A higher viscosity can be observed at both the minimum(0 1 %) and maximum(2 %) percent concentrations of Darvan C (fig 5 4) than the corresponding points for Darvan 821A (Fig. 5.10) In both the dispersants a minimum is observed around 0 5%, although the viscosities in case of Darvan 821A are shear thickening This behaviour is possible, due to the fact that the 821A chains are shorter and the steric resistance is therefore reduced even at high solids loading As discussed earlier, this concentration of the dispersant will form a diffuse layer of thickness enough to give the highest zeta-potential to the particles Addition of more polymer compresses the diffuse layer by (1) surrounding the particles due to further polymer adsorption, and (2) attraction

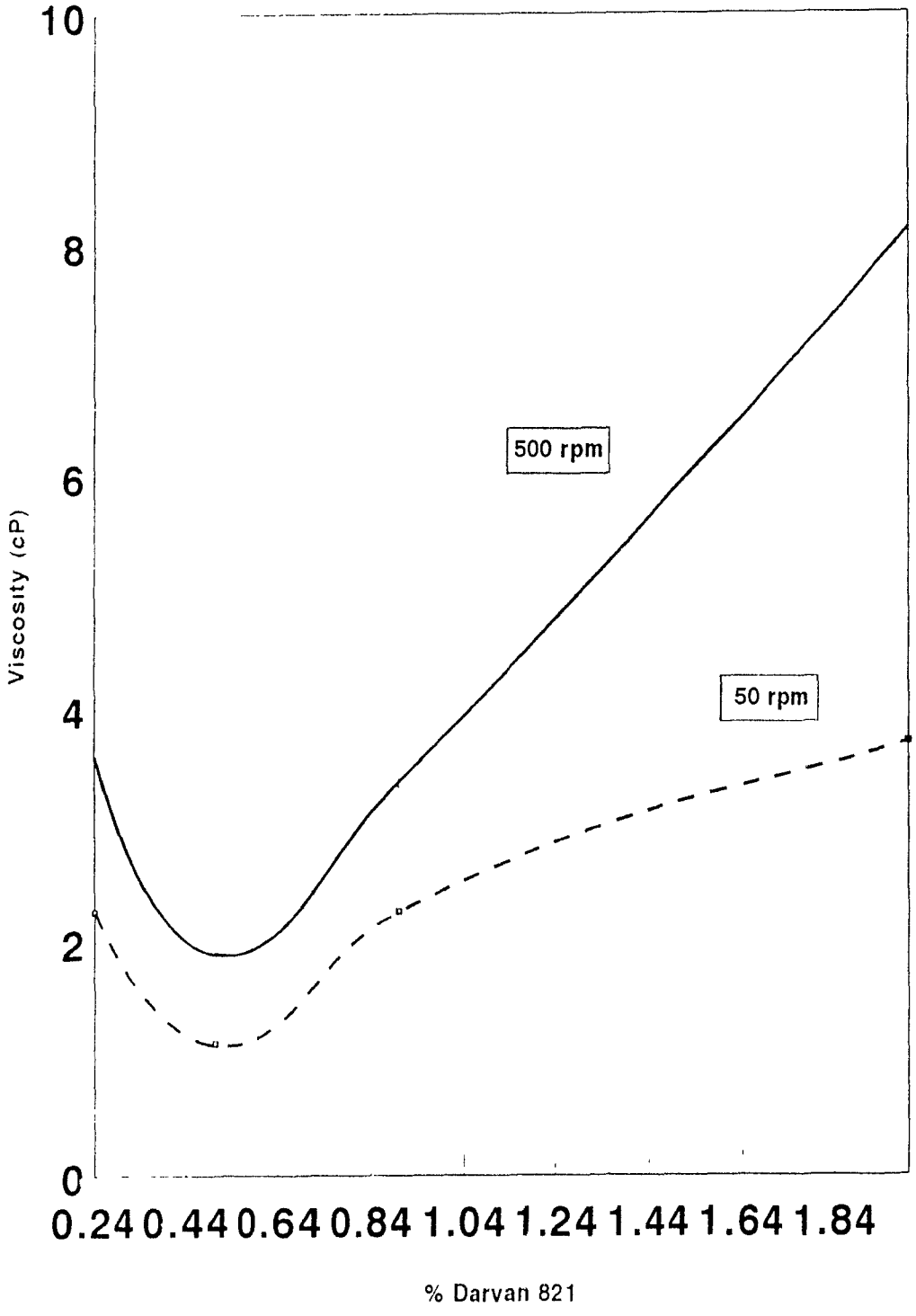

Figure 5.10: Viscosity vs % Darvan 821A
(solids loading 2.0)

between polymer chains due to van der Waals forces which result in bridging This leads to flocculation. A similar behaviour is observed at low concentrations of the dispersant In this case the forces which lead to flocculation are van der Waals attractive forces which leads to the formation of large agglomerates These tend to settle by gravity.

5.1.3 Aging behaviour of slips

Figures 5.11 and 5.12 show the time dependent behaviour of silicon nitride slips using Darvan C as a dispersant. In figure 5 11, 0 14% Darvan C represents the minimum amount required to render fluidity to the slip 0 5% concentration was selected based on previous investigations 0 9% and 2 0% concentrations were randomly selected From the figure it can be observed that the initial viscosity at (t=0) is high for 0 143%, and decreases with increasing amounts of Darvan C until 0 5% Increasing the concentration further, increases the viscosity

Over a period of about four hours, the viscosities at 0 14% concentration decrease sharply This can be explained as follows; due to a high particle concentration and poor deflocculation, the sedimentation rates were high and most of the solids settled almost immediately as shown schemetically in figure 5 13 The viscosity as observed, therefore represents that of the supernatant consisting mostly of water and a few particles Since the amount of solids settling increased with time, the viscosity decreased sharply from 25 cP to 9 cP. A minimum of 7 cP after 5 hours indicates almost complete settling Measurements of viscosity were not possible after 8 hours This is due to the fact that the solids settling jammed the rotating bob within the cylinder

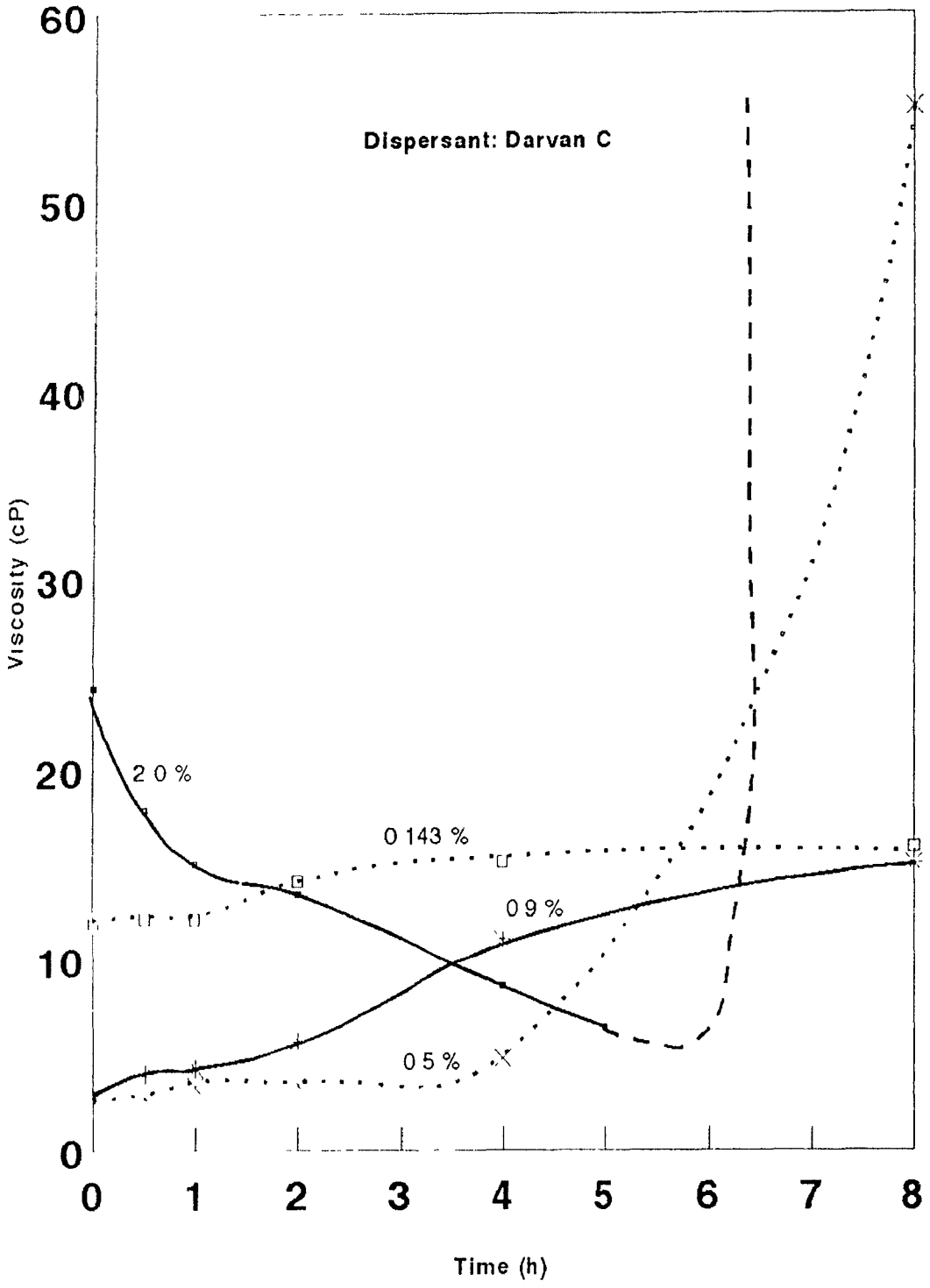

Figure 5.11: Time Dependent Behaviour of Viscosity at 50 rpm

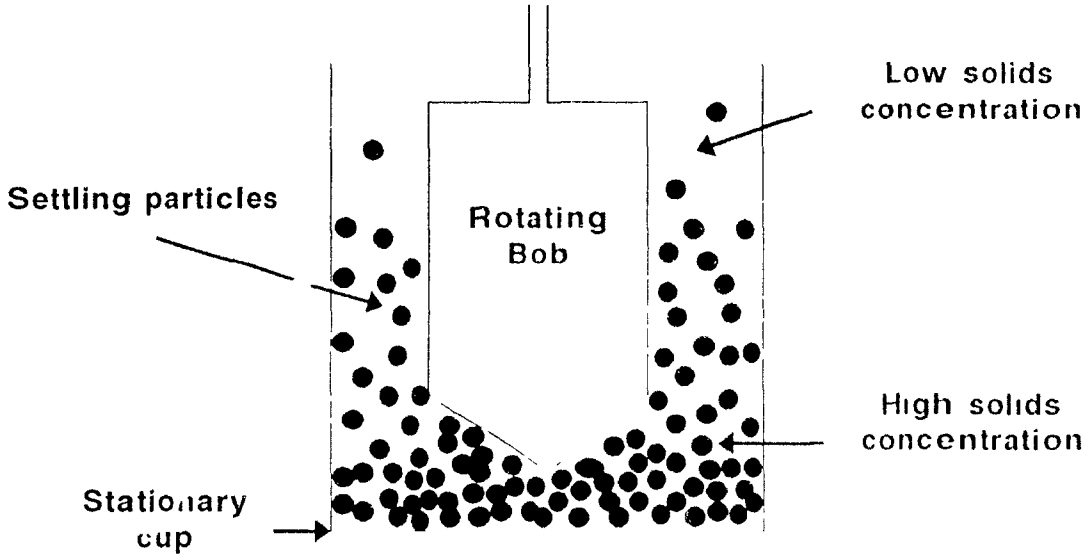

FIGURE 5 13. Cup and bob viscometer.

Thus, somewhere between 5 and 8hours the bob of the viscometer became jammed and viscosity became unmeasureable as represented by the dotted line on figure 5 11

Viscosities for 0.5% concentration were relatively constant over a four hour period. However, 0 9% and 2 0% show a gradual increase Since casting of the slip was done immediately after its preparation, and based on first four hours of viscosity behaviour, 0.5% was the best concentration of the Darvan C dispersant.

Figure 5 12 shows the data plotted in the form of viscosity versus % Darvan C different times (0, 2 and 4 hours). This figure again confirms the fact that minimum viscosities are observed for 0.5% concentration of Darvan C Similar values in the region of minimum viscosity, over a period of four hours, also indicates a Newtonian behaviour The difference in viscosities between 0 and 2h is very small, indicating almost no change in the system.

Figures 5 14 and 5 15 represent time dependent behaviour of the slurries using Darvan 821A Figures 5 14 and 5.11 show a similar behaviour with viscosities decreasing from 0 24% to a minimum at 0 5% and increasing again Viscosities for 0 24%, 0 5% and 0 9% of Darvan 821A appear to be fairly constant over a four hour period The viscosities of 2% concentration decrease gradually This is due to the fact, that a high concentration of the polymer tends to form long polymer chains, interlocking the solid particles A network consisting of polymer chains primarily due to steric effect is formed. This suspension consists of large molecules and anisometric particles Flow in such suspensions tends to orient the polymer chains and reduces its resistance to shear The viscosity, therefore decreases and the behaviour is typically shear thickening

During the first four hours, the viscosity at 0.5% concentration are the lowest. This data are re-plotted in figure 5.15. From the figure, once again the viscosities, within the first 4h, are lowest at 0.5% concentration of the dispersant.

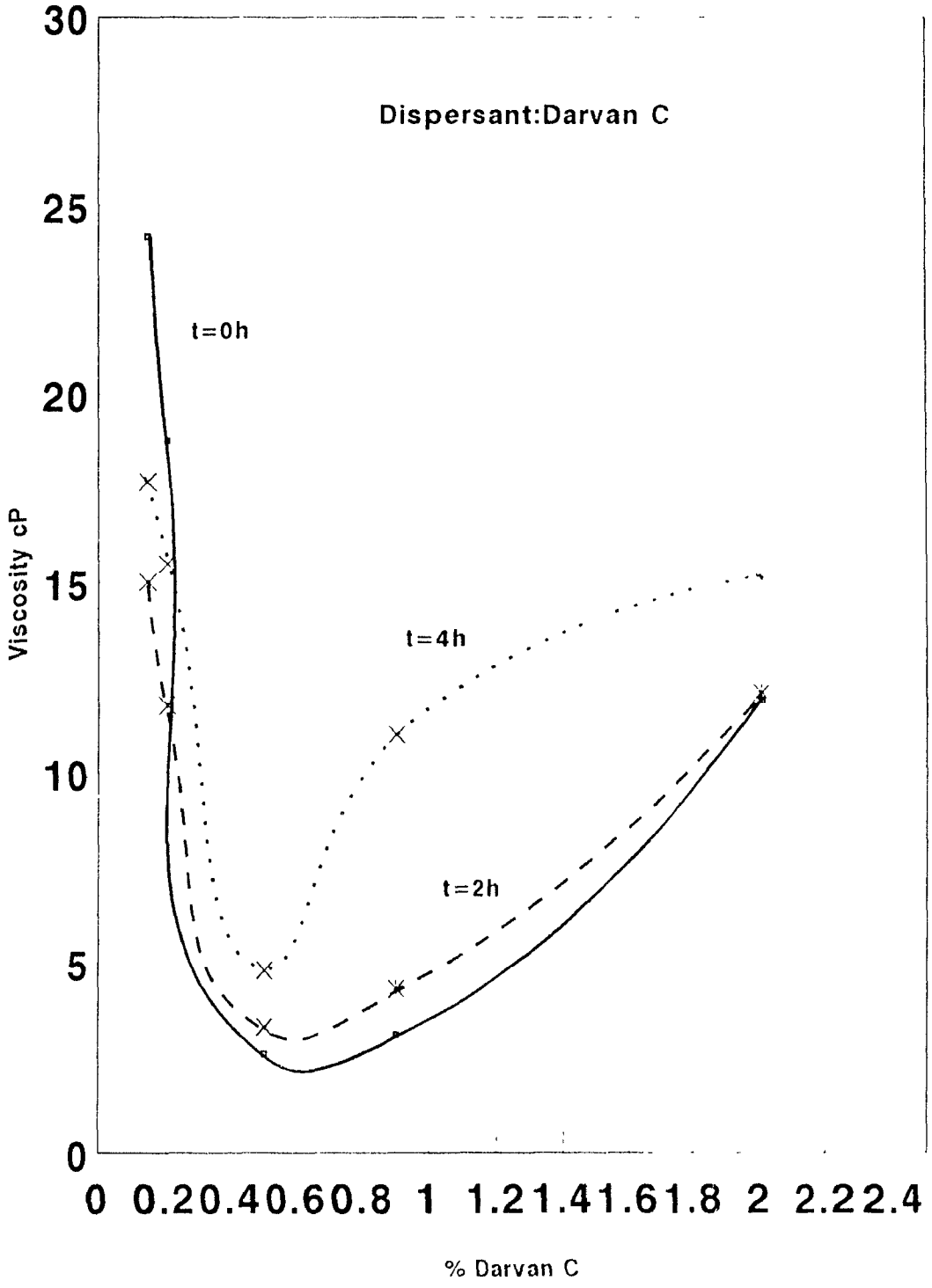

Figure 5.12: Slip Aging Characterstics at 50 rpm

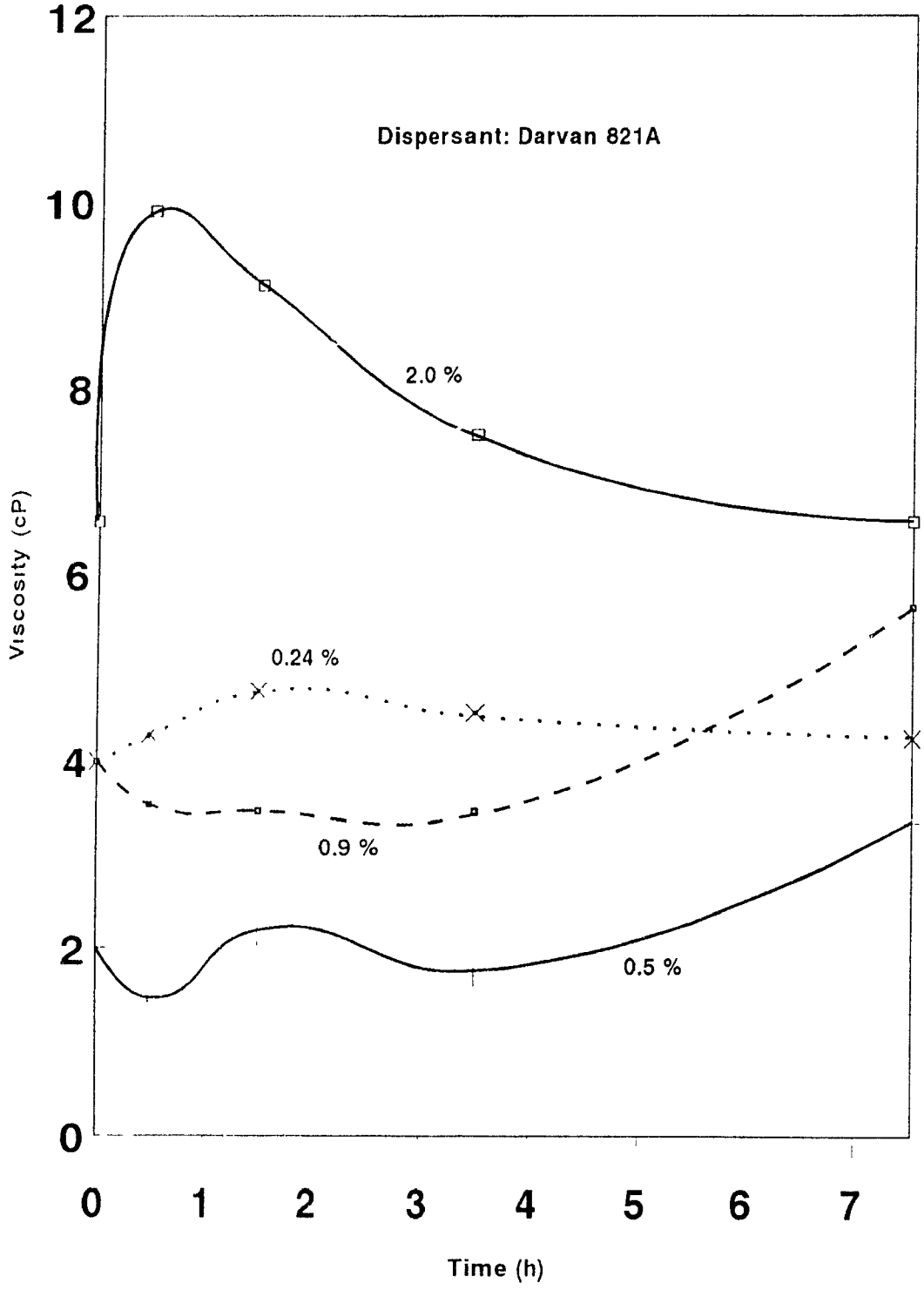

Figure 5.14 Time Dependent Behaviour of Viscosity at 50 rpm

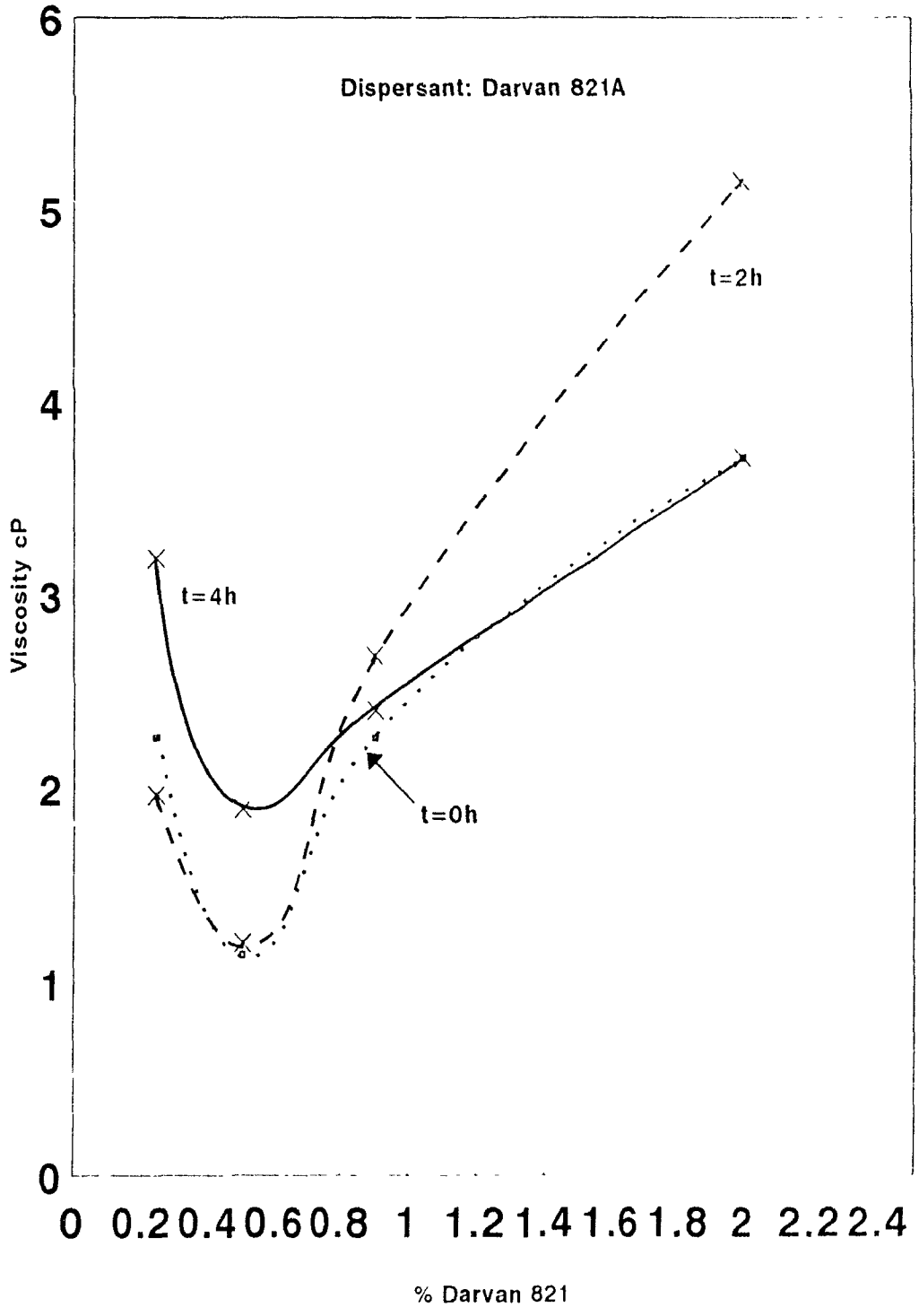

Figure 5.15: Slip Aging Characterstics at 50 rpm

5.1.4 Slip casting Behaviour.

Casting was done in the plaster moulds shown in figure 4 2, and bars of green dimensions 9 4mm×5 4mm×63 6mm were produced After casting, the bars had a thin hollow pipe running down the centre along the length, as shown in figures 5 16 and 5 17

This is typical for solid casting, where the heigh of the piece far exceeds the cross-sectional area In this case the length was 63mm and the cross-sectional area of the green bars was 45mm^2 Since the rate of casting along AB is equal to the rate of casting along the length XY, solid material cast along the AB direction prevented the flow of slip along the XY direction On subsequent drying the cake shrunk leaving a thin hollow pipe in the centre The micrograph of the fractured sample is shown in figure 5 17 Evidence of a 200-300μm diameter pipe can be clearly seen in the centre figure 5 17 also shows C shrinkage cracks and seggregation of additives.

This problem was overcome in two ways. Firstly, a waxed surface was placed on the bottom surface to replace the plaster, so that the solid cast would not form on the bottom surface The schematic of the mould is shown in figure 4.3(i) This allowed the cast to grew only along the AB direction shown in figure 5.16

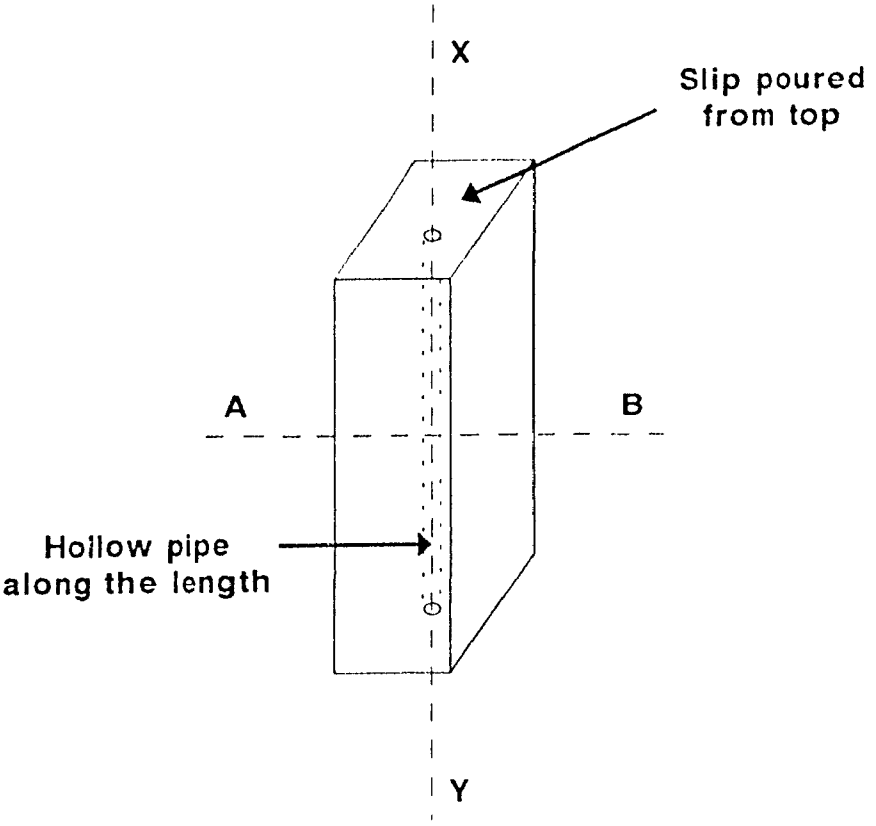

FIGURE 5.16 Hollow pipe running along the length of the cast

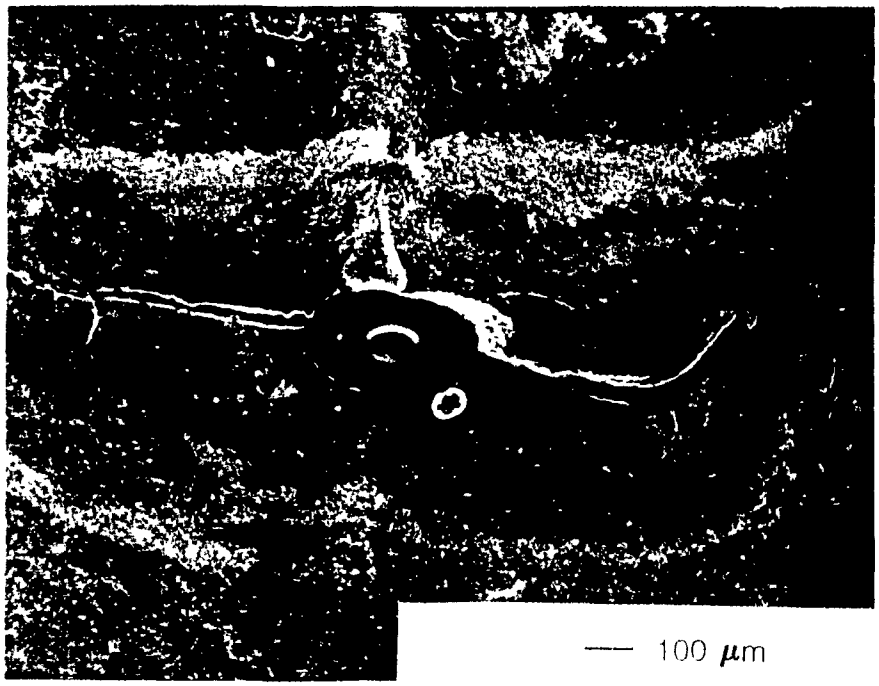

FIGURE 5.17 Micrograph showing the formation of a hollow pipe in the centre of the cast

Secondly, a reservoir was made on the top of the mould containing excess slip The reservoir made of plaster was also waxed to prevent dewatering and any cake build-up. Throughout the casting procedure it was ensured that the reservoir contained excess slip.

Slip cast densities and sintering behaviour

Tables V.3 and V.4 show the green and sintered densities of the slip cast samples. The green densities were calculated after binder burn out treatment The individual green and sintered density values are given in appendix A

TABLE V.3· Green densities of the slip cast samples

Dispersant	Number of samples	density (g/cc)	Standard deviation	as % Theoretical density
Darvan C	31	1 63	0 04	49 7
Darvan 821A	27	1 69	0 07	51 52

TABLE V.4· Sintered densities of the slip cast samples

Dispersant	Number of samples	density (g/cc)	Standard deviation	as % Theoretical density
Darvan C	31	3 21	0 03	97 87
Darvan 821A	27	3.20	0 02	97.26

Samples made with Darvan C showed slightly lower green densities than the ones prepared with Darvan 821A (Table V.3). The sintered densities, however in both the cases were greater than 97%. This data is quite consistent with the shrinkage observed Since Darvan C is a longer chained polymer than Darvan 821A, the organic loss after burn out treatment, is higher than the samples made with 821A This led to higher shrinkage values (18.02% in case of Darvan C, and 17.25% in case of Darvan 821A) and lower green strength

Figure 5.18 shows typical fracture surface of slip cast and sintered silicon nitride

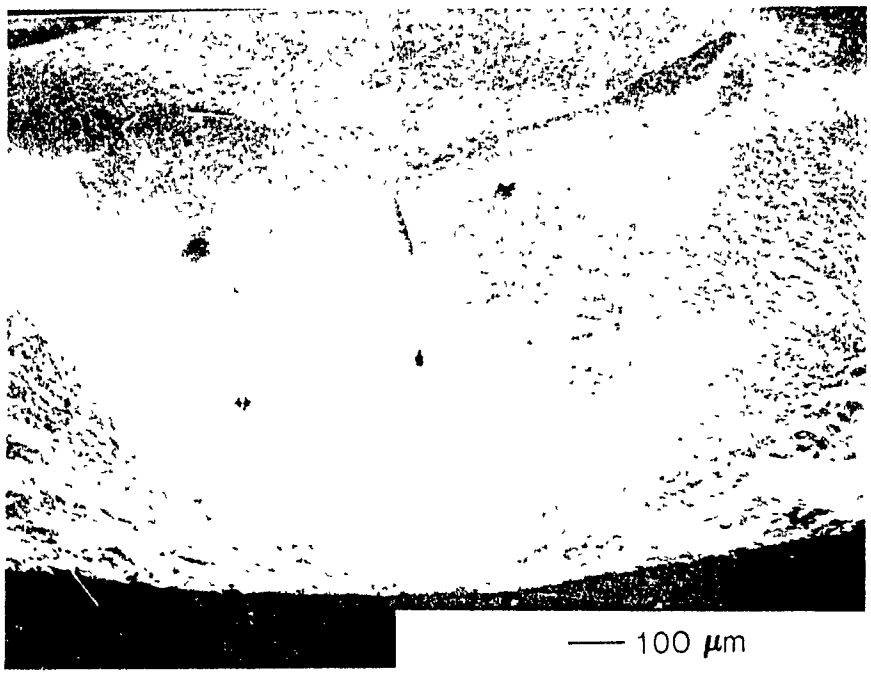

FIGURE 5.18: Micrograph of fracture surface of sintered slip cast silicon nitride

The micrograph in figure 5 18 shows a typical Mirror and Hackle fracture. The fracture initiating site, though close to the surface, is an internal flaw The smooth surface around the fracture origin is the fracture mirror. When such a crack propogates it encounters inclusions and experiences a shift in the direction of principal tensile stress This causes the formation of small radial ridges known as hackle The micrograph shows the uneven surface or the hackle around the fracture initiating site

5.2 Pressing and Sintering results

Samples prepared by die-pressing were isostatically pressed and sintered according to the procedure given in section 4 2 2 Green density measurements were carried out again by direct measurement of weight and dimensions The sintered density measurements were carried out by measurements of their dry, saturated and wet weights as outlined in ASTM C20-87 The results of green and sintered densities are given in table V.5 and V 6 respectively

TABLE V.5: Green densities of the pressed samples

Dispersant	Number of samples	density (g/cc)	Standard deviation	as % Theoretical density
Darvan C	23	1 74	0 05	53.5
Darvan 821A	25	1 70	0 04	51 8

TABLE V 6 Sintered densities of the pressed samples.

Dispersant	Number of samples	density (g/cc)	Standard deviation	as % Theoretical density
Darvan C	23	3.20	0.03	97.5
Darvan 821A	25	3 18	0 04	94.8

Comparing the values given in tables V.4 with V 6, it is clear that the sintered densities are independent of the green densities In the case of slip cast samples, the green densities are lower than the corresponding pressed samples, however the sintered densities are higher The sintered densities for both the processing routes are comparable and fall within a range of about 4%, although the slip cast samples show higher values

Pressureless sintering was carried out in both the cases. The use of sintering additives, as in this case, allow sintering of silicon nitride in pressureless conditions. In both, slip cast and pressed samples, the additive content (11-12%) was same, and pressureless sintering was carried out under same conditions, the resulting sintering densities are similar The main variation in the processing route of slip casting versus pressing is in the making of the green samples. Thus the slight difference in sintered density may be due to more even packing in the slip cast samples as opposed to pressed samples which often exhibit density gradients which lead to non-uniform sintering and lower sintered densities.

5.3 Mechanical strength of slip cast and die-pressed samples

Table V.7 and V 8 shows the results obtained from strength testing along with fracture initiating defects for both, slip cast and pressed samples, respectively Figures 5.19 and 5 20 show the Weibull plot for slip cast and pressed samples respectively Fractography was performed by locating the fracture initiating sites by tilting the samples by 20°. Fractography is of extreme importance in ceramics and especially in this case since silicon nitride is a high temperature material, and reliability can only be achieved by the elimination of failure causing defects

TABLE V 7 Results of mechanical testing of slip cast and sintered samples

	number of samples	Modulus of Rupture (MPa) σ	m	Fracture causing defects
Darvan C	39	383	3 1	50% pores 30% inclusions 20% machining
Darvan 821A	36	388	2 2	45% pores 35% inclusions 20% machining

TABLE V.8: Results of mechanical testing of die-pressed and sintered samples

	number of samples	Modulus of Rupture (MPa) σ	m	Fracture causing defects
Darvan C	23	519	3.2	22% pores 43% inclusions 35% machining
Darvan 821A	25	528	3.5	12% pores 48% inclusions 40% machining

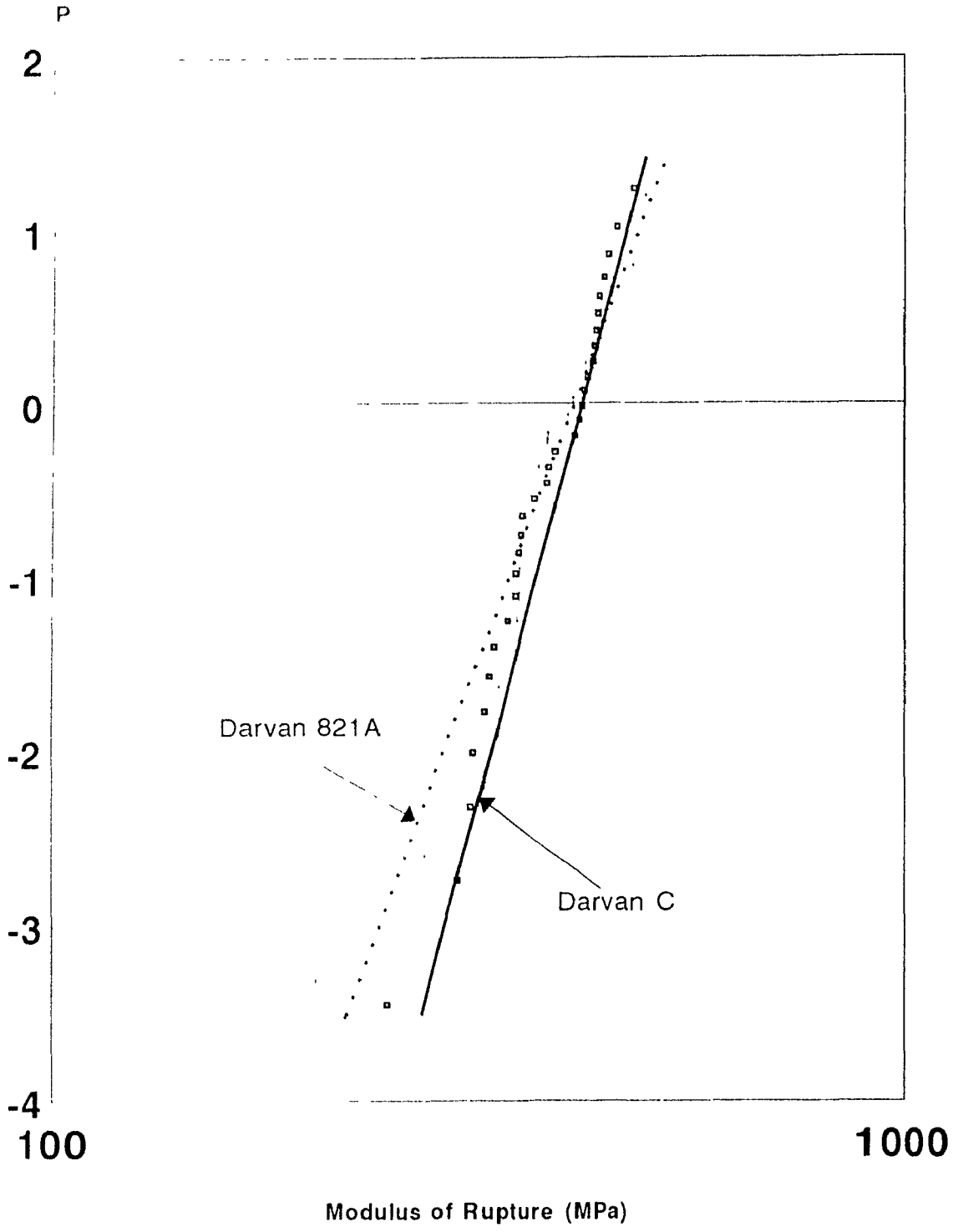

Figure 5.19: Weibull plot for slip cast samples

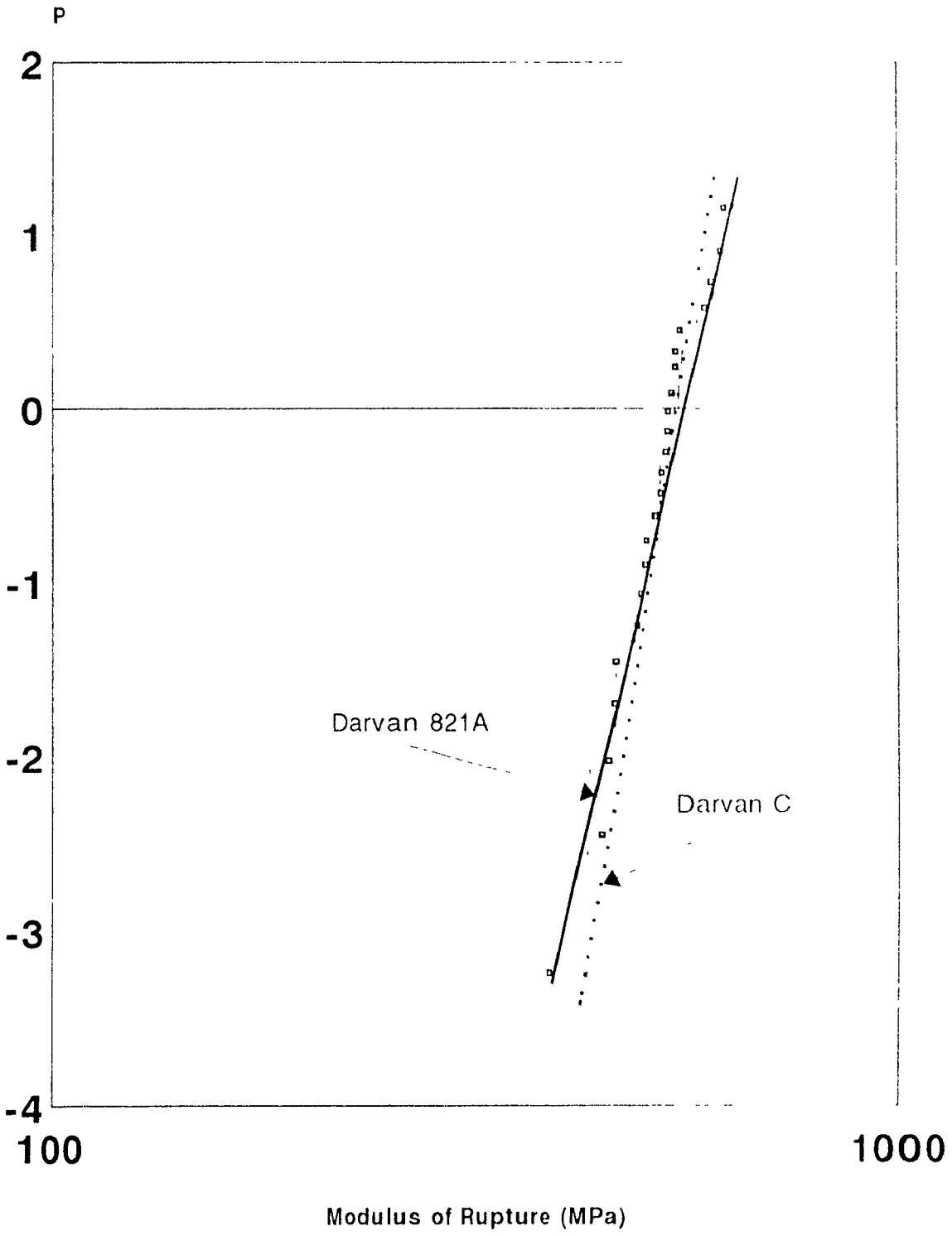

Figure 5.20: Weibull plot of die-pressed samples

From the results above it appears that the mechanical strength values of both slip cast and die-pressed samples are affected by their typical fracture causing defect. In the case of die pressed samples metallic inclusions resulted in lower strength values, whereas in case of slip cast samples, metallic inclusions and porosity both seem to have affected the values Metallic contamination is thought to result from attrition milling and is due to slight misalignment of the rotor in the chuck, resulting in iron fillings contaminating the samples A number of samples, showed inclusions which acted as fracture initiation sites. Figure 5.21 shows a micrograph of a fractured sample containing an inclusion Energy Dispersive X-ray analysis of the inclusions (figure 5.22), show distinct peaks for Al and Fe. Al could possibly be from the aluminium stub holding the sample.

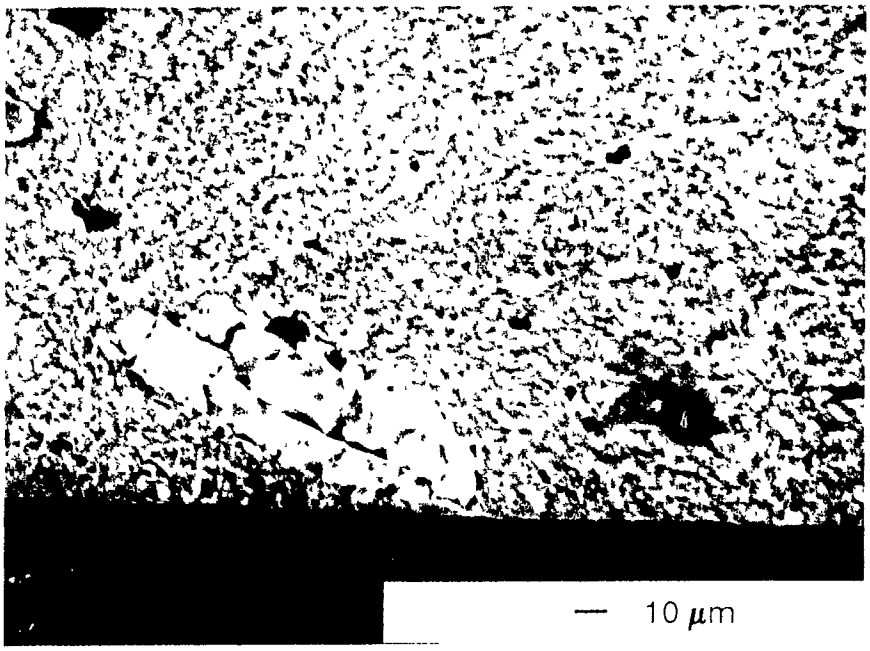

FIGURE 5 21: Micrograph of a fractured sample showing metallic inclusion.

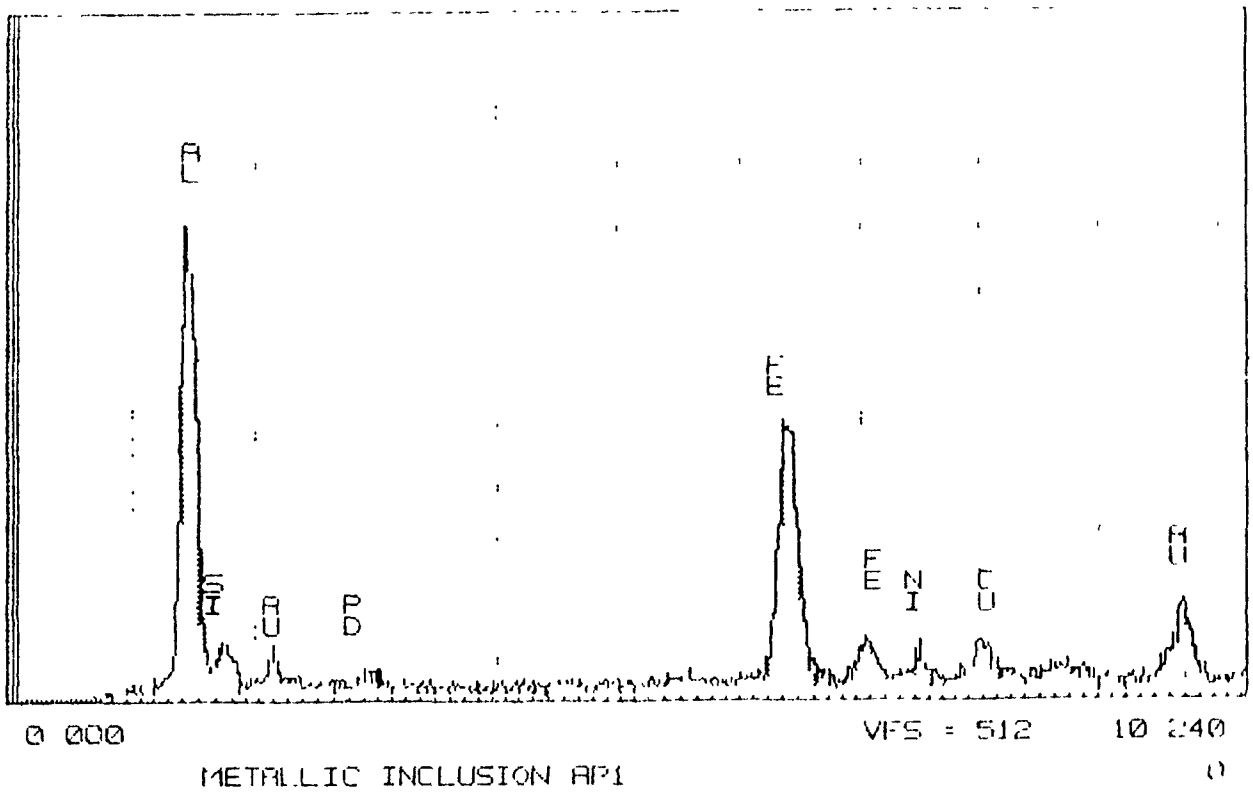

FIGURE 5 22· XPS of a metallic inclusion.

In case of slip casting, sub-surface pores caused fracture in most of the samples, which led to lower strength values as shown in Table V.6. Figure 5.23 shows the micrograph of an approximately 120 micron sub-surface pore. The origin of porosity can be due to improper filling of the mould or more likely due to trapped air bubbles in the slip.

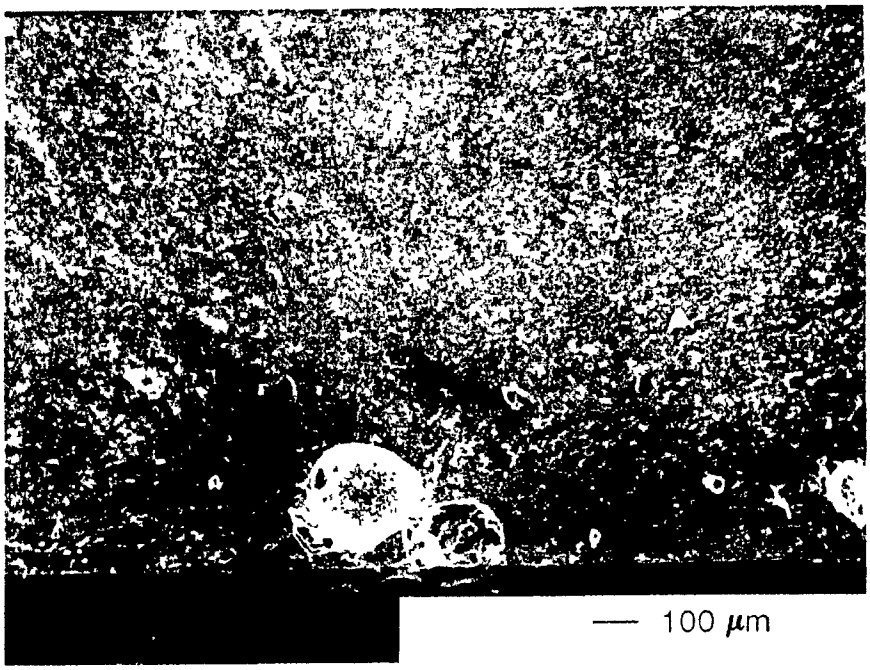

FIGURE 5.23: Micrograph of a slip cast sample showing a sub surface pore.

De-airing of . slip, under high vacuum, containing a high solids loading leads to evaporation of water from the surface of the slip This gives rise to the formation of a crust and changes the viscosity of the slip. Another method for removal of trapped air is by constant stirring of the slurry with the help of a propeller In this case the propeller is fully submerged within the slurry and stirring takes place at a very slow speed. The second method is an industrial approach where large batches of slurry are made and is especially useful when the slurry is to be aged before casting Since no de-airing of the slips were done after attrition milling, it is possible that the trapped air bubbles resulted in pores leading to the fracture of the samples

Figure 5 24 shows the micrograph of a slip cast sample containing metallic inclusions. Machining defects, as shown in figure 5 25, also limited the strength values in the slip cast samples Figure 5 25 shows a radial crack which is typical of a machining defect The samples being ground in the longitudinal direction, the stress concentration occurs in radial direction

The inclusions and machining defects were observed in both slip cast and pressed samples.

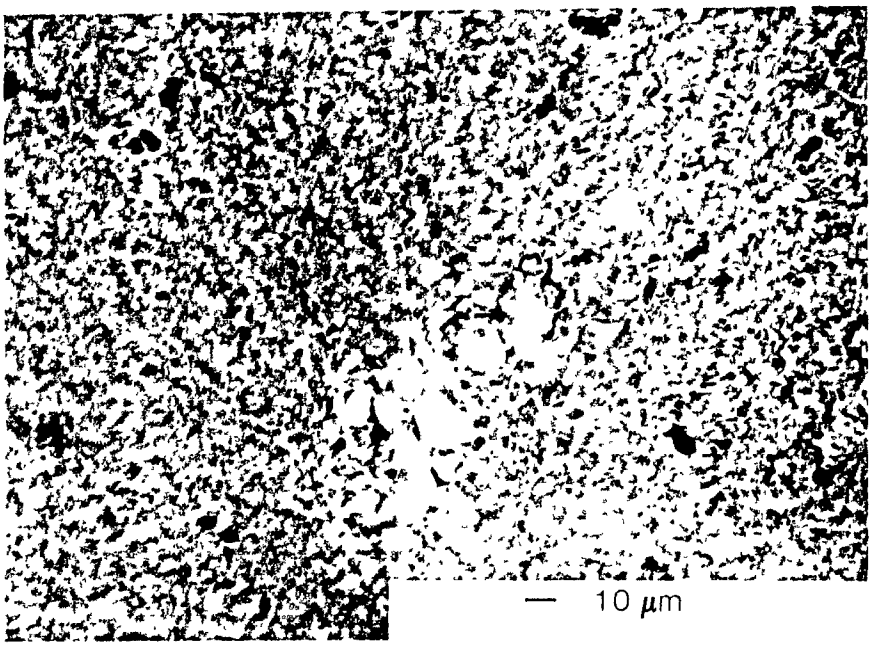

FIGURE 5.24. Micrograph of a slip cast sample showing a metallic inclusion.

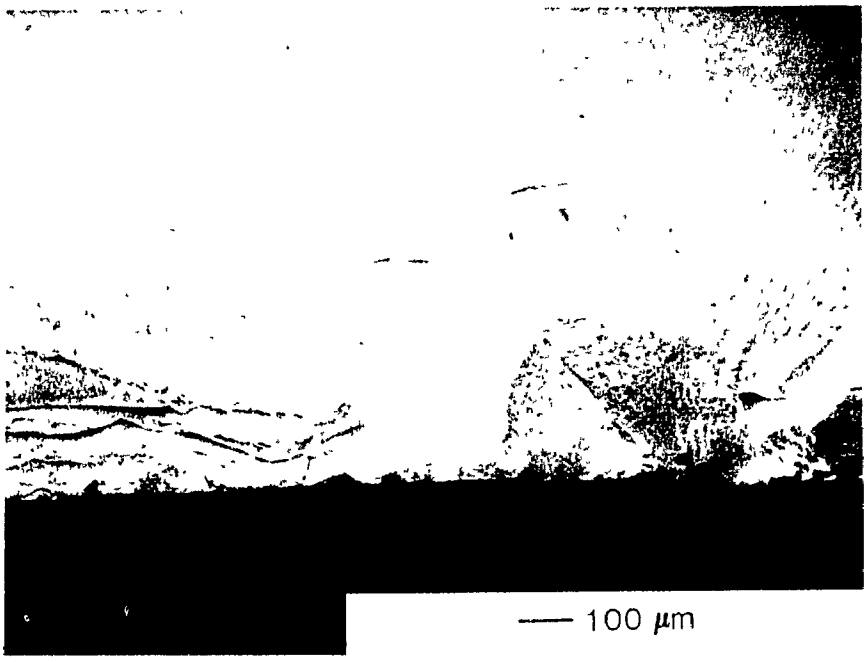

FIGURE 5.25. Micrograph showing a machining defect in a slip cast sample

CHAPTER VI CONCLUSIONS

Slip casting of silicon nitride was investigated by study of the rheology of the prepared slips With the aid of parameters such as viscosity, solids loading, zeta potential, amount and choice of dispersants and time dependent behaviour, it was possible to slip cast silicon nitride using traditional slip casting processes in an aqeous medium. Since the properties of the slurry greatly affect the casting rates, sintered microstructure and mechanical strength, it was important to control the rheology of the slips. Based on the results it can be concluded that:

1. Viscosities for a given solids loading decrease with increasing concentration of the dispersant, until a minimum is obtained On increasing the concentration of the dispersant the viscosity increases again

2. This minimum value of viscosity is associated with the highest zeta potential for the given solids loading, and can be used as a reference point for optimising a deflocculated slip.

3. A wide range of dispersant concentrations (0 14%-2% , and solids loading (1 0-2 5) were examined for both Darvan C and Darvan 821A, and it was concluded that 0 5% concentration and a solids loading of 2 0, gave the best and rheologically stable slips for casting.

4. Sintered densities ranging from 94-97%TD were independent of the green densities (48-54%TD)

5. For slip cast samples sintered densities upto 97% theoretical, could be achieved after sintering at 1800°C for 1 h with a slight nitrogen overpressure, and an additive content of 11-12%.

6 Mechanical strength values obtained were limited by metallic inclusions, porosity and machining flaws.

7. In the case of slip cast samples, an average strength of 383MPa was obtained. Porosity, and inclusions were the major fracture causing defects.

CHAPTER VII SUGGESTIONS FOR FUTURE RESEARCH

This research has shown the importance of particle size, solids loading, viscosity and other processing related parameters, their effect on sintered microstructure, and successful slip casting of silicon nitride. Future work can be directed towards·

1. Development of theoretical and experimental techniques for characterizing agglomerate formation and pore distribution during slip casting

2. Theoretical techniques for prediction of sintered properties of ips prepared by using different powders and a wide particle size distribution, especially non spherical particles.

3. Creation of multicomponent colloidal structural models through a knowledge of starting powders and processing parameters.

4. Using a combination of dispersing agents with a view to enhance flowability and green densities of slip cast silicon nitride

5. Development of a computer simulated software for the prediction of reliability of advanced and other structural ceramics prepared by slip casting

6. A purely economic approach directed toward the use and implementation of slip casting in conjunction with other possible colloidal techniques, for the development of advanced ceramics and composites in an industrial environment.

REFERENCES

1. D.R.Messier and W.J.Croft, "Silicon Nitride", *Preparation and Properties of Solid State Materials, Vol. 7*, 131-213. edited by W.R.Wilcox.

2 R A.L.Drew, "Silicon Nitride and Sialon Ceramics-A Review", *Canadian Metallurgical Quarterly, Vol 27,* No.1,59-64(1988).

3 G.Ziegler and G Wotting, "Powder Characteristics and Sintering Behaviour of Si_3N_4 Powders, *Powder Metallurgy International, Vol. 18,* No.1, 1986.

4. H.Mehner, German Patent 88999, 30 Sept. 1896.

5. L.Weiss and T.Engelhardt, "The Nitrogen Compounds of Silicon" *Z. Anorg. Allg. Chem.65,* 38-65(1910).

6 J.F Collins and R W Gerby, "New Refractory uses for Silicon Nitride" *J. Metals,* 612-615(1955).

7 E.T Turkdogan, P.M.Bills and V.A.Tippet, "Silicon Nitride: Some Physicochemical Properties", *J. Appl. Chem. Vol 8,* 296-302(1958).

8. N.L.Parr, "Silicon Nitride-A new Ceramic for High Temperature Engineering and other Applications", *Research (London) 13,* 261-269(1960)

9 N.L Parr and E R W.May, "The Technology and Engineering of Reaction-Bonded Silicon Nitride", *Proc. Brit Ceram. Soc., No.7,* 81-98, (1967).

10. K.H.Jack and W.I.Wilson, *Nature,* 238 (1972).

11. Y.Oyama and J.Kamigaito, *Japan. J. Appl. Phys.,* 10 (1971).

12. M Persson, L.Hermansson and R.Carlsson, "Some aspects of Slip Casting of Silicon Nitride and Silicon Carbide", *Ceramic Powders,* edited by P Vincenzini, 1983, Elsevier Scientific Publishing Company, Amsterdam.

13. P.K.Whitman and D L.Feke, "Colloidal Characterization of Ultrafine Silicon Carbide and Silicon Nitride Powders", *Advanced Ceramic Materials,* 1(4) 366-370 (1986).

14. A.Bellosi, C.Galassi, R.Lapasin and E.Lucchin, "Casting Conditions and Rheological Properties of Si_3N_4 based Materials" *Brit. Ceram. Proc., No.38*, 179-196 (1986).

15. C.A.M.Siskens, W.J.A.M.Hartman, F.K.V.Dijen and R.Metselaar, "Slip Casting parameters for commercial Si_3N_4 Powders", *Journal de Physique,Supplement au no.2,* Tome 47, 79-83, Fevrier 1986.

16. C.Olagnon, D.McGarry and E.Nagy, "The effect of Slip Casting Parameters on the Sintering and Final Properties of Si_3N_4", *Brit Ceram Trans. J.,* 88, 75-78, 1989.

17. M.J.Hoffmann, A.Nagel, P.Greil and G.Petzow, "Slip Casting of SiC-Whisker-Reinforced Si_3N_4", *J. Am. Ceram. Soc.,* 72(5) 765-769 (1898)

18. C.H.Schilling and I.A Aksay, "Slip Casting of Advanced Ceramics and Composites", *Pacific Northwest Laboratory Report,* DE-AC06-76RLO.

19. D.Hardie and K.H.Jack, "Crystal structure of Silicon Nitride", *Nature,* 180, 332-333 (1957).

20. S.N.Ruddlesden and P Popper, "The crystal structures of the nitrides of Silicon and Germanium", *Acta Cryst ,* 11, 465-468 (1958).

21. S.Wild, P.Grieveson and K H Jack, "The crystal structures of alpha and beta Silicon and Germanium nitrides", *Special Ceramics 5 (P Popper, ed.),* British Ceramic Research Association, England, 385-395 (1972).

22. I. Kohatsu and J.W.McCauley, "Re-examination of the crystal structure of alpha Silicon Nitride", *Materials Research Bulletin,* 9, 917-920 (1974)

23. R.Gruen, "The crystal structure of beta Silicon Nitride; Structure and stability considerations between alpha and beta Silicon Nitride", *Acta Cryst.,* B35, 800-804 (1979)

24. H.M.Jennings, " On reactions between Silicon and Nitrogen, Part 1, Mechanisms", *J. Mater Sci ,* 18, 951-967 (1983)

25. W.P.Kelley, *Cation Exchange in Soils,* Reinhold Pub. Corp., New York (1948).

26. E.J.W.Verwey and J.Th.G.Overbeek, *Theory of the Stability of Lyophobic Colloids,* Elsevier Pub. Co., New York (1948)

27 H.R Kruyt (Ed), *Colloid Science,* 2 vols., Elsevier Pub. Co., New York (1949).

28. W D.Kingery, *Introduction to Ceramics,* 33-56, John Wiley & Sons Inc., New York (1960).

29. M A.Ashby, *Acta Met.,* 22 (1974).

30 C Greskovick and H H Rosolowski, *J. Am. Ceram. Soc.,* p337, 59 (1976).

31 G Ziegler, J.Heinrich and G Wotting, "Review: Relationships between processing, microstructure and properties of dense and reaction-bonded Silicon Nitride", *J. Mater Sci.,* 22 (1987).

32 W.D Kingery, H.K.Bowen and D.R.Uhlman, *Introduction to Ceramics,* 2nd Ed , John Wiley & Sons Inc., New York (1976).

33 G C Deeley, J.M Herbert and N.C.Moore, *Powder Metall.,* 8 (1961).

34 G.W Phelps, S G Maguire, W.J.Kelly and R.K.Wood, *Rheology and Rheometry of Clay-Water Systems,* Chapter 10, p146, Cyprus.

35 W D.Kingery, *Ceramic Fabrication Processes,* Part I, The MIT Press, Cambridge, MA

36 P.Rado, "Slip Casting of non-clay Ceramics", *Interceram,* 36, (1987)(4).

37 W D Kingery, *Introduction to Ceramics,* p387, John Wiley & Sons Inc., New York (1960).

38 F M.Tiller and C.Tasai, "Theory of Filtration of Ceramics: I, Slip Casting", *J Am. Ceram Soc.,* 69, No.12, 882-887 (1986).

39 D.S.Adcock and I.C.Mcdowall, "The Mechanics of Filter Pressing and Slip Casting", *J Am Ceram. Soc.,* 40, No.10, 355-362 (1957).

40. J S Reed and Zheng, *J Am. Ceram Soc.,* 72(5), (1989).

41 Rumpf and Schubert, Chap. 27, *Ceramic Proc. before Firing,* edited by Onoda and Hench, (1978).

42 G.W.Phelps, S.G.Maguire, W.J.Kelly and R.K.Wood, *Rheology and Rheometry of Clay-Water Systems,* Chapter 2, p15, Cyprus.

43. B.Jirgensons, *Colloid Chemistry*, p118-124, John Wiley & Sons Inc., New York (1954).

44. T.G.M.Van de Ven, "VII. Polymer Colloid Interactions", *Class Notes*, McGill University (1989).

45. F.F.Lange, B.I.Davis and E.Wright, "Processing Related Fracture Origins: IV, Elimination of Voids Produced by Organic Inclusions", *J Am. Ceram. Soc*, 69(1) 66-69 (1986).

46. R.C.P.Cubbon and E.G.Walker, The Rheological Properties of Suspensions of Potters Plaster in Water. A new Quality Control Test", *British Ceramic Society Pottery Section*, Autumn Meeting, 1978

47. "Flexural Strength of High Performance Ceramics at Ambient Temperature", *MIL-STD*, 1942(MR).

48. P.J.Anderson and P.Murray, "Zeta Potentials in Relation to Rheological Properties of Oxide Slips", *J. Am Ceram Soc*, 42(2), 70-74 (1959)

49. T.P.Herball, M.R.Freedman and J.D Kiser, "Particle size reduction of Si_3N_4 Powder with Si_3N_4 Milling Hardware", *Tenth Annual Conference on Composites and Advanced Ceramic Materials*, Cocoa Beach Florida, January 1986.

50. T.G.M.Van de Ven, "VI. Electrical Double Layer", *Class Notes*, McGill University (1989).

51. D.W.Richerson, "Modern Ceramic Engineering", Marcel Dekker Inc., New York.

APPENDIX A: SAMPLES PREPARED BY SLIP CASTING AT THE CERAMICS AND COMPOSITES LAB, McGILL UNIVERSITY

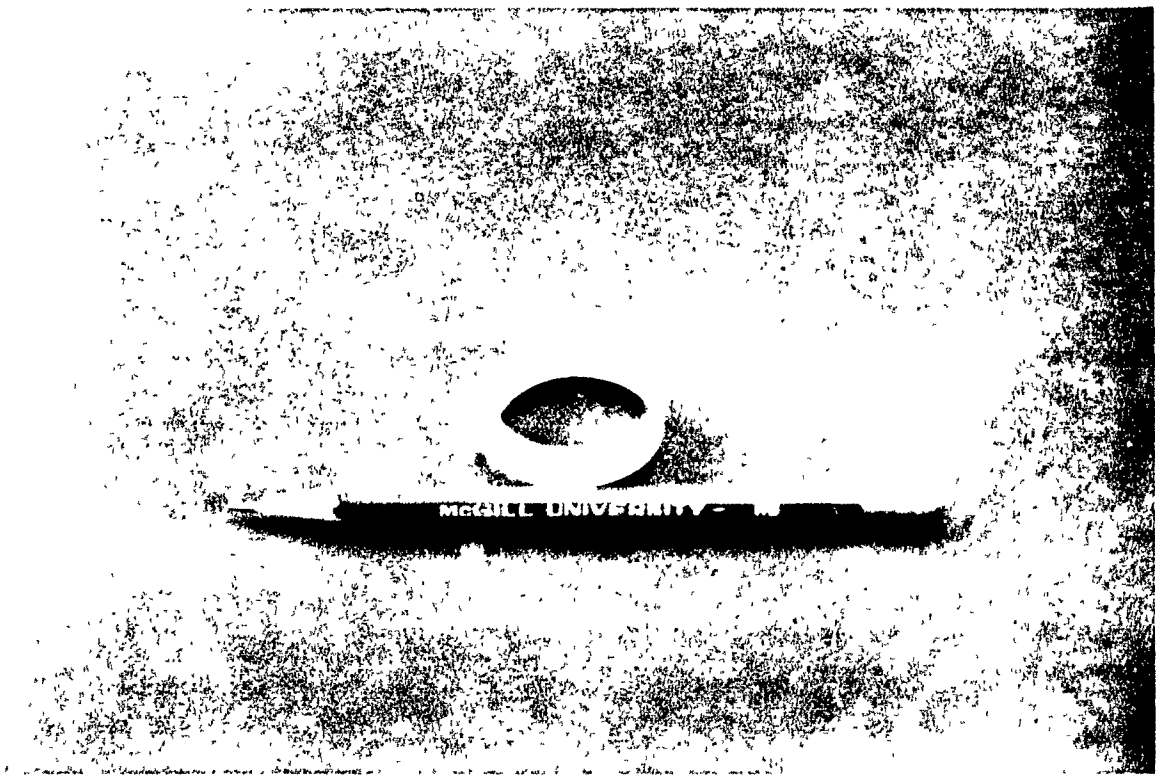

Figure A1: Green slip cast ring

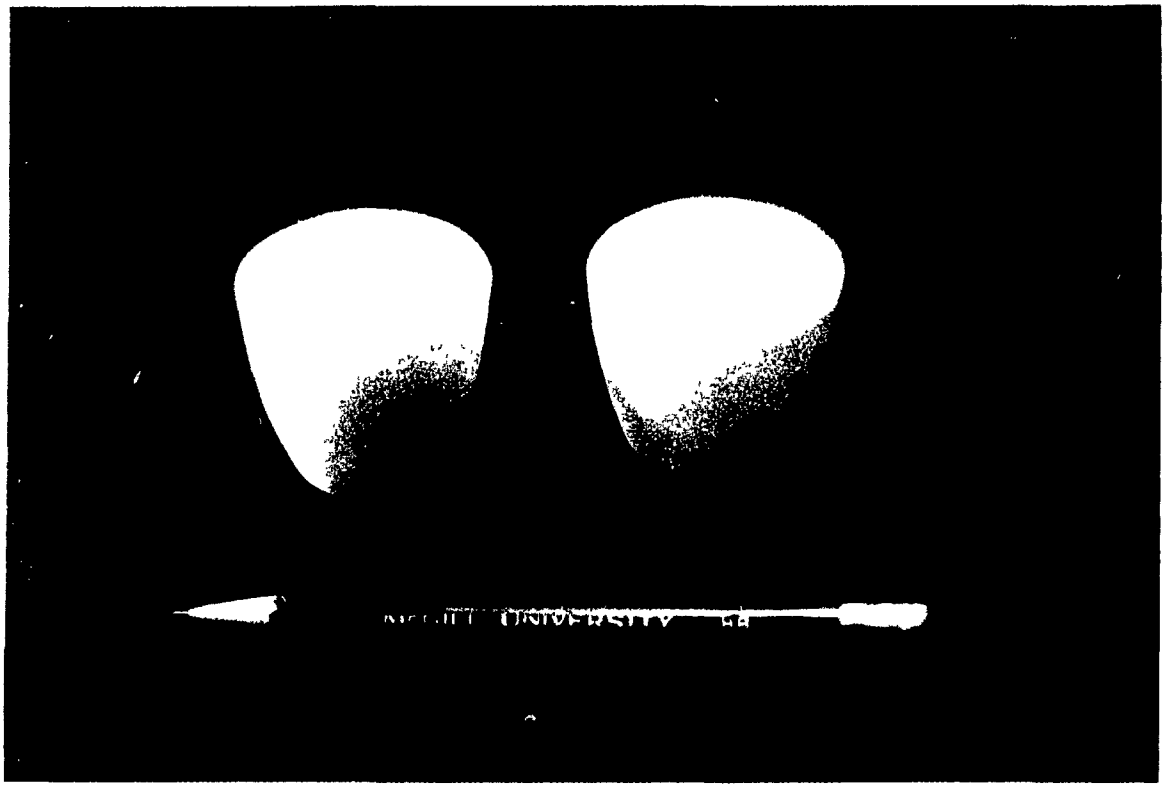

Figure A2: Green slip cast crucibles

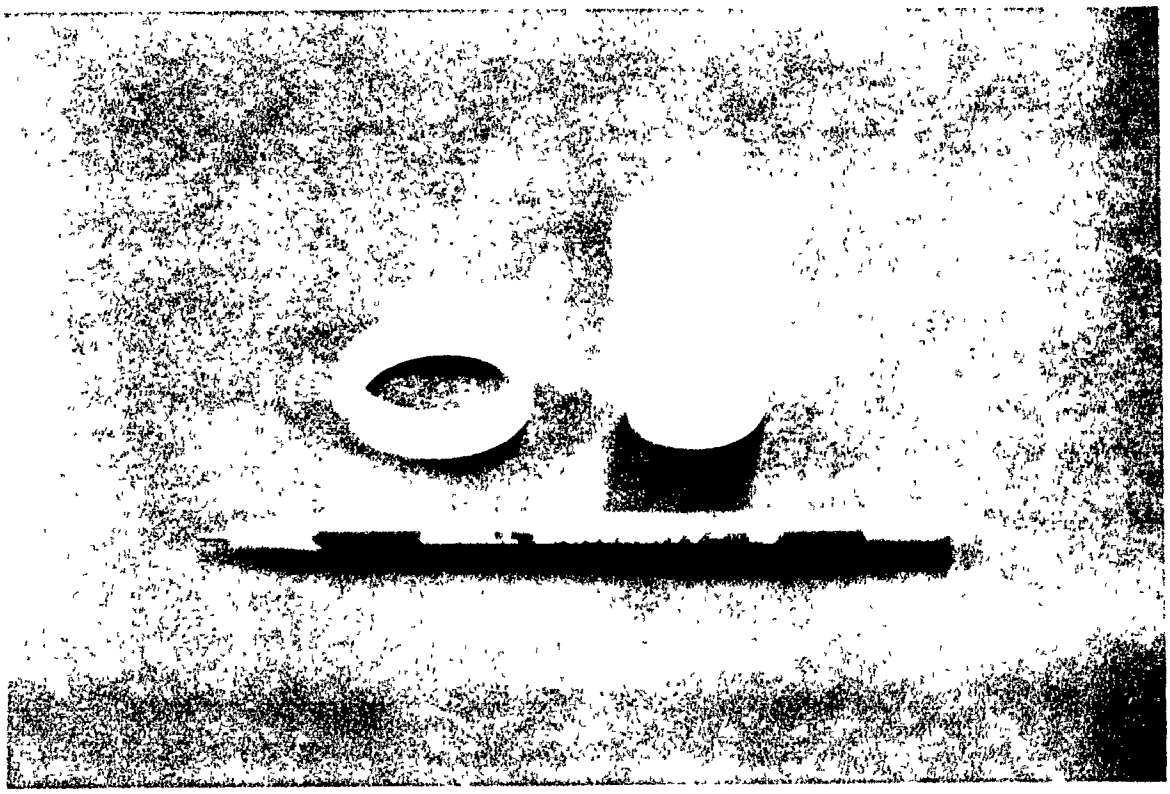

Figure A3: Green slip cast hollow cylinder

Figure A4: Sintered rings

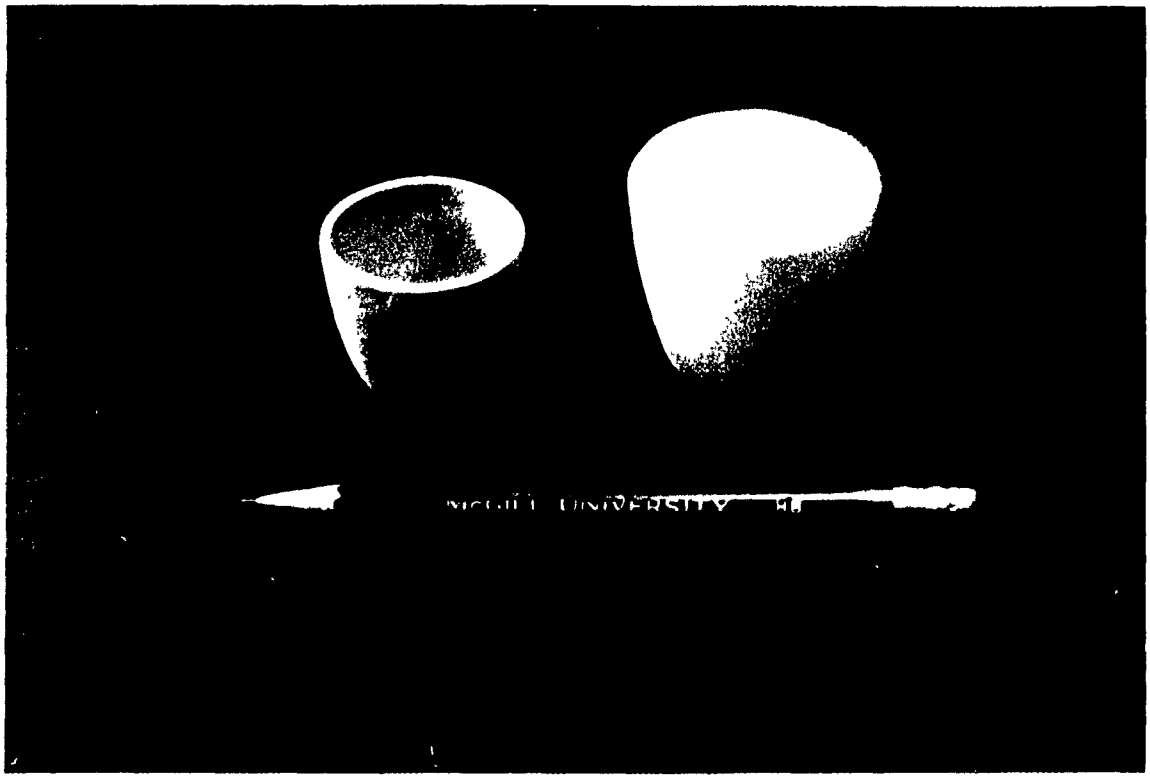

Figure A5: Sintered and green crucible

APPENDIX B: GREEN DENSITIES OF SLIP CAST AND PRESSED SAMPLES (gm/cc)

Sample number	SLIP CAST Darvan C	SLIP CAST Dar. 821A	PRESSED Darvan C	PRESSED Dar. 821A
1	1.64	1.68	1.76	1.71
2	1.62	1.67	1.71	1.7
3	1.62	1.66	1.75	1.69
4	1.62	1.67	1.84	1.68
5	1.63	1.69	1.67	1.68
6	1.58	1.59	1.73	1.68
7	1.54	1.61	1.77	1.61
8	1.62	1.62	1.69	1.71
9	1.64	1.69	1.62	1.78
10	1.65	1.65	1.7	1.69
11	1.65	1.74	1.71	1.66
12	1.63	1.71	1.79	1.67
13	1.64	1.54	1.81	1.72
14	1.65	1.69	1.81	1.73
15	1.61	1.68	1.77	1.66
16	1.65	1.71	1.76	1.76
17	1.66	1.72	1.72	1.72
18	1.56	1.72	1.71	1.76
19	1.68	1.72	1.74	1.66
20	1.60	1.76	1.73	1.69
21	1.63	1.73	1.7	1.75
22	1.64	1.67	1.71	1.69
23	1.72	1.66	1.74	1.7
24	1.69	1.56		1.73
25	1.71	1.88		1.72
26	1.72	1.85		
27	1.60	1.69		
28	1.61			
29	1.60			
30	1.61			
31	1.60			
32				
33				
34				
35				
Average	1.63	1.69	1.74	1.70
Standard Dev.	0.04	0.07	0.05	0.04

APPENDIX C: SINTERED DENSITIES OF SLIP CAST AND PRESSED SAMPLES (gm/cc)

Sample number	SLIP CAST Darvan C	SLIP CAST Dar. 821A	PRESSED Darvan C	PRESSED Dar 821A
1	3.22	3.21	3.19	3.14
2	3.21	3.17	3.19	3.16
3	3.24	3.18	3.11	3 22
4	3.21	3.22	3.12	3 25
5	3.24	3.21	3.21	3 23
6	3.25	3.17	3.19	3 11
7	3.26	3.19	3.21	3.17
8	3.22	3.19	3.21	3 19
9	3.21	3.19	3.22	3.18
10	3.21	3.2	3.25	3 14
11	3.24	3.22	3.26	3.15
12	3.19	3.19	3.24	3.17
13	3.18	3.2	3.21	3 21
14	3.21	3.21	3.23	3 21
15	3.23	3.2	3.25	3.18
16	3.18	3.19	3.21	3 23
17	3.17	3.16	3.2	3 21
18	3.21	3.17	3.22	3 21
19	3.23	3.24	3.18	3 23
20	3.21	3.22	3.18	3 23
21	3.20	3.22	3.19	3 13
22	3.18	3.21	3.22	3.19
23	3.19	3.23	3.21	3.11
24	3.22	3.21		3 17
25	3.23	3.19		3 18
26	3.23	3.18		
27	3.26	3.19		
28	3.21			
29	3.21			
30	3.15			
31	3.19			
32				
33				
34				
35				
Average	3.21	3 20	3 20	3 18
Standard Dev.	0.03	0.02	0 03	0 04

APPENDIX D· STRENGTH VALUES OF SLIP CAST AND PRESSED SAMPLES (MPa)

Sample number	SLIP CAST Darvan C	SLIP CAST Dar. 821A	PRESSED Darvan C	PRESSED Dar. 821
1	438.40	373.10	501.01	555.86
2	434.00	350.50	550.66	622.35
3	431.00	274.00	599.07	535.61
4	350.00	402.40	521.52	636.50
5	444.00	332.80	532.46	503.20
6	416.60	381.00	487.20	482.23
7	353.00	422.00	452.28	522.45
8	310.00	437.30	524.44	428.50
9	312.80	480.00	459.90	520.93
10	321.00	353.00	530.31	459.14
11	383.00	363.10	588.31	602.69
12	355.00	204.00	498.82	634.40
13	424.00	454.00	513.75	549.43
14	436.20	440.00	385.16	459.90
15	342.30	339.00	443.53	549.86
16	350.10	355 00	544.99	485.88
17	460.00	497.00	492.66	540.22
18	480.60	354.00	458.80	500.28
19	325.30	359.50	534.27	484.37
20	300.60	440.00	544.61	518.48
21	409.40	333.10	613.90	553.65
22	413.70	495.00	619.85	576.73
23	247.30	365.00	538.67	430.62
24	433.00	407.00		517.76
25	329.00	382.00		542.57
26	449.40	417.50		
27	381.00	321.10		
28	389.00			
29	420.00			
30	356.40			
31	369.40			
32				
33				
34				
35				
Average	382.76	382.68	518.96	528.54
Standard Dev.	55.27	64.62	55.69	56.19

APPENDIX E: pH MEASUREMENTS

Solids Loading	% Darvan C	pH	% Dar. 821A	pH
1	0.143	8 47		
1	0.5	8 48		
1	0.9	8.46		
1	2	8.67		
1.5	0.143	8.47		
1.5	0.5	8.47		
1.5	0.9	8.5		
1.5	2	8.87		
2	0.143	8.4	0.24	8.56
2	0.5	8.55	0.5	8.68
2	0.9	8.9	0 9	9.7
2	2	9.2	2	10 8
2.5	0.143	9.01		
2.5	0.5	9.45		
2.5	0.9	9.7		
2.5	2	11.02		

APPENDIX F: VISCOSITY DATA

Solids loading	% Darvan C	% Dar. 821A	Viscosity at 50rpm (cP)	Viscosity at 500rpm (cP)
1	0.1		1	1.1
1	0.2		0.9	1.2
1	0.3		0.6	1.1
1	0.4		0.35	0.94
1	0.45		0.2	0.92
1	0.5		0.23	0.93
1	0.6		1.1	1.3
1.5	0.2		4.8	4.4
1.5	0.3		2.6	2.3
1.5	0.4		0.7	1.2
1.5	0.5		1.2	1.5
1.5	0.6		1.55	1.6
1.5	0.7		1.8	1.6
1.5	0.8		1.8	1.55
1.5	0.9		1.55	1.8
1.5	1.5		2.6	2.2
1.5	2		3.5	2.4
2	0.143		24	7.5
2	0.5		2.6	2.6
2	0.9		2.5	3
2	2		4.5	12
2.5	0.5		11.4	25.8
2.5	1		5.5	9.5
2.5	1.5		6.3	14
2.5	2		8.3	26.5
2		0.24	2.2	3.5
2		0.5	2	2.7
2		0.9	2.3	3.5
2		2	3.8	8